Stony Brook University

Structure-Function Studies on Mammalian Mitochondrial DNA Polymerase

A Dissertation Presented

by

Zhixin Chen

To

The Graduate School

In Partial Fulfillment of the

Requirements

For the Degree of

Doctor of Philosophy

In

Biochemistry and Structural Biology

Stony Brook University

August 2007

Stony Brook University

The Graduate School

Zhixin Chen

We, the dissertation committee for the above candidate for the

Doctor of Philosophy degree,

hereby recommend acceptance of this dissertation.

Caroline Kisker, Ph.D.
Advisor
Professor, Rudolf-Virchow-Center, University of Würzberg, Germany
Formerly Associate Professor, Department of Pharmacological Sciences,
Stony Brook University

Arthur P. Grollman, M.D.
Co-Advisor
Distinguished Professor, Department of Pharmacological Sciences, Stony Brook Univeristy

Rolf Sternglanz, Ph.D.
Chairman
Distinguished Professor, Department of Biochemistry and Cell Biology,
Stony Brook University

Dax Fu, Ph.D.
Assistant Professor, Department of Pharmacological Sciences, Stony Brook University
(Department of Biology, Brookhaven National Laboratory)

Daniel F. Bogenhagen, M.D.
Professor, Department of Pharmacological Sciences, Stony Brook University

This dissertation is accepted by the Graduate School.

Lawrence Martin
Dean of the Graduate School

Abstract of the Dissertation

Structure-Function Studies on Mammalian Mitochondrial DNA Polymerase

by

Zhixin Chen

Doctor of Philosophy

In

Biochemistry and Structural Biology

Stony Brook University

2007

Mitochondrial DNA polymerase (pol γ) is the only DNA polymerase within mitochondria, and is responsible for both mtDNA replication and repair. Mutations of pol γ have been implicated in several human diseases and cause accelerated aging in mice. In contrast to yeast, which only contains the catalytic subunit, an accessory subunit (pol γB) has been observed in higher eukaryotes like *Drosophila* and mammals and shown to enhance processivity and substrate binding of the catalytic subunit (pol γA). *Drosophila* pol γ has been reported to be a heterodimer containing one pol γA and one pol γB polypeptide. However, mouse pol γB, when crystallized, forms a homodimer. In this study, using various biophysical approaches, human pol γ has been determined to be a heterotrimer formed by one catalytic subunit and two accessory subunits. Furthermore, the integrity of the stoichiometric composition of pol γA and pol γB within the human pol γ holoenzyme is shown to be important for maintaining pol γ processivity. A deletion

derivative of pol γB which is unable to dimerize consequently is impaired in its ability to stimulate processive DNA replication. For a better understanding of the subunit interaction, regions within pol γB and pol γA were identified that are required for complex formation. A pol γB interacting domain was mapped to the spacer region of pol γA which is located between the catalytic domain and the exonuclease domain of pol γA. In addition, the structure of human pol γB was determined at 3.10 Å by molecular replacement.

Table of Contents

List of Abbreviations

Å: Angstrom (10^{-10} m)

BME: β-mercaptoethanol

C_α: Alpha Carbon

cv: Column volume

Da: Dalton

dATP: Deoxyadenosine 5'-triphosphate

DLS: Dynamic Light Scattering

E.coli: *Escherichia coli*

EDTA: Ethylenediamine tetraacetic acid

EM: Electron microscopy

EMSA: Electrophoretic mobility shift assays

EtBr: Ethidium Bromide

Exo: Exonuclease

FID: Free interface diffusion

H: Enthalpy

HEPES: N-(2-hydroxyethyl)-piperazine-N′-2-ethanesulfonic acid

IPTG: Isopropyl-β-D-1-thiogalactopyranoside

ITC: Isothermal titration calorimetry

K_a: Association constant

K_d: Dissociation constant

KSCN: Potassium thiocyanate

2-ME: 2-Mercaptoethanol

mtDNA: Mitochondrial DNA

$O.D_{600}$: Optical density at 600 nm

PEO: Progressive external ophthalmoplegia

PDB: Protein data bank

PEG: Polyethylene glycol

PEG MME 5000: Polyethylene glycol monomethyl ether 5000

Pol: Polymerase

PVDF: polyvinylidene difluoride

rms: Root mean square

rRNA: Ribosomal ribonucleotide

tRNA: transfer ribonucleotide

RU: Resonance unit

SDS-PAGE: Sodium dodecyl sulfate-polyacrylamide gel electrophoresis

Sf9: *Spodoptera frugiperda 9*

SPR: Surface plasmon resonance

Tris: Tris (hydroxymethyl) aminomethane

TTP: Thymidine 5'-triphosphate

WT: Wild-type

List of Figures

List of Tables

Acknowledgement

I would like to thank Elena Yakubovskaya and Daniel F. Bogenhagen for their great efforts on this co-laboratory project. I would also like to recognize James J. Truglio for his assistance with the X-ray crystallography studies of human pol γB. In addition, I would like to acknowledge Liqun Wang for the cloning work of pol γA fragments. I thank my committee members, Arthur P. Grollman, Rolf Sternglanz, Dax Fu, and Daniel Bogenhagen for their suggestions and guidance. I would also like to especially thank my advisors, Caroline Kisker and Daniel Bogenhagen from whom I have learned a great deal. Lastly, I dedicate this dissertation to my husband Hengyao Niu, my daughter Vivian, and my parents Guofang and Xiufang. This work would not have been possible without their support.

CHAPTER 1: General Introduction

DNA polymerases are essential for maintaining the integrity of the genome, both through faithful DNA replication and by repairing damages to DNA. These enzymes can be classified into six main families based on phylogenetic relationships with *E. coli* pol I (Family A), *E. coli* pol II (Family B), *E.coli* pol III (Family C), Euryarchaeotic pol II (Family D), human pol β (Family X), and *E. coli* UmuC/DinB and the eukaryotic RAD30/xeroderma pigmentosum variant (Family Y) (BRAITHWAITE and ITO 1993; CANN and ISHINO 1999; ITO and BRAITHWAITE 1991; OHMORI *et al.* 2001). All known eukaryotic DNA pols are either Family A, B, X or Y enzymes (Table 1). Among the 16 known eukaryotic DNA polymerase, 15 are involved in maintaining nuclear genetic information and they are highly specialized functionally. Pol α, δ and ε are required for nuclear DNA replication. The remaining nuclear DNA polymerases function in nuclear DNA repair and specialized DNA synthesis processes which contribute to the maintenance of genetic integrity, reviewed in Shcherbakova, Bebenek et al. (2003) and Bebenek and Kunkel (2004). In contrast, the replication and maintenance of the mitochondrial genome relies solely on pol γ. As the only DNA pol detected in mammalian cell mitochondria, pol γ is uniquely responsible for all DNA synthetic reactions in replication, repair and recombination of mitochondrial DNA (mtDNA).

I. The Mitochondrial Genome and its Replication and Repair:

A. Mitochondrial Genome: Mitochondria became the energy centers of a primordial eukaryotic cell about 1.8 billion years ago. The mitochondrion contains its own genomic DNA, which is derived from the early bacteria, α-proteobacterium (LANG *et al.* 1999). In mammals, mtDNA is a double stranded circular molecule (16569 nucleotides), which is very compact and does not contain introns or long non-coding segments. The human mitochondrial genome comprises 37 genes, all of which encode polypeptides essential for energy production and storage. Thirteen of these genes encode protein subunits involved in electron transport and oxidative phosphorylation, and the remaining 24 genes encode tRNAs (22 genes) and rRNAs (2 genes) required for mitochondrial protein synthesis (ATTARDI 1985; ATTARDI and SCHATZ 1988). All the other proteins required for mtDNA maintenance and expression, including pol γ, the single-stranded DNA binding protein (mtSSB), DNA helicase (Twinkle), and other accessory proteins and transcription factors, are encoded by nuclear genes, synthesized on cytosolic ribosomes and imported into the mitochondria (CLAYTON 1991).

B. MtDNA Replication: In comparison to nuclear DNA replication, mtDNA replication might be expected to be simple due to the small size of mtDNA, its circular character and limited number of genes. A long-standing model of mammalian mtDNA replication is termed the strand displacement or asymmetric model (CLAYTON 1982; SCHMITT and CLAYTON 1993; SHADEL and CLAYTON 1997) (Fig. 1.1). In this model, replication of

mtDNA is initiated by transcription at the origin of heavy (H)-strand synthesis (O_H) and proceeds unidirectionally by displacement of the parental H-strand as single-stranded DNA. The resulting triplex structure is termed a D-loop. After two-thirds of the H-strand has been replicated, the origin of light (L)-strand synthesis (O_L) is exposed, permitting initiation of L-strand synthesis in the opposite direction (FERNANDEZ-SILVA *et al.* 2003). A key aspect of this model is that both strands can be replicated continuously. Recently this established model has been challenged by an alternative mechanism of mtDNA replication, termed the strand-coupled model (Fig. 1.1), which is based on the presumed ribonucleotide substitution pattern in mtDNA and analysis of replication intermediates by 2D-gel electrophoresis (BOWMAKER *et al.* 2003; HOLT *et al.* 2000; YANG *et al.* 2002). In the strand-coupled model, a symmetric, semidiscontinuous replication is initiated from a zone within a broad area beyond the D-loop. Within this zone, both strands are synthesized bidirectionally as the double-stranded replication forks proceed through the length of mtDNA. Both models of mtDNA replication with their supporting evidence have been reviewed recently (BOGENHAGEN and CLAYTON 2003a; BOGENHAGEN and CLAYTON 2003b; HOLT and JACOBS 2003). The controversy between the two models may be resolved with a new analysis of replication intermediates by atomic force microscopy (AFM). AFM analysis is consistent with the strand displacement model and suggests that this model is the dominant or even sole mode of mtDNA replication in mouse liver (BROWN *et al.* 2005).

C. MtDNA Repair: MtDNA is more prone to damage than nuclear DNA due to two factors. First, mtDNA is not protected like nuclear DNA by histone proteins; second, mtDNA is associated with the mitochondrial inner membrane where reactive oxygen species (ROS) are generated. In addition to damage from ROS, mtDNA is also damaged by exposure to ionizing or ultraviolet radiation, antiviral compounds or through other endogenous and exogenous factors. Repair of damaged DNA is important for maintaining the function of mitochondria as energy providers in eukaryotic cells. The major DNA repair mechanism in mitochondria is base excision repair (BER) (CROTEAU and BOHR 1997; SAWYER and VAN HOUTEN 1999). In BER, a DNA glycosylase recognizes a damaged or inappropriate base and removes it by cleaving the N-glycosylic bond between the base and the sugar. Following this, an apurinic/apyrimidinic endonuclease (AP endonuclease) catalyzes incision of the DNA phosphate backbone at the AP site. A lyase then removes the 5'-terminal 2-deoxyribose-5-phosphate (dRP) sugar moiety from the downstream DNA. The resulting 3'-hydroxyl moiety can be extended by a DNA pol and finally DNA ligase joins the two free DNA ends (BOGENHAGEN 1999). The targets of mitochondrial BER are oxidatively modified DNA bases, such as 7, 8-dihydro-8oxoguanine (8-oxo-G) and thymine glycol. Other repair mechanisms, such as mismatch repair, recombination and nonhomologous end-joining, have not been well studied in mammalian cells, although these pathways have been found in yeast mitochondria. Reports of translesion synthesis past DNA adducts by pol γ are also limited. More remarkably, no nucleotide excision repair (NER) has been found in vertebrate

mitochondria, and the bulky adducts induced by carcinogenic compounds are generally not repaired in mitochondria (CROTEAU *et al.* 1999; SAWYER and VAN HOUTEN 1999).

D. Significance of mtDNA: Mutations and partial deletions in mtDNA can be accumulated during mtDNA replication and organelle proliferation in an age dependent manner (MICHIKAWA *et al.* 1999). When mitochondrial function is disrupted by accumulated mtDNA mutations, a variety of diseases with respiratory defects and tissue degeneration may result (MICHIKAWA *et al.* 1999). Functional defects of mtDNA have been linked to apoptosis, oxidative aging, and side effects of commonly used HIV drugs (LEWIS *et al.* 1996; WANG *et al.* 2001a; WANG *et al.* 2001b). As the only DNA pol found in mitochondria, pol γ is implicated to generate mutations in mtDNA. Recent studies have indicated that POLG, the gene for the catalytic subunit of pol γ, is an important disease locus. Dysfunction of pol γ has been associated with disorders as progressive external ophthalmoplegia (PEO), Parkinsonism, Alpers syndrome etc (LUOMA *et al.* 2004; NAVIAUX and NGUYEN 2004; VAN GOETHEM *et al.* 2001). Two recent developments have stressed the effects of a defective pol γ. Mutations in the catalytic subunit of human pol γ cause mitochondrial disorders, and a transgenic mouse engineered to express an error-prone form of DNA pol γ lacking the 3'→5' proofreading ability accumulates errors in mtDNA and undergoes accelerated aging (KUJOTH *et al.* 2005; TRIFUNOVIC *et al.* 2004).

II. Activities and Subunit Composition of Polymerase γ

Pol γ was first identified as an RNA-dependent DNA pol in human Hela cells (FRIDLENDER *et al.* 1972), and subsequently localized to animal mitochondria (BOLDEN *et al.* 1977). It contributes only 1-5% of the total cellular DNA polymerase activity and replicates ~1% of the cellular DNA. It has been well established that pol γ contains a catalytic subunit of 115-143 kDa (γA) and in higher eukaryotes an accessory subunit of 35-55 kDa (γB). Based on sequence homology, Pol γ has been grouped into the family A DNA pol, which contains pol I of *E.coli* as prototype (Fig. 1.2). Like other family A polymerases, in addition to its 5'→3' DNA polymerase activity, the catalytic subunit of pol γ has an intrinsic 3'→5' exonuclease activity which is highly mismatch-specific and improves the fidelity of mtDNA replication. Genetic and biochemical studies of the yeast enzyme showed that its 3'→5' exonuclease activity contributes several 100-fold to error avoidance *in vivo*. The knock-in mouse with a proofreading-deficient form of the catalytic subunit of pol γ developed a mtDNA mutator phenotype with up to a 5-fold increase in the number of point mutations as well as a significant increase in mtDNA deletions (TRIFUNOVIC *et al.* 2004).

A third catalytic activity, 5'-deoxyribose phosphate lyase activity has also been described for pol γ and other family A polymerases (LONGLEY *et al.* 1998a; PINZ and BOGENHAGEN 1998; PINZ and BOGENHAGEN 2000). This dRP lyase activity catalyzes the release of a 5'-terminal dRP sugar moiety from incised AP sites in BER. Moreover, pol γ has been characterized as a highly faithful, catalytically efficient, processive and

salt-tolerant DNA polymerase that can utilize a wide variety of DNA substrates including singly-primed M13 DNA and several homopolymers like poly(dA): oligo(dT) besides its natural DNA templates. Pol γ also possesses reverse transcriptase activity, which distinguishes it from other cellular DNA pols, although the significance of this activity *in vivo* remains unclear (ANDERSON *et al.* 1981). However, this activity makes pol γ highly sensitive to inhibition by anti-HIV nucleotide analogues such as AZT-TP (3′-azido-3′-deoxythmidine-5′-triphosphate), dideoxynucleotides, and other antiviral nucleotide analogues.

Almost all higher organisms have two DNA pol γ subunits. How they function together has become an interesting question. Pol γA is the catalytic subunit, conserved throughout all species. Transcription and western analysis show that it is expressed in a relatively steady state in different tissues, even in the absence of mitochondrial DNA maintenance and replication (DAVIS *et al.* 1996; SCHULTZ *et al.* 1998). A slight decrease of pol γA mRNA has been detected when *Drosophila* embryos start mtDNA replication (LEFAI *et al.* 2000). *In vitro* DNA polymerase assays show that recombinant human pol γA alone displays salt sensitivity and modest processivity. Interestingly, a study with the accessory subunit found that its mRNA increases when *Drosophila* embryos initiate mtDNA replication. Mutations of the gene encoding the *Drosophila* accessory subunit led to loss of mtDNA and lethality. Recombinant human pol γB raises the salt optimum of pol γA, stimulates the polymerase and exonuclease activities, and increases the processivity of the enzyme up to 100 fold *in vitro* (CARRODEGUAS et al. 1999), suggesting

that pol γB, instead of pol γA, could be an important target regulator for mtDNA replication and repair. To answer the question of how they function together will largely depend on the identification of the interaction between the two subunits and how such an interaction helps the catalytic subunit to increase its processivity and stimulates its replication and repair.

In contrast to the conserved sequence of the catalytic subunit, the composition of DNA Pol γB is not that well conserved throughout evolution. First, the pol γB subunit exists only in higher eukaryotes, but not in yeast (WOLF and KOONIN 2001). Interestingly, *S. cerevisiae* pol γ, contains a 200-aa C-terminal extension compared to its human homologue, and has been reported to be highly processive (ERIKSSON *et al.* 1995). However, the DNA polymerase assay used to examine the processivity of *S. cerevisiae* pol γ in Eriksson et al. 1995 is not very convincing. Since they didn't use unlabeled primer-template as competitor, the pol γ that dissociates from the labeled primer-template will be very likely to rebind a labeled molecule and thus the processivity of the enzyme might be over-evaluated. Why nature introduces an additional subunit through evolution only for higher organisms does appear to be an interesting question. Second, besides the difference between multi-cellular and uni-cellular organisms, the number of accessory subunits in the holoenzyme within higher organisms may also not be conserved. The recently solved crystal structure of mouse pol γB supports the formation of a homodimer, while *Drosophila* pol γB lacks the dimerization domain and is suggested to form a 1:1 heterodimer with pol γA in the holoenzyme (CARRODEGUAS *et al.* 2001; FAN and KAGUNI

2001). Why does this difference exist? Currently, there is not a very good answer to this question. The evolutionarily diversified DNA pol γ holoenzyme composition provides a very good experimental system to elucidate the function and evolutionary role of the different subunits. Further comparison of the structure and function of DNA polymerase γ is required to obtain insight into these differences.

III. Structural Analysis of the Pol γ Subunits

A. Structural Analysis of Pol γA: Unlike the accessory subunit, no X-ray crystal structure of a pol γ catalytic subunit exists to date. Most structural information about family A proteins came from *E.coli* DNA polymerase I (OLLIS *et al.* 1985), *Thermus aquaticus* KlenTaq polymerase I (KIM *et al.* 1995; KOROLEV *et al.* 1995), *Bacillus stearothermophilus* DNA pol I (KIEFER *et al.* 1997) and bacteriophage T7 DNA polymerase (DOUBLIE *et al.* 1998), for which crystal structures have been solved. All available structures of DNA polymerases share a common overall architecture of a right hand comprising palm, fingers, and thumb domains, and they all use a two-metal ion catalyzed mechanism for phosphoryl transfer (STEITZ 1999). The three domains of the pol form a deep cleft, with the active site located within the palm domain at the bottom of the cleft. The finger domain includes important interactions with the incoming nucleoside triphosphate as well as the template base to which it is paired, while the thumb domain plays a role in positioning the duplex DNA and in processivity and translocation. Whereas the palm domain is homologous among the A/B/Y pol families, the finger and thumb domains differ substantially in all of the five polymerase families for which representative crystal structures are known, although they share some analogous structural features and function in similar ways.

The crystal structures of family A DNA polymerases revealed a high degree of structural conservation. The interaction between the polymerase and its template-primer DNA has also been revealed in molecular detail by structural determination of binary and

ternary pol:DNA complexes, with and without the incoming nucleotide and in biochemical studies (BEESE *et al.* 1993; EOM *et al.* 1996; KIEFER *et al.* 1998; LI *et al.* 1998). Among the structures of Family A pol, T7 DNA pol distinguishes itself from the bacterial pols by its heterodimeric structure in which the catalytic core forms a complex with an accessory subunit, *E. coli* thioredoxin (DOUBLIE *et al.* 1998) (Fig.1.3). This association makes the holoenzyme an efficient, processive replicative DNA pol, unlike the repair DNA pol, DNA pol I. Based on the available crystal structures of Family A DNA pols and their sequence homology, a structural model of the pol domain of human pol γ was developed (BIENSTOCK and COPELAND 2004; GRAZIEWICZ *et al.* 2004). The model comprises amino acid residues 871 to 1145 of human pol γA which includes all three highly conserved pol motifs. This pol γ active site model provides structural insights into the function of many amino acids in the active site, and has been used to predict the potential effect of disease mutations and incorporation of nucleotide reverse transcriptase inhibitors by pol γ (BIENSTOCK and COPELAND 2004; GRAZIEWICZ *et al.* 2004). While the homology between pol γA and T7 DNA polymerase is sufficient to permit modeling of the polymerase active site as noted above, the primary sequence conservation in other regions is weak. Therefore, it is not feasible to model other regions of pol γA except the polymerase active site in light of the T7 DNA polymerase structure.

Family A DNA polymerases contain an N-terminal exo domain and a C-terminal DNA pol domain. In addition to the highly conserved three exo motifs and three pol motifs shared in all family A pols, pol γ from higher eukaryotes contain six moderately

conserved sequence elements, γ1 to γ6 in the catalytic subunit (Fig.1.2) (KAGUNI 2004), which are not conserved in other members of the Family A group. These subfamily-specific elements were recognized upon the initial cloning of a higher eukaryotic DNA pol γ by Ye and Bogenhagen (1996) (YE *et al.* 1996). Two of these are located near the C-terminal end, and the other four elements lie between the exo and pol domains, in the region termed linker or spacer. This linker region in the pol γ catalytic subunit ranges in length from 337 amino acids in yeast to 482 amino acids in humans, thus much longer than that of other Family A DNA pols as shown in Fig 1.2. In T7 DNA pol, the linker region of 293 amino acids contains a 71 amino acid loop that is part of the thumb domain and enables the interaction with its accessory subunit, *E.coli* thioredoxin (DOUBLIE *et al.* 1998). Although no specific function has been assigned to the spacer region in pol γ, a mutational study by Kaguni and colleagues suggests that the conserved motifs in this region are related to DNA binding, subunit interaction and functional coupling between the pol and exo activities (LUO and KAGUNI 2005). Determination of the crystal structure of pol γA or of the complex formed between pol γA and pol γB will help to understand the function of this region.

B. Structural Analysis of Pol γB: Largely due to the recent crystal structure of mouse DNA polymerase γB (Fig.1.4A) (CARRODEGUAS *et al.* 2001), we currently have more information for the accessory subunit than the catalytic subunit of Polγ. Structural comparison shows that the fold is highly homologous to glycyl-tRNA synthetases, but it

has diverged sufficiently to inactivate the tRNA synthetase activity. The similarity between them might reflect the role of pol γB in RNA primer recognition and binding in mtDNA replication (FAN *et al.* 1999; MURAKAMI *et al.* 2003). DNA binding assays proved that mouse pol γB can bind dsDNA, but in a dimer-dependent manner (CARRODEGUAS *et al.* 2002). Similar to pol γA, the dimeric pol γB binds dsDNA with moderate strength and specificity. The direct DNA binding ability of pol γB makes it different from other processivity factors such as PCNA, the β subunit of *E.coli* pol III and even *E.coli* thioredoxin, the processivity factor of T7 DNA pol. Both PCNA and the β subunit of *E.coli* pol III require additional proteins known as clamp loaders to load them onto DNA in an ATP-dependent manner. Thioredoxin doesn't form direct interactions with DNA in the absence of its catalytic subunit (KELMAN and O'DONNELL 1995). In addition, pol γB does not have a toroidal shape to encircle dsDNA, and the mechanism whereby this protein keeps the catalytic subunit engaged on the template-primer is not known. Using the structure as a guide, several deletion mutants were generated to explore the roles of various domains (Fig.1.4B) (CARRODEGUAS *et al.* 2001). In addition, the ability of pol γB variants to bind pol γA and to stimulate processive synthesis by pol γA has been studied in our lab recently. Mutant I4 with a deletion of the two-helix bundle dimerization motif (see Figure 1.4) abolished dimer formation and its DNA binding activity. It retains some ability to stabilize pol γA on a primer-template, but does not stimulate processive replication *in vitro*. Mutants I6 and I7, designed to remove two solvent exposed loops between domains 1 and 3 (see Figure 1.4), were found to abrogate

dsDNA binding, however, they did not interfere with binding to pol γA or stimulation of processivity. This suggests that DNA binding is not necessary for the action of pol γB as a processivity factor.

A sequence alignment of different pol γB's shows that the C-terminal domain, which is similar to the anti-codon binding part of glycyl-tRNA synthetase, is highly conserved among different species (Fig.1.5), while the N-terminal part of *Drosophila* pol γB, which does not form a dimer *in vivo*, is largely different from its mouse and human homologues. The conservation in the C-terminal part of the protein suggests that this part may be important for the basic function of the accessory subunit and may work more directly together with the relatively conserved catalytic subunit to enhance processivity (CARRODEGUAS and BOGENHAGEN 2000; FAN and KAGUNI 2001). This is further supported by the fact that the small subunits of *Xenopus,* mouse and human pol γ can all stimulate replication of the human catalytic subunit *in vitro* primarily by acting as a processivity factor (CARRODEGUAS *et al.* 1999).

IV. Interactions of the Two Subunits

As mentioned above, regulation of the catalytic subunit between a high processivity form and a low processivity form by the accessory subunit is not well understood. Further clarification requires detailed information on how these two subunits interact with each other. Most of the published data currently available on the interaction of pol γA and pol γB was obtained through *in vitro* biochemical analysis of *Drosophila* pol γ. Fan and Kaguni (2001) (FAN and KAGUNI 2001) mapped an important interaction region within pol γA which includes the N-terminal exo domain and the middle linker region, and in pol γB the central and the C-terminal domain. Experimental data from our lab show that deletions in both the amino terminal and carboxyl terminal regions of pol γB, which are separated in the folded protein, affect binding and/or stimulation of pol γA, suggesting that mammalian pol γB contacts pol γA in more than one region, as Kaguni reported for the *Drosophila* protein (FAN and KAGUNI 2001). Recent mutational studies suggest that the conserved sequences in the spacer region of the catalytic subunit contain sites for interaction with the accessory subunit. A deletion mutagenesis study of the *Drosophila* pol γ catalytic subunit indicated that γ1 and γ4 might participate in subunit interaction (FAN and KAGUNI 2001; LUO and KAGUNI 2005). It has also been found that a human disease mutation is located in the spacer region of human pol γA (A467T) and biochemical studies show that this mutation has lost interaction with the accessory subunit and displays dramatically decreased catalytic activity (CHAN *et al.* 2005; LUOMA *et al.* 2005). Further structural and biochemical analysis of the two subunits is required to

identify the actual binding sites and provide us with more information on how the accessory subunit aids the catalytic subunit in mtDNA replication and repair. For structural and biochemical analysis, sufficient amounts of homogeneous pol γA protein are required. However, available amounts of pol γA were a limiting factor for subsequent studies. A great effort has been taken to improve the overexpression level and purification of human pol γA in insect cells.

Creek Name	HUGO Name	Class	Other Names	Proposed Main Function
α (alpha)	**POLA**	**B**	***POL1***	**DNA replication**
β (beta)	**POLB**	**X**		**Base excision repair**
γ (gamma)	**POLG**	**A**	***MIP1***	**Mitochondrial replication**
δ (delta)	**POLD1**	**B**	***POL3***	**DNA replication**
ε (epsilon)	**POLE**	**B**	***POL2***	**DNA replication**
ζ (zeta)	**POLZ**	**B**	***REV3***	**Translesion synthesis**
η (eta)	**POLH**	**Y**	***RAD30*, XPV**	**Translesion synthesis**
θ (theta)	**POLQ**	**A**	**mus308, eta**	**DNA repair**
ι (iota)	**POLI**	**Y**	**RAD30B**	**Translesion synthesis**
κ (kappa)	**POLK**	**Y**	**DinB1, theta**	**Translesion synthesis**
λ (lambda)	**POLL**	**X**	***POL4*, beta2**	**Base excision repair**
μ (mu)	**POLM**	**X**		**Non-homologous end joining**
σ (sigma)	**POLS**	**X**	***TRF4*, kappa**	**Sister chromatid cohesion**
	REV1L	**Y**	***REV1***	**Translesion synthesis**
	TDT	**X**		**Antigen receptor diversity**

Table 1.1 Eukaryotic DNA polymerases and their proposed main functions.
S. cerevisiae genes (in italics) and conflicting names are listed under "Other Names." (BURGERS *et al.* 2001)

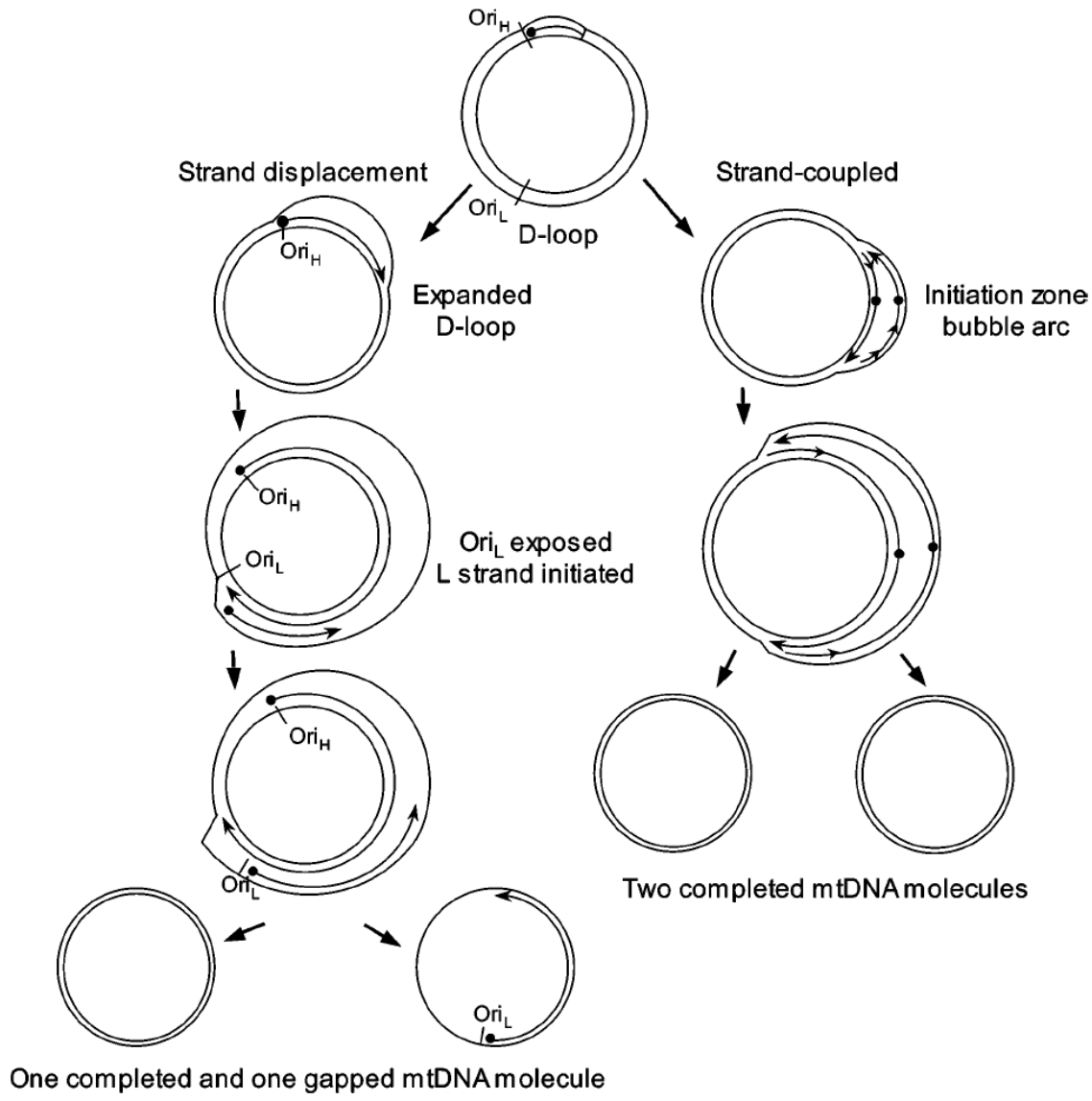

Figure 1.1 Models of mitochondrial DNA replication. The asymmetric or strand displacement model is shown in the left pathway while the strand-coupled model is shown in the right pathway.
Chem. Rev. 2006**,** 106, 383-405

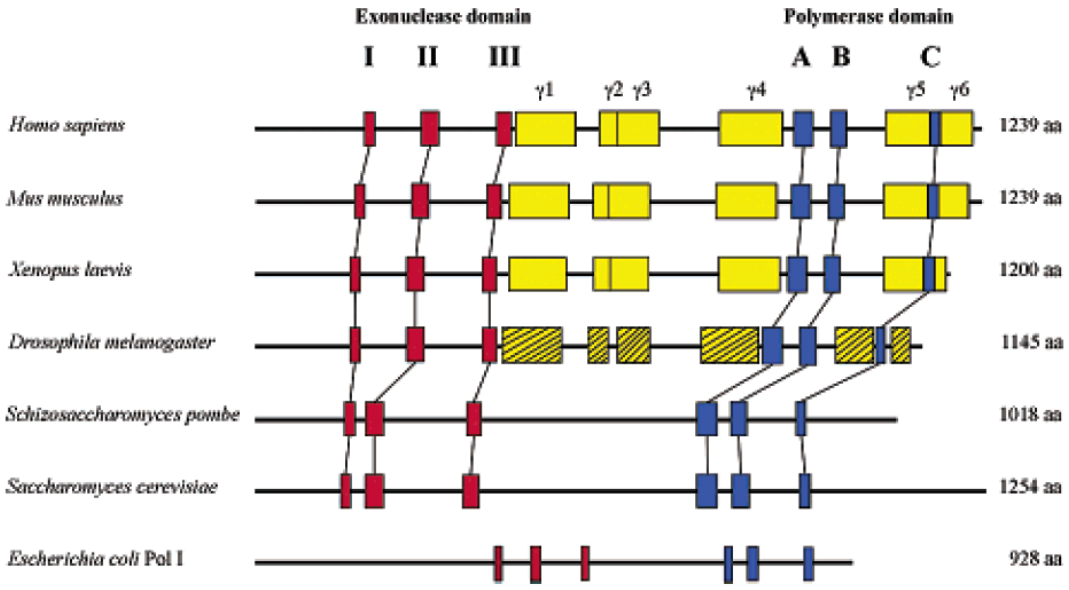

Figure 1.2 Schematic alignment of the pol γ catalytic subunit and family A DNA pols. The conserved 3′-5′ exonuclease domains (*red*) are encoded by the three motifs I, II, and III while the DNA polymerase domains (*blue*) are encoded by the three ABC motifs. *Yellow* boxes indicate DNA polymerase *γ*-specific sequences highly conserved in vertebrates, weakly conserved in insects, and absent in single-cell eukaryotes. The *E. coli* DNA pol I linear organization is included for comparison.
Chem. Rev. 2006**,** 106, 383-405

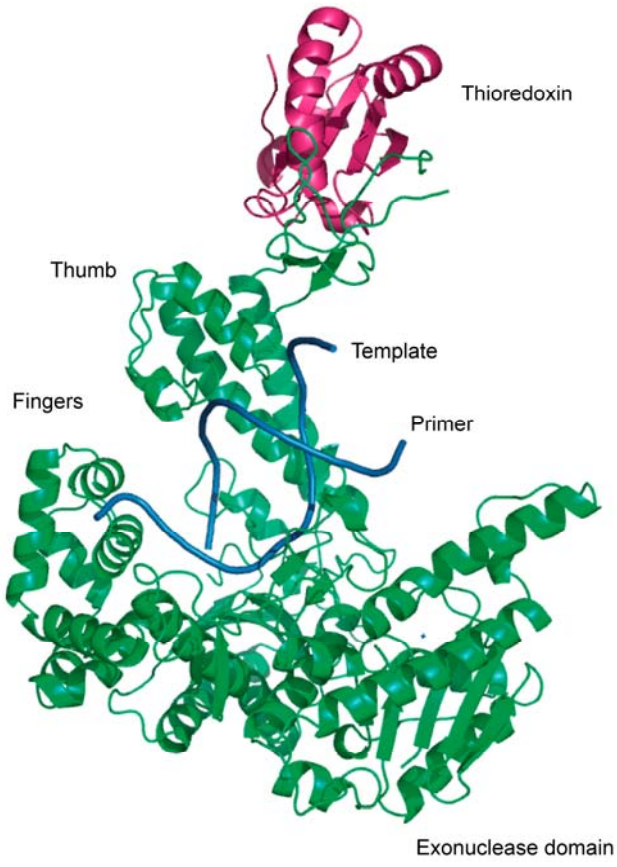

Figure 1.3 Crystal structure of the bacteriophage T7 DNA pol complex with a template-primer and thioredoxin. T7 DNA pol is shown in green and thioredoxin in pink. The template and primer are shown in blue. (PDB code 1T7P)

A

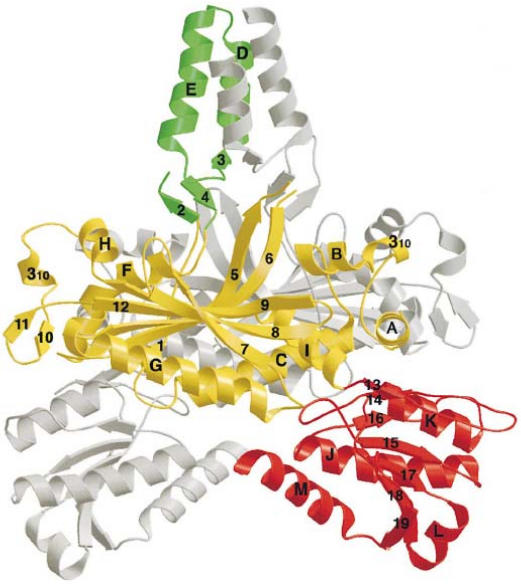

B

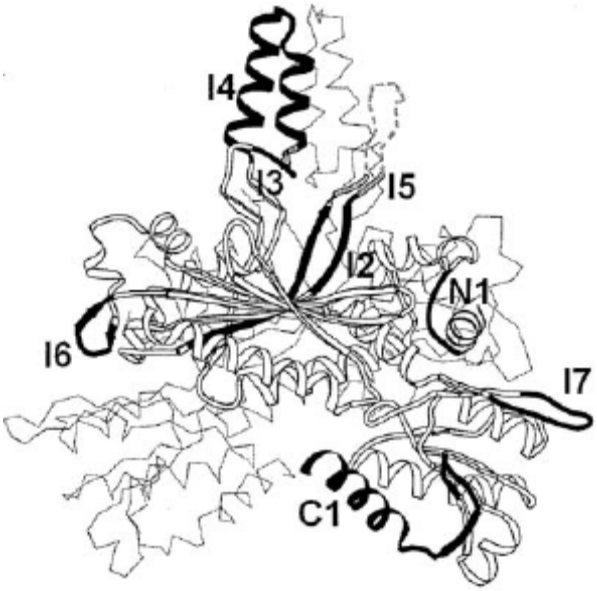

Figure 1.4 Crystal structure of mouse pol γB. ***(A)*** Overall structure of the Pol γB dimer, with one subunit colored by domains and the other in gray. Helices are marked by letters and β-strands are marked by numbers; yellow, green, and red correspond to domains 1, 2, and 3. ***(B)*** Location of characterized deletions in the structure of pol γB. Deletions are shown in black with overlapping regions in gray.
This Figure is reproduced from reference: Carrodeguas, Theis et al. 2001

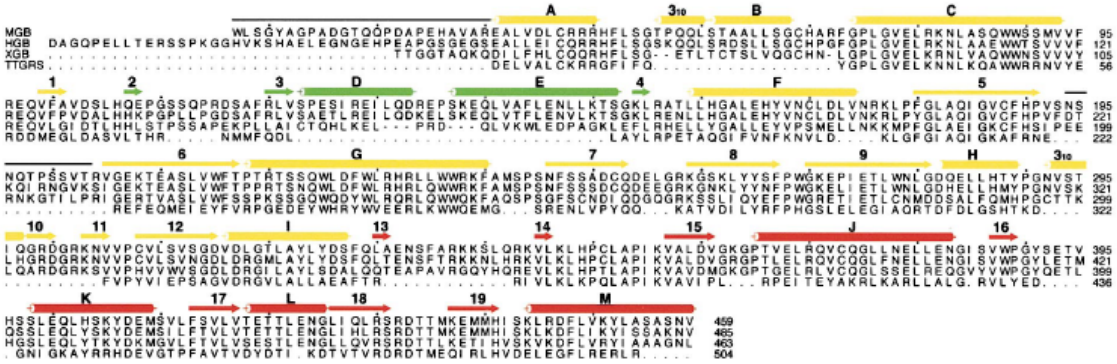

Figure 1.5 Sequence alignment of pol γB from different species and glycyl-tRNA synthetase from *Thermus thermophilus*. Sequence alignment of mouse, human and Xenopus laevis Pol γB (accession numbers AF177202, AF177201, and AF124606) and segments of the *Thermus thermophilus* glycyl-tRNA synthetase (Logan et al., 1995). The secondary structure of Pol γB is indicated above the sequence and colored by domains, cylinders refer to α-helices and arrows to β-strands; yellow, green, and red correspond to domains 1, 2, and 3. β-strands are labeled with numbers, α helices with letters.
This Figure is reproduced from reference: Carrodeguas, Theis et al. 2001

CHAPTER 2: Functional Human Mitochondrial DNA Pol γ Forms a Heterotrimer.

I. Introduction:

Human pol γ is isolated from mitochondria as a complex containing two subunits, a catalytic subunit, pol γA, of 139 kDa and an accessory subunit, pol γB, of 53 kDa. Initial characterization of pol γ suggested that the enzyme forms a heterodimer containing one copy of each subunit (INSDORF and BOGENHAGEN 1989; WERNETTE and KAGUNI 1986). However, when the first crystal structure of mouse pol γB was solved, it became apparent that this accessory factor forms a homodimer with remarkable structural similarity to prokaryotic tRNA synthetases (PDB code 1G5H (CARRODEGUAS *et al.* 2001)). Based on these results it seemed very unlikely that this dimerization is a crystal packing artifact, especially because additional experiments showed that wild-type pol γB sedimented more rapidly than a deletion derivative lacking a major portion of the dimerization interface (CARRODEGUAS *et al.* 2001).

The incorporation of pol γB in the pol γ holoenzyme appears to be a relatively recent event in evolutionary terms. The protein has not been reported in yeast, where pol γ was first cloned as a product of the *mip1* gene (FOURY 1989), and efforts to find evidence for it have been unsuccessful (LUCAS *et al.* 2004). *Drosophila* pol γ differs from the enzyme in vertebrates as it is reported to contain only one subunit each of pol γA and pol γB (OLSON *et al.* 1995; WERNETTE and KAGUNI 1986), because the amino acids required for dimerization of human pol γB are absent in the *Drosophila* ortholog. Thus, pol γ provides an interesting example of a eukaryotic DNA polymerase with variable quaternary structure. A number of publications have speculated that pol γA or pol γB alone may have

roles in mtDNA replication or repair independent of the other subunit (CARRODEGUAS and BOGENHAGEN 2000; JOHNSON *et al.* 2000; LONGLEY *et al.* 2001; LONGLEY *et al.* 1998a). We have therefore undertaken the studies described here to examine the stoichiometry and association kinetics for human pol γA and pol γB by using a range of different methods. Our studies represent the first extensive investigation of the interaction between subunits of human pol γ and show that the native enzyme is a heterotrimer that contains one molecule of the catalytic subunit and two molecules of the processivity factor. The tight binding between the two subunits suggests that the free subunits do not exist *in vivo* and that individual subunits do not play important roles in mitochondrial DNA replication and repair.

In this chapter, a variety of biophysical and functional approaches were used to examine the stoichiometry and association kinetics for human pol γA and pol γB. This work is published in "Elena Yakubovskaya, Zhixin Chen, Jose´ A. Carrodeguas, Caroline Kisker, and Daniel F. Bogenhagen (2006) Functional Human Mitochondrial DNA Polymerase γ Forms a Heterotrimer, *the Jounal of Biological Chemistry, Vol 281:* pp. 374-382". The data described in this chapter have been obtained in a close collaboration between the Bogenhagen laboratory and the Kisker laboratory at Stony Brook University. My contribution to this work is as follows: Purification of proteins, analytical ultracentrifugation experiments and data analysis, analytical size exclusion chromatography and isothermal titration calorimetry experiments and data analysis.

II. Materials and Methods:

A. Purification of Proteins—His-tagged recombinant exo$^-$pol γA was purified from Sf9 cells infected with the pVL1393 baculovirus engineered to express exo$^-$pol γA as described by Longley *et al* (LONGLEY et al. 1998c). Cells were grown in suspension culture in JRH Excell 420 culture medium supplemented with 2.5% fetal calf serum and 100 IU penicillin plus 100 μg/ml streptomycin. 5-Liter batches of cells were harvested on the 4th day of infection yielding 40 g of cells. The 40 g cells were lysed by sonication in 150 ml of Buffer I (20 mM Hepes, pH 8.0, 5% glycerol, 1 mM EDTA, 5 mM 2-mercaptoethanol, 0.2 mM PMSF, 1 μg/ml pepstatin A, 5 μg/ml leupeptin) with 0.3 M KCl and 0.1% Triton X-100. The lysate was centrifuged at 96,000 *g* for 1 h at 4 °C. The supernatant was treated with 0.04% polyethyleneimine and centrifuged for 30 min at 96,000 *g* to remove the DNA. The lysate was adjusted to contain 60 mM imidazole and 5 mM $MgCl_2$ and loaded onto Ni-IDA HisTrap resin (Amersham Biosciences) equilibrated in Buffer II (20mM Hepes, pH 8.0, 5% glycerol, 0.2 mM PMSF, 1 μg/ml pepstatin A, 5 μg/ml leupeptin) with 0.2 M KCl and 50 mM imidazole. After washing with 10 column volumes of Buffer II, the protein was eluted with a linear gradient of imidazole (0.05–1 M) in Buffer II with 0.1 M KCl. Fractions of the eluate containing pol γA were diluted with Buffer I to adjust the conductivity to below 0.1 M KCl. The enzyme was applied to a 1.0-ml HR 5/5 Mono S column (Amersham Biosciences) equilibrated in Buffer I with 0.08 M KCl. After washing with 5 column volumes, the protein was eluted with a 15-column volume linear gradient of 0.08 to 0.7 M KCl in Buffer I. Fractions containing

peak absorbance at 280 nm were loaded onto a Hiload 16/60 Superdex 200 size exclusion column (Amersham Biosciences) equilibrated in Buffer I containing 0.3 M KCl. The exo$^-$ pol γA eluted from this column at 62 ml. All chromatographic steps were performed at 4 °C. The enzyme was concentrated to 1mg/ml using a 100,000*M*r Vivaspin ultrafiltration device. The yield of the protein was about 0.7 mg/liter culture.

The His-tagged recombinant pol γB and pol γBΔI4 mutant proteins were expressed in *Escherichia coli* BL21 RIL codon plus cells (Novagen) transfected with plasmid pET22b+ constructs as described by Carrodeguas *et al.* (CARRODEGUAS et al. 2001) When proteins were prepared without a His tag, the construct was modified by introducing a stop codon at the NotI restriction site of the pET22b+ vector. Pellets from 2 liters of bacterial culture expressing pol γB were suspended in 40 ml of Buffer I with 0.3 M KCl and 0.1% Triton X-100, and cells were lysed in a French press. The lysate was centrifuged at 16,000 *g* for 30 min at 4 °C. The supernatant was treated with 0.14% polyethyleneimine and centrifuged using the same conditions to remove the DNA. The lysate was adjusted to contain 50 mM imidazole and 5 mM $MgCl_2$, and the protein was purified by nickel affinity, cation exchange, and size exclusion chromatography as described for pol γA above. The enzyme was concentrated to 16 mg/ml using a 30,000*M*r Centricon ultrafiltration device. The yields of pol γB and polγBΔI4 proteins were about 2 and 8 mg/liter culture, respectively.

Reconstituted pol γ holoenzyme was prepared by mixing 1 volume of Sf9 lysate containing His-tagged exo$^-$ pol γA and 0.7 volume *E. coli* lysate containing recombinant

pol γB without a His tag. The relative volumes used for this reconstitution varied somewhat from one preparation to another based on the specific protein concentrations of the lysates as assessed by SDS-PAGE. The lysates were mixed for 30 min at 4 °C on a rotator and adjusted to contain 60 mM imidazole and 5 mM $MgCl_2$. The holoenzyme was purified and concentrated using the same protocol as for pol γA. The extinction coefficients used to determine the protein concentration were calculated following Gill and von Hippel (Gill and von Hippel 1989). The ε280 for pol γA was 243,790 *A*280/M and that used for both WT pol γB and pol γBΔI4 was 71,940 *A*280/M, because the deletion did not remove any residues that contribute to the absorption at 280 nm. The absorbance measurements were routinely made on native protein preparations and were blanked against the dialysate used in preparing the protein. Controls indicated that absorbances at 280 nm were identical within 3% when the proteins were denatured with guanidine hydrochloride.

B. Analytical Ultracentrifugation—Sedimentation equilibrium experiments were conducted using a Beckman XL-I Optima analytical ultracentrifuge and a Ti-60a rotor. Six-channel, charcoal-filled Epon center-pieces with quartz windows were filled with 100 μl of sample (in 20 mM Hepes, pH 8.0, 300 mM KCl, 1mM EDTA, 2mM β-mercaptoethanol, 5% glycerol) at protein concentrations between 1.88 and 5.64 μM. Absorbance profiles were acquired at 280 nm. Sedimentation equilibrium studies were performed at 4°C, using three different velocities (15,000, 18,000, and 22,000 rpm for

wild-type pol γB and 20,000, 25,000, and 30,000 rpm for pol γBΔI4). The data were analyzed by two programs, Heteroanalysis (National Analytical Ultracentrifugation Facility at the University of Connecticut) and the XL-A/XL-I data analysis software (Beckman), and consistent results were obtained. Solvent density was calculated as 1.026 (Sednterp software (LEBOWITZ *et al.* 2002)), and the partial specific volumes of the proteins were approximated from their amino acid compositions (0.7299 for wild-type pol γB and 0.7283 for pol γBΔI4) (Sednterp).

C. Surface Plasmon Resonance—Surface plasmon resonance (SPR) to analyze binding kinetics was performedon a Biacore 2000 instrument (Biacore AB, Uppsala, Sweden) at 25°C. Pol γA was immobilized on a Sensor Chip S CM5 using the amine coupling kit (Biacore AB) in 10 mM phosphate buffer, pH 6.0, with immobilization levels of 1400 resonance units (RU). Analytes (WT pol γB and pol γBΔI4) were injected at concentrations ranging from 0 to 320 nM over the sensor chip with immobilized pol γA for 3 min followed by 8 min of dissociation and 10 s of regeneration using 3mM NaOH, 1 mM KCl. Mass transfer and linked reaction experiments were performed. The kinetics of pol γB and pol γBΔI4 interaction with immobilized pol γA were evaluated using alternative predefined models in the BIAevaluation 4.1 software (Biacore AB). A model was judged appropriate if it fit to every experiment with $\chi^2 < 1.5$. The conformational change model assumes a two-state reaction, where analyte B binds to ligand A followed by a conformational change of the complex AB to AB^*. The overall dissociation constant

K_D is calculated from the rate constants as follows: $K_D = 1/(k_{a1}/k_{a2} \times (1 + k_{a2}/k_{d2}))$. For stoichiometry determinations, a sensor Chip S CM5 with immobilization levels of pol γA at 600 RU was used. Analytes (pol γB and pol γBΔI4) were injected at increasing concentrations (from 50 to 500 nM) over immobilized pol γA for 5 min followed by 8 min of dissociation and 10 s of regeneration using 3 mM NaOH, 1 mM KCl. When the saturated concentration was achieved, R_{max} values for pol γB (420 RU) and pol γBΔI4 (217 RU) were measured, and the stoichiometry was calculated based on the equation: $Sn = (M_{r(pol\ \gamma A)}/M_{r(pol\ \gamma B)}) \times R_{max}/RL$, where RL is the resonance signal at a given ligand concentration. The affinity of the enzymes for DNA was investigated using the streptavidin-coated sensor chip (SA chip; Biacore). A solution (2 nM) of a 5'-biotinylated oligonucleotide (5'-BioTEG) 26:45-mer (Qiagen) in HBS-EP BIAcore buffer was used to yield an increase of 10 RU (1 min) on flow cell 1 and 150 RU (10 min) on flow cell 2. Two other flow cells without an oligonucleotide were used as reference cells. After immobilization, running buffer with low salt was used (30 mM KCl, 0.005% surfactant P20, 10 mM Hepes, pH 7.4). To compare the affinity of enzymes for DNA at different salt concentrations, 50 nM analytes (pol γA, pol γAB_2, and pol γABΔI4) in buffers with different ionic strengths (30-200 mM for KCl and 1-40 mM for $MgCl_2$) were injected over immobilized oligonucleotide for 8min followed by 30 s of regeneration using 1 M KCl. In experiments with varied $MgCl_2$ concentration, 30 mM KCl was used.

D. Isothermal Titration Calorimetry—Isothermal titration calorimetry (ITC) experiments

were performed with a VP-ITC calorimeter (Micro-cal) at 25°C with a mixing speed of 302 rpm. The WT pol γB (160 μM) or pol γBΔI4 (130 μM) proteins were titrated as 5-μl injections (first injection 2 μl) into the sample cell containing 7.2 μM exo$^-$ pol γA. Samples were prepared by dialyzing all interacting components extensively against a buffer containing 20 mM Hepes, pH 8.0, 300 mM KCl, 5% glycerol, 1 mM EDTA, 5 mM 2-mercaptoethanol, 0.2 mM PMSF, 1 μg/ml pepstatin A, 5 μg/ml leupeptin. The heats of dilution of both proteins with buffer were determined and subtracted prior to analysis. Data were analyzed using the ORIGIN software supplied with the instrument according to the one- and two-binding sites models.

E. Electrophoretic Mobility Shift Assays—Native gel electrophoretic mobility shift assays (EMSA) were conducted as described (CARRODEGUAS *et al.* 2001) using the 26:45-mer primer-template labeled on the 5' end of the 45-mer (CARRODEGUAS and BOGENHAGEN 2000), except that the assays were conducted as challenge assays to assess the stability of the DNA-protein complexes. Binding reactions were assembled in 30 μl containing 4 nM labeled primer-template, 4 nM pol γA, and where indicated, 8 nM pol γB or pol γBΔI4 (both forms of pol γB calculated as a monomer). Binding reactions continued for 10 min. At this time 4 μl were removed as a binding control, and 3 μl of 200 nM cold 26:45-mer were added as a competitor to bind any protein that dissociated from the labeled complex. A second 4-μl sample was removed within 10 s after the competitor was mixed into the reaction and was considered a 0.2-min time point during the time series. The binding

control and 0.2-min sample were loaded directly into the lanes of a running native gel. Additional 4-μl samples were removed at 1,2,4,8, 16, and in some cases 32 min after addition of the competitor. Following electrophoresis, gels were dried onto Whatman DE81 paper and exposed to a PhosphorImager to quantify the radioactivity of bound and free DNA.

F. DNA Polymerase Assays—DNA polymerase assays were performed as described (CARRODEGUAS *et al.* 1999) with 0.2 pmol of pol γA and varied amounts of pol γB or pol γBΔI4 in 30-μl reactions using either 120 μg/ml activated calf thymus DNA or 10 μg/ml poly(dA)-oligo(dT) as template. The standard polymerase reaction buffer was 50 mM KCl, 8 mM $MgCl_2$, 10 mM Tris, pH 8, 2 mM dithiothreitol, 100 μg/ml bovine serum albumin. Where indicated, reactions contained 140 mM KCl. Primer-extention processivity experiments were performed as described by Carrodeguas et al. (CARRODEGUAS *et al.* 1999) and in the legend of Fig. 2.9.

III. Results:

A. High Level Expression of Both Subunits of Human pol γ and Reconstitution of the Holoenzyme—We and others have been unable to express pol γA in bacteria in an intact form. To obtain quantities of recombinant enzyme sufficient for biophysical studies, we expressed the protein in insect cells from a baculovirus construct. Although it is possible to express the holoenzyme entirely in insect cells by co-expressing the A and B subunits, we chose to express the B subunit in bacteria using the T7 system. This permits us to test the activity of a number of pol γB variants without making an independent baculovirus construct for each protein of interest. In this study, we compared the binding of wild-type pol γB to a deletion derivative that we refer to as pol γBΔI4. This derivative, which contains a glycine residue in place of residues 147–178 of pol γB, was first reported by Carrodeguas et al. (CARRODEGUAS *et al.* 2001) to test the role of the four-helix bundle observed in the dimer of the mouse pol γB crystal structure in dimerization. This derivative has some ability to bind to primer-templates along with pol γA but has little ability to stimulate activity of the catalytic subunit. Thus, we set out to compare the association of wild-type pol γB and pol γBΔI4 to pol γA in this study.

Mixing a lysate of insect cells containing His-tagged pol γA with a lysate of bacterial cells expressing nontagged pol γB permits association of the subunits and purification of pol γ holoenzyme using a three-step procedure. As described under "Materials and Methods", this procedure consists of an affinity chromatography on a Ni-IDA (His-trap®) resin followed by ion exchange and size exclusion chromatography. In a typical

preparation beginning with 21 g of SF9 cells expressing pol γA and 15 g of BL21 cells expressing pol γB, we obtained a final yield of ~4.5 mg of pol γ holoenzyme. Pol γA is prepared similarly without the addition of pol γB. These procedures have provided a sufficient quantity of enzyme for the biophysical studies analysing the association of the polymerase subunits reported here. The purity of typical protein preparations is shown in Fig. 2.1. It is apparent that the amount of the small subunit bound to pol γA is diminished by approximately half when the reconstitution is performed with pol γBΔI4 rather than with wild-type pol γB.

We previously compared the sedimentation properties of pol γB and pol γBΔI4 by velocity sedimentation in glycerol gradients using a preparative ultracentrifuge (CARRODEGUAS *et al.* 2001). We characterized these proteins in more detail by equilibrium ultracentrifugation as shown in Fig. 2.2. For wild-type pol γB, sedimentation equilibrium distributions were fit to a single species. When the molar mass was treated as the unknown parameter in the global analysis, an average molecular mass of 105,747 Da was obtained (compared with the expected molecular mass of 106,916 Da for dimeric pol γB). Attempts to fit the data to a self-association model failed to yield better results. This is consistent with other data suggesting that the wild-type protein is a tightly bound homodimer with effectively no monomer present under these conditions. We estimated that the pol γB dimer association is characterized by a K_D somewhat tighter than 0.1 nM. In contrast, analysis of the data for the I4 mutant was complex. When the data were analyzed using a single component model the apparent molecular mass calculated by the

software was 70 kDa, a value intermediate between a monomer and a dimer. Moreover, the residuals indicated that the single-component model was a poor fit to the data (data not shown). A better fit was obtained using a self-association model for a monomer-dimer equilibrium. The fitted monomer molecular mass was 48,370 Da, and the dissociation constant (K_D) was 5.8 μM. The fact that pol γBΔI4 retains a weak ability to dimerize is consistent with the inference drawn from the crystal structure of mouse pol γB. In this model, we estimated that domain 2, which is deleted in pol γBΔI4, contributes 2675 $Å^2$ to the total dimerization interface of 6850 $Å^2$. Thus, it is reasonable that pol γBΔI4 retains a weak ability to dimerize at high protein concentrations but behaves as a monomer at protein concentrations significantly below the K_D value, as in most *in vivo* or *in vitro* reactions involving pol γ.

Because the final step in our purification is a high resolution size exclusion step, we applied this as an analytical method to study the stoichiometry of the holoenzyme. Fig. 2.3 shows the results of a titration in which known molar quantities of pol γA and pol γB, as determined using the calculated extinction coefficients, were applied to a 60-cm Amersham Biosciences Superdex 200 size exclusion column. The elution profiles of free pol γA and pol γB are shown in the background of each panel. All added pol γB was bound to pol γA until saturation was reached at a 1:2 molar ratio of A to B. As the quantity of pol γB was further increased, a peak of excess free pol γB was apparent. This is consistent with the crystallographic finding that pol γB is a dimer. A similar binding titration performed with pol γA and pol γBΔI4 showed saturation at a ratio of 1:1 (data

not shown).

B. Isothermal Titration Calorimetry Confirms the 1:2 Stoichiometry of A and B Subunits and Estimates the Affinity of the Interaction—Isothermal titration calorimetry (ITC) was used to measure the enthalpy of holoenzyme formation, stoichiometry of the complex, and the dissociation constant. The ionic strength of the reaction buffer was chosen based on dynamic light scattering data, which demonstrated that aggregation was minimal under these conditions (data not shown). ITC was performed in parallel with both wild-type pol γB and pol γBΔI4 (Fig. 2.4). K_D values for complexes of native pol γB and pol γBΔI4 subunits with pol γA (Table 2.1) were similar and within experimental error. A 2-fold difference in stoichiometry of the complexes formed by WT pol γB or the pol γBΔI4 mutant in binding to pol γA was observed, which is a logical consequence of the proposed monomeric nature of the I4 mutant. These results, along with our size exclusion chromatography data (Fig. 2.3), confirm that the stoichiometry of the complex between pol γA and WT pol γB is 1:2. The interaction of pol γA with the pol γB dimer is characterized as an exothermic process with ΔH of -6.4 kcal/mol and a K_D of ~0.15 μM. Association of pol γA with the monomeric pol γBΔI4 mutant protein is nearly as tight as with the wild-type protein. Because this experiment was performed under stoichiometric binding conditions, *i.e.* with a pol γA concentration (7 μM) in excess of the K_D value, we considered that this experiment overestimates the K_D for the interaction between the subunits.

C. Surface Plasmon Resonance Analysis of the pol γA-pol γB Interaction— SPR analysis was employed to study the interaction of pol γA with either pol γB or pol γBΔI4 in real time. Pol γA was injected onto the activated sensor chip surface to immobilize the protein to the carboxymethyl-activated dextran to the extent of 1400 resonance units (RU), corresponding to ~1.4 ng/mm^2 of covalently linked protein. According to mass transfer tests, the influence of diffusion on binding of pol γB to pol γA was negligible under our experimental conditions. Baseline drifts due to covalent linkage ruptures between the immobilized pol γA and the dextran matrix were also minimal for at least 10 consecutive ligand injections.

Typical association and dissociation curves characterizing the interaction of pol γB with pol γA are shown in Fig. 2.5*A*. Association and dissociation rate constants were obtained using curve fitting as implemented in the BIAevaluation software version 3.0. Because standard Langmuir kinetics modeling resulted in a poor fit (χ^2>20), a two-state reaction model was used, which led to considerably better results. Kinetic and equilibrium constants obtained as well as fitting details are summarized in Table 2.2. Similar experiments with the I4 mutant, which is unable to form a dimer at these low protein concentrations, demonstrated similar association and dissociation kinetics (Fig. 2.5*B*). The overall dissociation constant for the WT protein is 27 nM. The association between pol γBΔI4 and pol γA is weaker by approximately a factor of 2. These measurements are comparable with the apparent K_D of 35 nM for the pol γB-pol γA interaction estimated from polymerase stimulation kinetics by Johnson et al. (JOHNSON *et*

al. 2000).

D. The I4 Mutant Stabilizes the Interaction of pol γA with Primer-Template DNA Nearly as Well as Wild-type pol γB—We were surprised at the relatively small difference in affinity of pol γA for binding pol γBΔI4 as compared with the wild-type subunit. Therefore, we conducted experiments to examine the relative ability of these proteins to stabilize the interaction of pol γA with DNA primer-templates. One of the standard methods used to study DNA polymerases is to characterize their interactions with oligonucleotide primer-templates, often using an electrophoretic mobility shift assay. We have used this assay in the past to study the interaction of pol γB mutants with pol γA in primer-template complexes (CARRODEGUAS and BOGENHAGEN 2000; CARRODEGUAS *et al.* 1999; CARRODEGUAS *et al.* 2001). We have shown that the I4 mutant participates with pol γA in binding primer-template, but we have not studied previously the stability of this interaction. We therefore designed a binding challenge assay in which complexes containing different forms of pol γ bound to radio-labeled primer-template were assembled and then challenged with a large excess of cold primer-template to follow the kinetics of dissociation. Following addition of a 50-fold excess of cold primer-template, any polymerase released from the labeled complex would be much more likely to bind the unlabeled competitor than the original radio-labeled oligonucleotide. The kinetics of the dissociation reaction can be followed by withdrawing aliquots from the reaction at various times after addition of competitor and loading them directly on a running native

gel. Similar use of EMSA to study dissociation kinetics has been employed since the initial development of this method (FRIED and CROTHERS 1981). Fig. 2.6*A* shows that pol γA alone dissociates quickly from a 26:45 primer-template. The pol γAB2 holoenzyme complex migrates more slowly on the native gel, as expected, and shows considerable stabilization, with a half-life of almost 2 min (Fig. 2.6*B*). A parallel EMSA challenge assay performed with pol γ reconstituted with the I4 mutant protein revealed that this complex was almost as stable as that formed with wild-type pol γB (Fig. 2.6*C*).

One limitation of the EMSA to study nucleic acid-protein interactions is that this method provides little ability to vary solution conditions because ions in the reaction buffer are quickly separated from macromolecules as complexes enter the gel. We used SPR to study the primer-template binding of pol γA alone and complexes of pol γA with either wild-type pol γB or pol γBΔI4 at varied concentrations of monovalent and divalent ions (Fig. 2.7). Each curve in Fig. 2.7 represents the results of 10 titration experiments conducted at varied KCl or $MgCl_2$ concentrations to determine the maximal amount of protein bound to the biotinylated 26:45-mer oligonucleotide immobilized on a streptavidin chip. The data are normalized to the maximum resonance signal obtained at low ionic strength. As expected, high concentrations of KCl or $MgCl_2$ destabilized the binding of pol γA to the oligonucleotide, whereas the presence of wild-type pol γB in the pol γ holoenzyme significantly stabilized the binding of the polymerase to DNA. Pol γBΔI4 provided an intermediate level of stabilization.

The foregoing results showing that pol γBΔI4 binds pol γA with high affinity and

stabilizes the polymerase on primer-template oligonucleotides were somewhat surprising in light of our previous work showing that this monomeric derivative had very limited ability to stimulate DNA synthesis by pol γA (CARRODEGUAS *et al.* 2001). Previous polymerase reactions with this mutant used only low quantities of pol γBΔI4, <400 fmol, and used only poly(dA)-oligo(dT) as the primer-template. Therefore, we reinvestigated the ability of this derivative relative to wild-type pol γB to stimulate pol γA activity at higher protein concentrations and on heteropolymeric DNA as well as the synthetic homopolymer. As can be seen in Fig. 2.8*A*, in reactions using 0.2 pmol of pol γA (6.7 nM) and a poly (dA)-oligo (dT) primer-template, DNA synthesis is maximally stimulated by 1 pmol of pol γB (0.5 pmol of B_2 dimer; 16 nM). Significantly higher concentrations of pol γBΔI4 were required to stimulate pol γA, and the maximal activity obtained was ~50% compared with wild-type pol γB. This reduced ability to stimulate pol γA was observed when activated DNA was used as substrate as well, but a dependence on pol γB was only seen at elevated KCl concentrations, as reported previously (CARRODEGUAS *et al.* 1999; LIM *et al.* 1999) (Fig. 2.8*B*). Although the monomeric pol γBΔI4 did retain some ability to stimulate pol γA, the overall reaction rate was always diminished.

We performed single-round primer-extension reactions (Fig. 2.9) to study polymerase processivity in greater detail. Pol γ was pre-incubated with a primer-template consisting of 5'-^{32}P-oligo(dT_{16})-poly(dA). Extension of primers bound by pol γ was initiated by addition of TTP mixed with a nonradioactive primer-template to serve as a binding competitor to trap polymerase molecules that dissociated from the radioactive primers.

This 26:45-mer oligonucleotide would require dATP as the first incoming nucleotide and is incapable of supporting polymerization with only TTP. *Lanes 5* and *6* of Fig. 2.9 show that wild-type pol γ extended primers to products as long as 200–300 nucleotides (median extension about 60–80 nucleotides) before dissociation within the first 1.5 min. The size range of products did not continue to increase when the reaction time was doubled. These results and the controls in *lanes 7* and *8* of Fig. 2.9 indicate that the oligonucleotide competitor provided an effective trap to prevent re-utilization of labeled primers. Thus, we conclude that the distribution of product lengths shown in *lanes 5* and *6* of Fig. 2.9 represent the products synthesized following a single polymerase binding event. When pol γABΔI4 was used in parallel reactions, the primers were typically extended by fewer than 40 nucleotides, indicating that the monomeric pol γBΔI4 was greatly impaired as a processivity factor. Virtually no extension of the primer was seen using pol γA alone.

IV. Discussion

A. pol γ Holoenzyme Subunit Stoichiometry—This is the first extensive investigation of the assembly of the pol γ holoenzyme. Our sedimentation equilibrium data show that pol γB forms a dimer in solution, while analytical gel filtration and isothermal titration calorimetry establish that the pol γB dimer binds tightly to the pol γA monomer to form a heterotrimer with the structure AB_2. We performed the first detailed study of the association of these subunits in the absence of DNA. Interestingly, the K_D of 27 nM for the subunit interaction, determined by SPR, agrees well with the binding affinity measured in the presence of DNA in the enzyme kinetic studies of Johnson *et al* (JOHNSON et al. 2000). The recombinant pol γAB_2 complex would have a calculated mass of 245 kDa. This appears to be somewhat larger than the estimated 194 kDa of the polymerase isolated from mitochondria (GRAY and WONG 1992; LIM *et al.* 1999). We cannot rigorously rule out the possibility that differences in post-translational modification of the recombinant polypeptides or their inclusion of His tags may influence the higher order structure of the polymerase. However, considering the high biological activity of the recombinant enzyme, we think it is more likely that the smaller apparent size of the enzyme purified from mitochondria may be due to the fact that the hydrodynamic measurements in these studies used much lower protein concentrations. It is possible that the holoenzyme may be in equilibrium with A and B_2 subunits during overnight glycerol gradient sedimentation of dilute protein samples, leading to an underestimate of the sedimentation coefficient.

Unfortunately, there is currently no way to estimate the concentrations of polymerase subunits in mitochondria. The interaction between the pol γA and B_2 subunits is probably sufficiently tight to prevent frequent dissociation of the holoenzyme to the free subunits *in vivo*. Our previous experiments revealed no excess of free pol γA or pol γB subunits when the holoenzyme was purified from crude mitochondrial lysates (CARRODEGUAS and BOGENHAGEN 2000; CARRODEGUAS *et al.* 1999). Therefore, we think it unlikely that models for the role of pol γ in mtDNA replication and repair should consider any independent roles for the pol γ subunits under most circumstances. An exception to this generalization derives from the fact that these two subunits are synthesized and imported into mitochondria separately. Very little is known about the kinetic process by which single subunits are assembled into a holoenzyme in the organelle. Although we cannot rule out the possibility that single subunits may be free to engage in nucleic acid binding, no pool of free subunits has been documented.

We also compared the behavior of wild-type pol γB with that of a mutant form designated I4 that lacks a two-helix bundle domain important for dimerization. Analytical ultracentrifugation experiments showed that dimerization of this mutant protein is markedly impaired, with an apparent K_D of 5–14 μM for the monomer-dimer equilibrium. Nevertheless, pol γBΔI4 retains the ability to bind to pol γA in a 1:1 complex with an affinity comparable with that of the wild-type pol γB dimer. Despite the difference in stoichiometry, both complexes are formed with nearly the same ΔG^0 (see Table 2.1). This implies that most of the interactions that pol γA forms with pol γB are preserved when it

binds pol γBΔI4. As has been suggested for the *Drosophila* pol γ subunits, it is likely that human pol γA and pol γB share an extensive interaction interface (FAN and KAGUNI 2001). One simple model for the structure of the holoenzyme might propose that a dimeric pol γB may provide two identical interfaces for the interaction with pol γA. Such a model would be consistent with the assembly of an A_2B_2 tetramer. This structure, however, is not compatible with our results, which clearly indicate the formation of a heterotrimeric complex. We suggest an asymmetrical model for the interaction between pol γA and pol γB. According to this model, pol γA mainly interacts with one pol γB subunit in the pol γB dimer, but this interaction sterically inhibits interaction of a second catalytic subunit with the other pol γB subunit. When pol γA binds to the pol γBΔI4 mutant it is possible that pol γA forms additional contacts with pol γB surfaces that are exposed in the monomeric pol γBΔI4 permitting binding of this complex to primer-template but inhibiting polymerization. Both models are consistent with our data, and it will be extremely interesting to obtain a crystal structure of the pol γ holoenzyme to understand how this unusual processivity factor functions to stimulate the catalytic subunit.

B. Influence of pol γB on pol γA DNA Binding and Polymerase Activity—We have taken advantage of the contrast between wild-type pol γB and pol γBΔI4 to explore the contribution of the accessory subunit to the interaction of the polymerase with DNA primer-templates. Through electrophoretic mobility shift assays and SPR experiments,

we showed that the heterodimeric enzyme formed by association of pol γBΔI4 to pol γA binds tightly to primer-template and dissociates slowly in the presence of competitor primer-template. The apparent K_D value for the binding of wild-type holoenzyme to a 26:45-mer oligonucleotide at 30 mM KCl is 0.06 nM, although pol γA and the pol γA-pol γBΔI4 complex bind the same substrate with K_D values of 0.6 and 0.4 nM, respectively. These binding affinities are considerably tighter than those reported by Johnson *et al.* (JOHNSON et al. 2000) based on polymerase kinetic measurements made at a higher salt concentration, 100 mM NaCl. Several labs have shown that activity of pol γA is reduced at high salt but is stimulated by pol γB (CARRODEGUAS *et al.* 1999; LIM *et al.* 1999). Our SPR experiments show both pol γB and pol γBΔI4 dramatically stabilize binding of pol γA to primer-template at higher salt concentrations (Fig. 2.7). Like other DNA-binding proteins, pol γA presumably displaces cations upon binding to DNA (RECORD *et al.* 1977). pol γB and, to a lesser extent, pol γBΔI4 appear to modify the interaction of pol γA with DNA to enable it to resist competition by free cations.

Although pol γB clearly increases the processivity of pol γA, it affects other activities of the catalytic subunit as well. Johnson *et al.* (JOHNSON et al. 2000) have shown that the accessory subunit decreases the K_m value for binding nucleotides and increases the polymerization rate, although Longley *et al.* (LONGLEY et al. 2001) have demonstrated that these effects result in decreased polymerase fidelity. Our biophysical studies comparing the interaction of pol γB and pol γBΔI4 with pol γA have not directly addressed the influence of these proteins on kinetic parameters of polymerase function.

However, we note that the tight binding of pol γBΔI4 to pol γA and the consequent stabilization of the enzyme on primer-templates does not lead to stimulation of polymerase activity (Figs. 2.8 and 2.9). Indeed, the monomeric pol γBΔI4 may have a weak ability to act as a dominant negative form of pol γB, because it competes well for binding to pol γA but is very ineffective in stimulating polymerization.

C. Comparison of pol γB to Other Processivity Factors—The available data suggest that the interaction between pol γB and pol γA is structurally distinct compared to that of most other pairs of processivity factors with their cognate polymerases. Pol γB is structurally unlike any of the sliding clamp processivity factors such as proliferating cell nuclear antigen, *E. coli* pol III β, and T4 phage glycoprotein 45 that stabilize polymerase binding to DNA by encircling the DNA duplex (KRISHNA *et al.* 1994). In these examples, as well as in the binding of thioredoxin to T7 phage DNA polymerase, the interaction of the accessory subunit with the polymerase is mainly mediated by a small interface that can be delimited to a peptide domain (BEDFORD *et al.* 1997; DOUBLIE *et al.* 1998). This is also true for cytomegalovirus UL44 (APPLETON *et al.* 2004; LOREGIAN *et al.* 2004) and herpes simplex virus UL42 (ZUCCOLA *et al.* 2000) proteins that do not form complete toroidal rings. Breyer and Mathews (BREYER and MATTHEWS 2001) have suggested that processivity can be conferred in either of two ways, by topological linkage, as illustrated by sliding clamps, or through the involvement of a large interaction surface. We suggest that pol γ may exemplify this latter category.

As noted in the Introduction, pol γ provides a unique example of an essential DNA polymerase that has a variable structure in different organisms. The obvious relationship between mammalian pol γB and homodimeric prokaryotic tRNA synthetases (CARRODEGUAS *et al.* 2001) has been cited as an illustration of horizontal gene transfer during evolution (WOLF and KOONIN 2001). An exceptional contrast is provided by *Drosophila* pol γ, which is a heterodimer containing one copy each of the A and B subunits (KAGUNI 2004; OLSON *et al.* 1995). Although *Drosophila* pol γB shares only 15% sequence identity with human pol γB, the only significant internal deletion in the alignment of the two proteins suggests that the *Drosophila* protein contains a discrete deletion of domain 2 of the mammalian proteins containing the two-helix structure, a deletion similar to that used to generate human pol γBΔI4. We suggest that the *Drosophila* protein may have experienced a deletion of this domain during evolution from a common ancestor with the mammalian lineage. Our observation that pol γBΔI4 is able to stabilize pol γ on primer-templates suggests that this deleted protein could retain substantial function. Additional mutations may have occurred to enable monomeric *Drosophila* pol γB to stimulate its catalytic partner. These mutations may have occurred either before or after deletion of this domain. It will be of great interest to compare the structures of the *Drosophila* and mammalian pol γ holoenzymes.

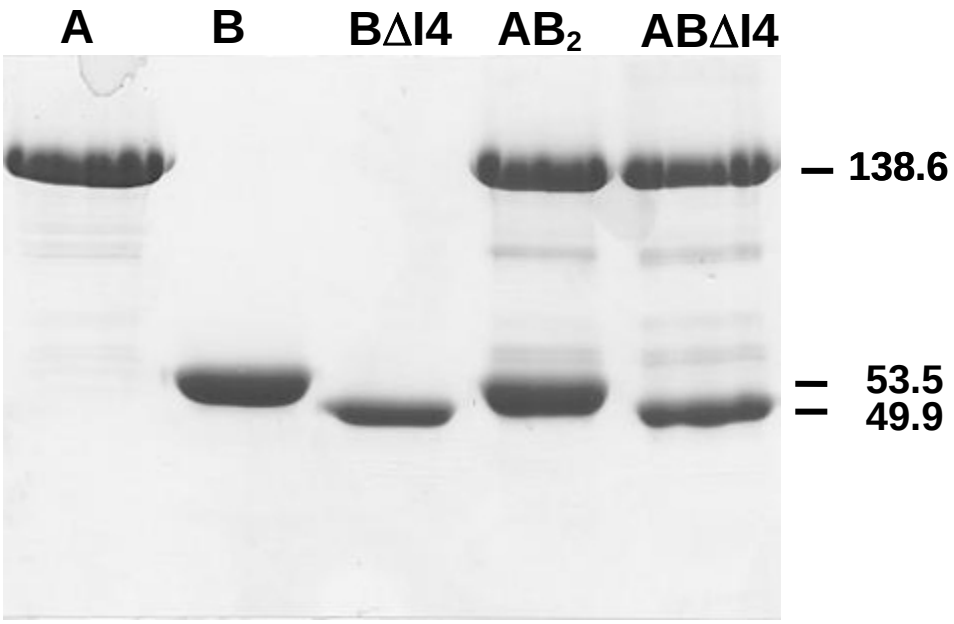

Figure 2.1 Purity of pol γ subunits and reconstituted holoenzyme. 2 pmol of the indicated protein preparations (*lane A* for pol γA, *lane B* for pol γB, etc.) were analyzed by SDS-PAGE, and the gel was stained with Coomassie Blue. The molecular masses indicated are those of the recombinant proteins and were consistent with commercial mobility markers (not shown).

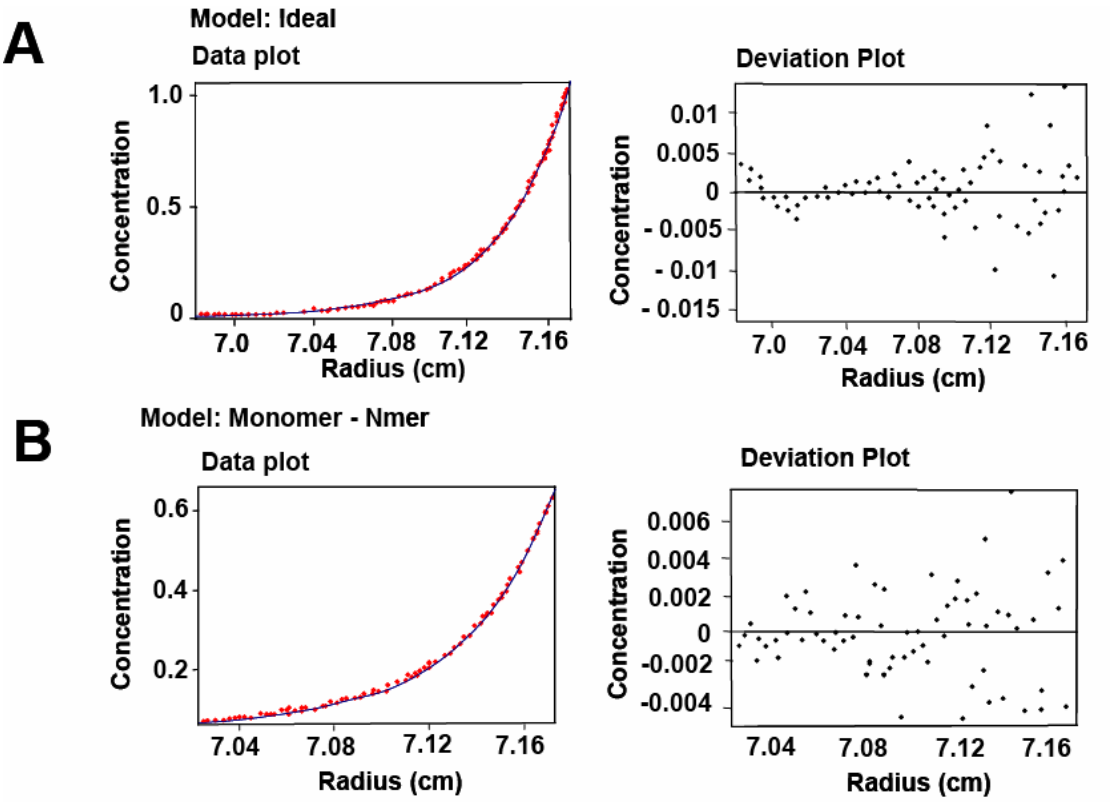

Figure 2.2 Analytical ultracentrifugation shows that pol γB is a homodimer and that pol γBΔI4 is a monomer that can dimerize at high protein concentrations. ***(A)*** Sedimentation equilibrium data for WT pol γB (3.77 μM), collected at 18,000 rpm after 30 h at 4 °C and fitted to a model for a single ideal species. *Left panel,* data points represent the experimental data, and the *solid line* is the model applied. The fitted molecular mass is 105,747 Da using a partial specific volume of 0.7299 and a solvent density of 1.026. *Right panel,* residuals for the fit are shown revealing small, random deviations from the model (rms deviation = 0.00385; variance = 1.4229). ***(B)*** Sedimentation equilibrium data for pol γBΔI4 (2.00 μM) collected at 20,000 rpm after 38 h at 4 °C and fitted to a model for monomer-dimer equilibrium. *Left panel,* the *dotted line* is the experimental data, and the *solid line* is the model applied. The fitted mass is 48,370 Da using a partial specific volume of 0.7283 and a solvent density of 1.026. The apparent association constant is 1.7×10^5 M^{-1}. *Right panel,* residuals for the fit show small, random deviations from the model (rms deviation = 0.00228; variance = 1.4982).

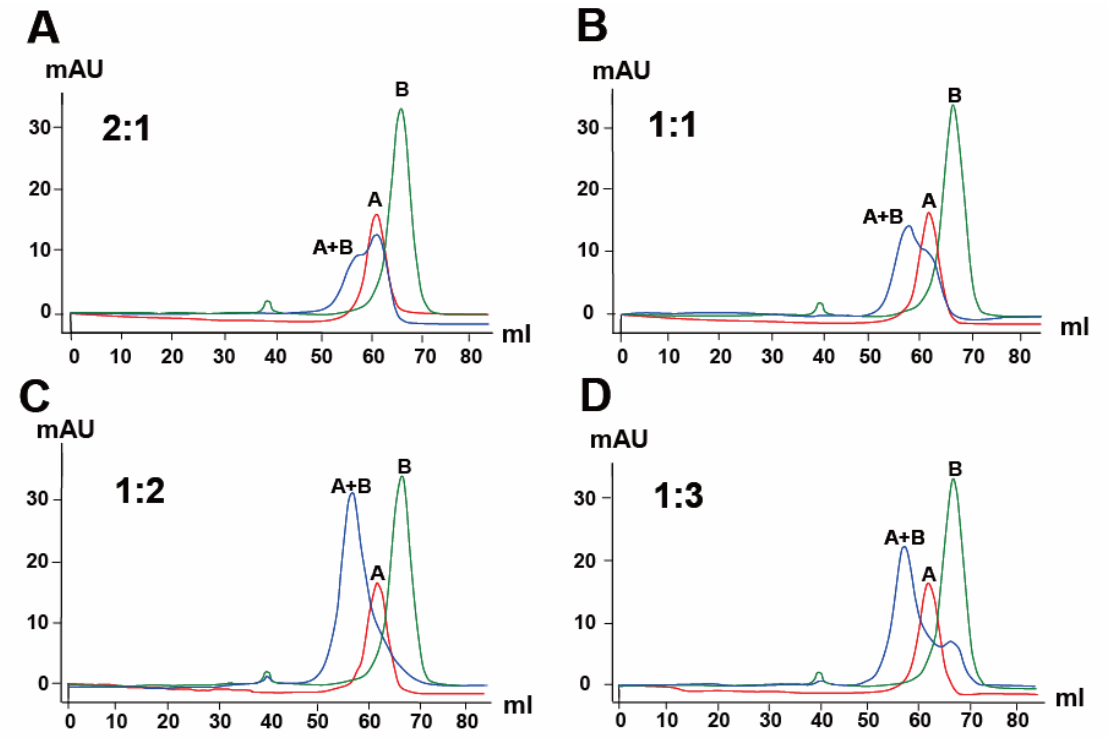

Figure 2.3 Analytical size exclusion analysis of the assembly of pol γ holoenzyme. The A_{280} profiles from four size exclusion chromatography experiments of mixtures of pol γA and pol γB are shown superimposed over the control elution profiles of separate runs with purified pol γA and pol γB. The marker profiles labeled *A* and *B* are the same in ***(A)*** – ***(D)***. Each analytical run used 0.2 mg of pol γA (1.44 nmol) mixed with 0.5, 1, 2, or 3 molar equivalents of pol γB, calculated as monomer. *mAU*, milliabsorbance units.

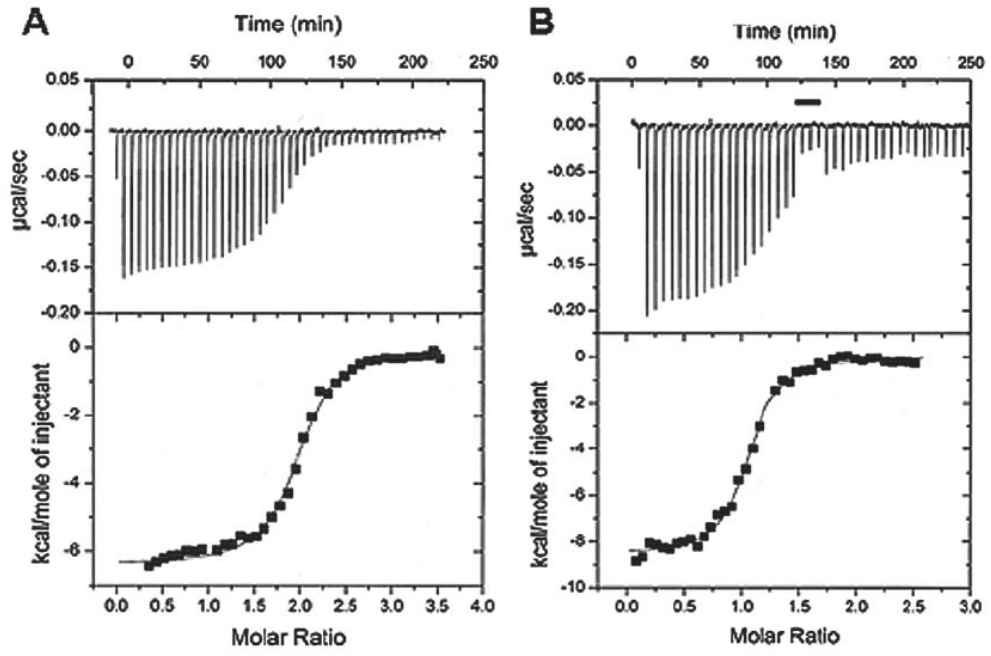

Figure 2.4 Isothermal titration calorimetry of WT pol γB *(A)* or pol γBΔI4 *(B)* binding to pol γA at 25 °C. The *top panel* shows the heat signal for injections of the WT pol γB (160 μM) or pol γBΔI4 (130 μM) into the calorimeter cell containing 1.4 ml of 7.2 μM pol γA. The *horizontal bar* in *B* shows that the injection volume was reduced from 5 to 2 μl for three successive injections at this time. The *bottom panel* shows the integrated heat for each injection after peak integration and subtraction of basal values fitted to a simple single-site binding model (*solid line*). The apparent thermodynamic parameters describing the fit are presented in Table 2.1.
This figure was contributed by Elena Yakubovskaya and Zhixin Chen.

Table 2.1

Thermodynamic parameters for pol γB and or pol γBΔI4 binding to exo⁻pol γA

	N^a	K_D	$\Delta G^{\circ b}$	ΔH°	$-T\Delta S^{\circ}$
		μM		*cal/mol*	
WT pol γB	1.97 (0.011)[c]	0.15 (0.014)	-9305	-6373 (52.5)	-2932
Pol γBΔI4	1.06 (0.062)[c]	0.14 (0.014)	-9344	-8522 (75.0)	-822

[a] *N* indicates stoichiometry of binding.

[b] ΔG° estimated from titration curve using MicroCal software (experiments were performed at 25°C).

[c] The errors shown in parentheses are the means ±S.D.

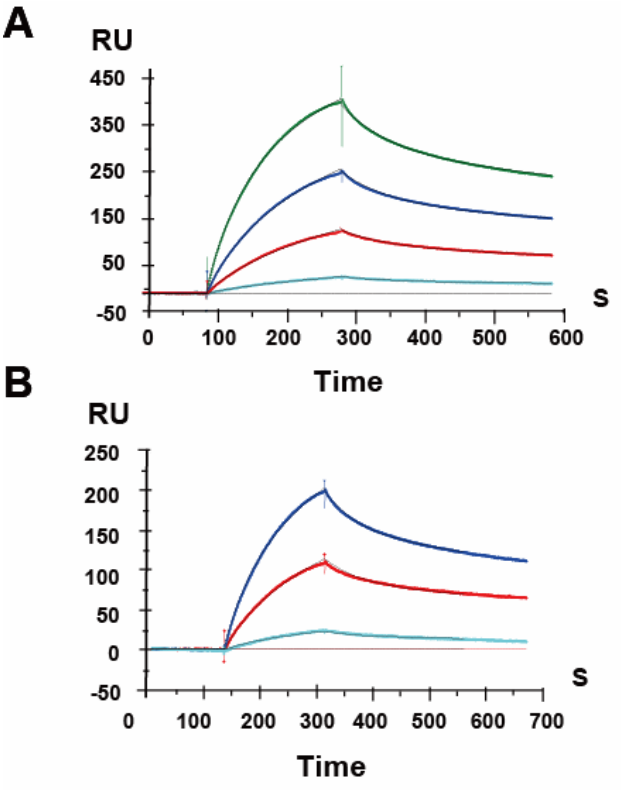

Figure 2.5 Kinetic analysis by SPR of pol γB_2 and pol γBΔI4 interactions with pol γA. Different concentrations (0, 40, 80, 160, and 320 nM) of pol γB_2 ***(A)*** or (0, 40, 80, and 160 nM) of pol γBIΔ4 ***(B)*** were injected in duplicate over 1400 RUs of amine-coupled pol γA. The *black points* correspond to the experimental data and the *solid lines* to the fit using the two-state reaction model (conformational change). Residuals for the fit are shown. The kinetic and thermodynamic constants and systematic error related to the fits are listed in Table 2.2. The overall dissociation constant K_D is calculated from the rate constants: $K_D = 1/(ka1/kd2) \times (1 + ka2/kd2)$).
This figure was contributed by Elena Yakubovskaya.

Table 2.2
Kinetic parameters for pol γB and or pol γBΔI4 binding to exo⁻pol γA in SPR

	k_{a1}[a]	k_{d1}[a]	k_{a2}[a]	k_{d2}[a]	K_D[b]
	$1/_{MS}$			$1/s$	
WT pol γB	2.81×10^{4} (166)[c]	6.21×10^{-3} (1.26×10^{-4})	4.93×10^{-3}(1.14×10^{-4})	7.09×10^{-4}(5.44×10^{-5})	2.78×10^{-8}(3.15×10^{-11})
Pol γBΔI4	3.61×10^{4} (526)	9.75×10^{-3} (3.25×10^{-4})	7.13×10^{-3}(1.75×10^{-4})	1.46×10^{-3}(3.42×10^{-5})	4.60×10^{-8}(2.50×10^{-10})

[a] For k_{a1}, k_{d1}, k_{a2}, k_{d2}, the rate constants were obtained from nonlinear least squares global fitting of the respective sensorgrams using SP *Revolution* software version 3.0 and a model permitting conformational change.

[b] $K_{D(M)}$ *is* the equilibrium dissociation constant derived from the rate constants by the equation $K_D=1/(k_{a1}/k_{d1})(1+k_{a2}/k_{d2})$.

[c] The errors shown in parentheses are the means ±S.D.

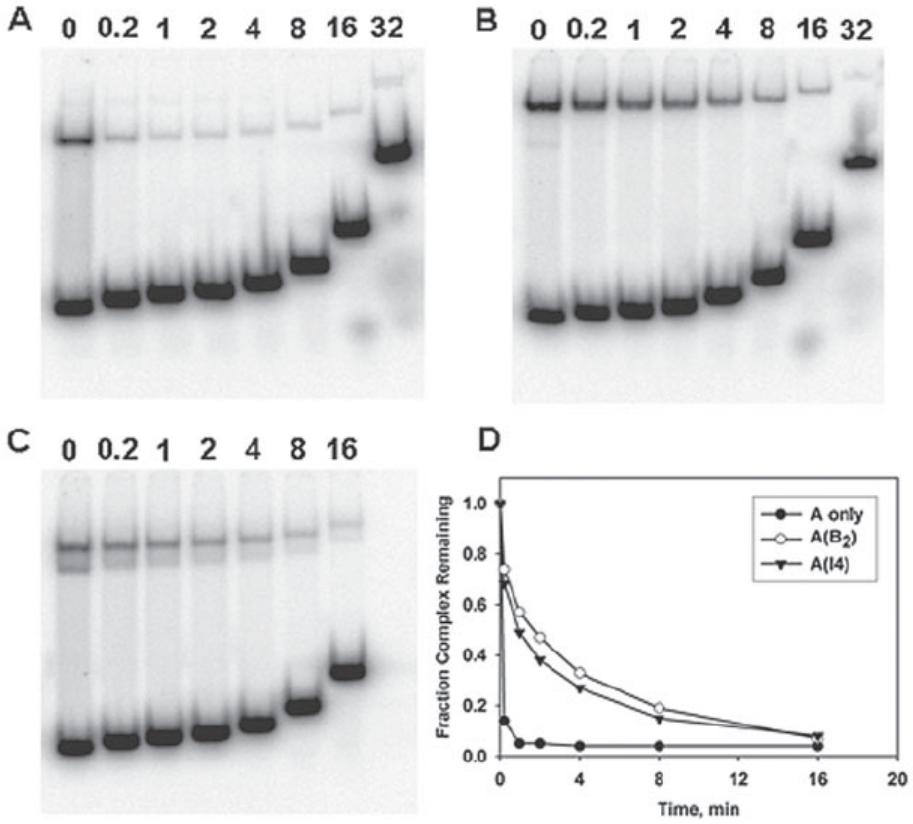

Figure 2.6 The monomeric I4 deletion derivative of pol γB stabilizes pol γA on an oligonucleotide primer-template nearly as well as the WT dimeric pol γB. EMSA challenge assays were conducted as described under "Materials and Methods" using pol γA alone ***(A)***, pol γA plus WT pol γB ***(B)***, or pol γA plus pol γBΔI4 ***(C)***. ***(D)*** The fraction of complex remaining intact in the presence of the cold binding competitor as a function of time.

This figure was contributed by Jose A. Carrodeguas.

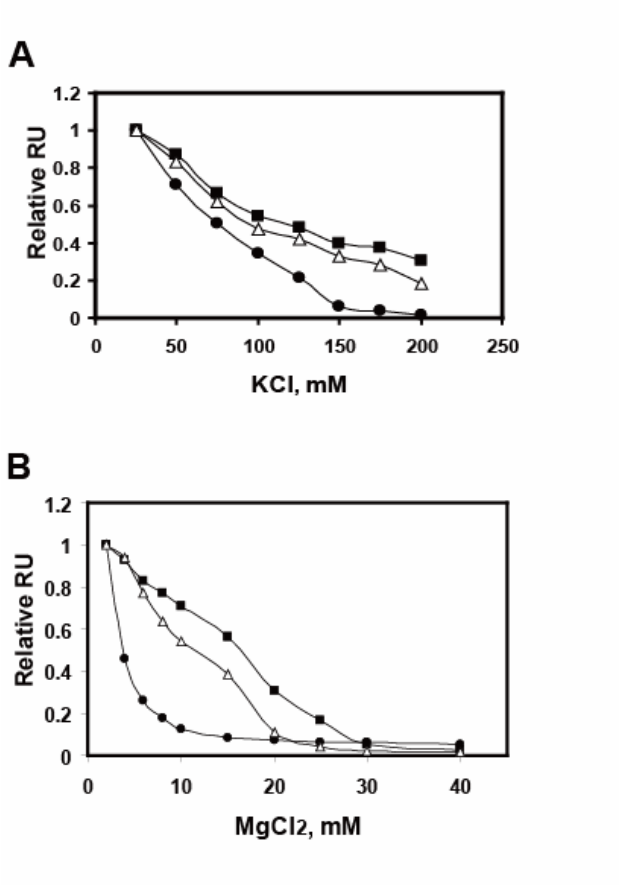

Figure 2.7 SPR analysis of the contribution of pol γB to the stabilization of the polymerase on DNA primer-template at varied ionic strength. Relative binding of 50 nM pol γAB_2 (■), pol γABΔI4 (Δ), and pol γA (●) to 10 RU of 26:45-mer DNA at varied concentration of KCl ***(A)*** or $MgCl_2$ ***(B)***. Similar results were obtained with a parallel flow cell loaded with 150 RU of 26:45-mer DNA (data not shown).
This figure was contributed by Elena Yakubovskaya.

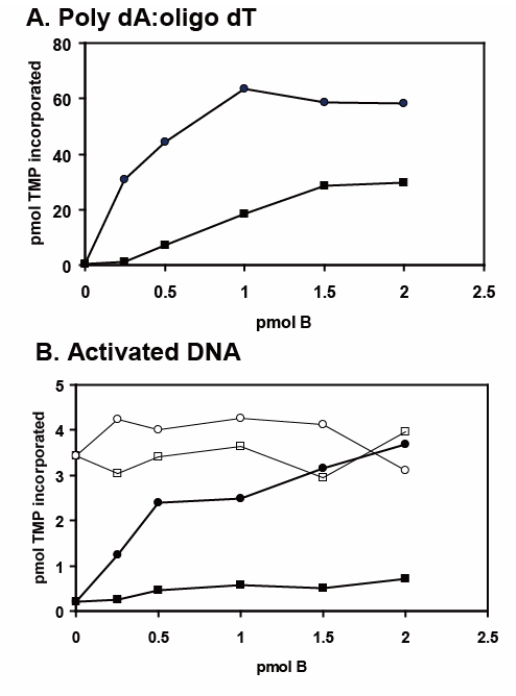

Figure 2.8 Stimulation of pol γA activity by pol γB_2 or pol γBΔI4. ***(A)*** Reactions were performed using 0.2 pmol of pol γA on poly(dA)-oligo(dT) primer-template in the presence of increasing concentrations of pol γB_2 (●) or pol γBΔI4 (■). ***(B)*** Reactions were performed using 0.2 pmol of pol γA on activated calf thymus DNA in the presence of increasing concentrations of pol γB_2 (●, ○) or pol γBΔI4 (■, □). *Filled symbols*, reactions performed in 140 mM KCl; *open symbols*, reactions performed in 50 mM KCl.
This figure was contributed by Daniel F. Bogenhagen.

Figure 2.9 Processivity of pol γAB$_2$ and pol γABΔI4 analyzed by single-round primer extension. 50 pmol of either pol γA, pol γAB$_2$, or pol γABΔI4 were mixed with 5'-^{32}P-labeled oligo(dT$_{16}$)-poly(dA) primer-template in standard polymerase reactions (50 mM KCl, 8mM $MgCl_2$) in a final volume of 15 μl and pre-incubated on ice for 5 min and then at 30 °C for 1 min. For the reaction shown in *lanes 1* and *2*, the polymerase reaction was started by addition of TTP to a final concentration of 25 μM along with 4 pmol of 26:45 unlabeled oligonucleotide competitor. 4 μl samples were removed at 1.5 (*lane 1*) and 3 min (*lane 2*) and added to 6 μl of formamide loading solution. The reaction shown in *lanes 3* and *4* was conducted in the same manner, except that the nonradioactive 26:45 competitor was added to the pre-incubation mixture before polymerase was added. *Lanes 5–8* and *9–12* show the products of reactions similar to those in *lanes 1-4*, except that pol γAB$_2$ and pol γABΔI4 were used, respectively. A PhosphorImager analysis of a polyacrylamide-urea gel to analyze the products of primer extension is shown. *Lane 0* shows the starting labeled oligonucleotide in the primer-template. *Lane M* shows mobility markers of end-labeled MspI fragments of pUC 18 DNA labeled according to size in nucleotides.

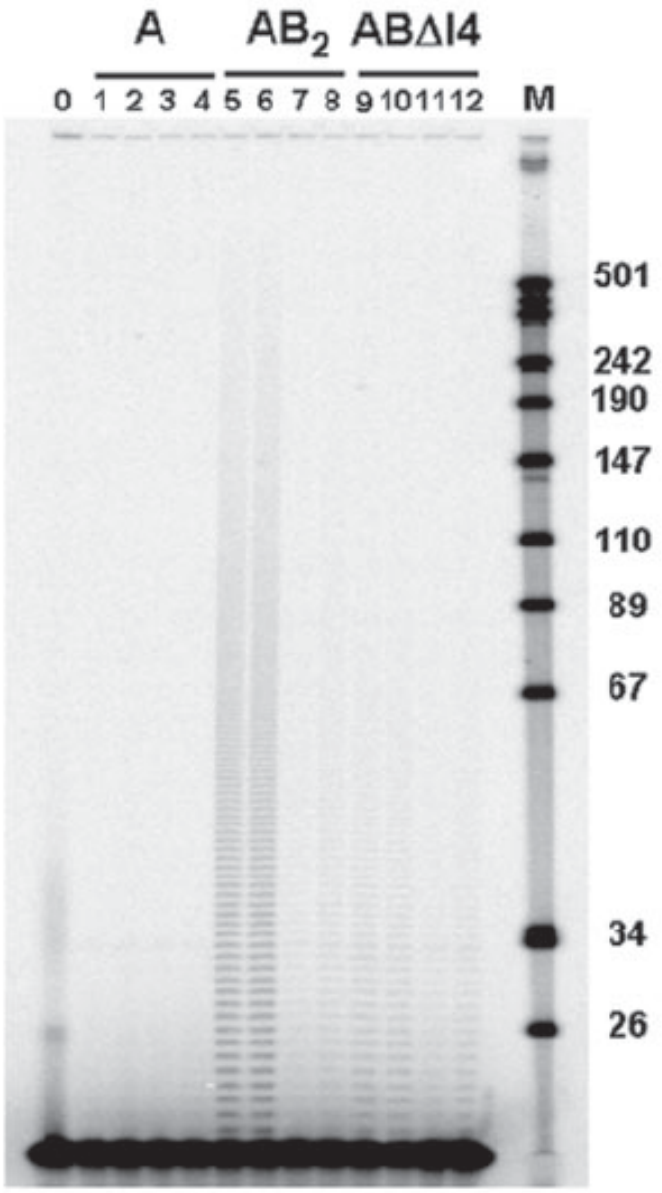

This figure was contributed by Daniel F. Bogenhagen.

CHAPTER 3: Pol γ Holoenzyme and Subunits Crystallization

I. Introduction:

As the sole DNA polymerase responsible for replication and repair in mammalian mitochondria, pol γ has been well studied with regard to its catalytic activities and subunit composition (GRAZIEWICZ *et al.* 2006). However, the molecular mechanism by which the accessory subunit stimulates the activity of the catalytic subunit and increases the processivity of the holoenzyme is not well understood. Studies of the interactions between the two subunits of pol γ in mammals are also limited. Although the structure of mouse pol γB has been solved (CARRODEGUAS *et al.* 2001), it is not homologous to other processivity factors such as PCNA and the β subunit of *E.coli* pol III which have a toroidal shape, and it doesn't provide any clue to explain the mechanism whereby this protein keeps the catalytic subunit engaged on the primer-template. For the catalytic subunit, no three-dimensional structure from any organism exists to date. The catalytic subunit of pol γ is homologous to other members of family A DNA polymerase, but is much larger than T7 DNA polymerase or DNA polymerase I whose X-ray crystal structures have been solved (DOUBLIE *et al.* 1998; OLLIS *et al.* 1985; YE *et al.* 1996). Most of the size difference is due to the linker region between the N-terminal exonulease domain and the C-terminal polymerase domain. Based on physical studies and mutational analysis of *Drosophila* pol γ (FAN and KAGUNI 2001; LUO and KAGUNI 2005; LUOMA *et al.* 2005), the two subunits interact with each other through more than one region and part of the pol γB interaction domain of pol γA might be located in some of the conserved sequences of the linker region in pol γA.

In this study, crystallization of pol γ has been attempted to obtain structural information of the catalytic subunit and its interaction with the accessory subunit. Crystallizations attempts were performed for both the catalytic subunit alone and for the reconstituted holoenzyme in the absence and in the presence of the primer-template DNA. Originally wt pol γA was purified and subjected to crystallization trials. Due to the limitted yield of wt pol γA, I used a proof-reading defective pol γA (exo$^-$ pol γA) which contains two mutations (D198A and E200A) in exonuclease motif I since this construct provides a much higher yield of recombinant protein than wt pol γA. The polymerase activity of this mutant pol γA is identical to that of the wt enzyme based on DNA activity assay. In order to achieve a more favorable protein conformation for crystallization, the optimal salt concentration and pH in protein solution have been studied by Dynamic Light Scattering. In addition, the primer-template DNA used for co-crystallization with pol γA and the reconstituted holoenzyme was compared among several designed oligonucleotides and confirmed by EMSA experiments. Crystallization trials have been set up using various crystallization formulations from different companies and different crystal growth techniques have been applied.

Currently, several techniques for setting up crystallization trials are available, including vapor diffusion, batch, free interface diffusion and microdialysis (Fig. 3.1). Each technique has its advantages and disadvantages. In this study, three of the techniques have been applied: hanging and sitting drop vapor diffusion, microbatch under oil and free interface diffusion. Vapor diffusion crystallization is mostly popular because

it is easy to set up, requires a small amount of sample, and is ideal for screening a broad spectrum of crystallization conditions. Hanging and sitting drop crystallization are the two common procedures for conducting vapor diffusion crystallization experiments. Using the hanging drop technique, a small amount of the sample (1 to 10 μl) is mixed with an equal volume of crystallization solution on a siliconized glass cover slide and inverted over a well containing the same crystallization solution (Fig. 3.1B). Over time equilibration of conditions between the drop and the reservoir solution occurs by diffusion of vapor within the sealed well. During this process, the sample is also concentrated. The sitting drop technique uses the same vapor diffusion principles as the hanging drop method, except that the protein droplets are placed on a platform as shown in Fig. 3.1A. For the microbatch under oil technique (Fig. 3.1E), a droplet of the sample combined with the crystallization solution is pipetted under a layer of oil which can be paraffin oil, a mixture of paraffin oil and silicon oil, or straight silicon oil. Paraffin oil allows little to no evaporation in the drop, but others allow water vapor to permeate from the drop and allow the sample and solution to concentrate. In this method, water will leave the drop until only solids remain. One advantage of this method is that it avoids the unwanted evaporation with the use of very small sample and solution volumes. Free interface diffusion (FID) crystallization is not a frequently used method, but it has been applied with the TOPAZ® screening chip by Fluidigm. In FID, the sample in liquid contacts with the reagent with a clearly defined interface (Fig. 3.1D). The sample and reagent are placed most commonly in a capillary right next to each other allowing the

solutions to mix by diffusion. This process generates a gradient of different protein and reservoir concentrations therey analyzing a wide range of different crystallization conditions. Crystallization may occur when favorable concentrations of the sample and precipitant are achieved. This method allows one to screen a gradient of combinations of the sample and precipitant concentrations. The TOPAZ® screening chip with the integrated fluidic circuit provides a format for FID which requires far less sample and reagents compared to the requirements of other methods.

Among the various crystallization trials, some promising crystallization conditions were identified. However, they didn't produce any crystal of pol γA or the reconstituted holoenzyme. As a side product of attempts to crystallize the pol γ holoenzyme, crystals of human pol γB were obtained from TOPAZ crystallization screening. The structure of human pol γB was solved at 3.1 Å resolution by molecular replacement showing that it closely resembles the structure of pol γB from mouse as expected from the high degree of sequence homology.

For a better understanding of the subunit interaction, regions within pol γB and pol γA required for complex formation were studied by limited proteolysis experiments. A pol γB interacting domain was mapped to the spacer region of pol γA which is located between the catalytic domain and the exonuclease domain of pol γA.

Using the limited proteolysis results as a guide, a number of pol γA constructs have been designed to remove the flexible regions for crystallization and interaction studies with pol γB. The overexpression and purification of these pol γA variants from *E.coli*

were attempted. The proteins tended to form aggregates during purification, indicating that the truncated fragments might not be able to fold properly in solution.

II. Materials and Methods:

A. Purification of WT Human pol γA: Recombinant wt human pol γA with an N-terminal histag was purified from Sf9 cells infected with the pFastBacI baculovirus engineered to express wt pol γA. The EcoRI-NotI pol γA fragment in pQE9 which was kindly provided by the Copeland lab was subcloned into a baculovirus vector — pFastBacI. The hexa-Histag is fused to the amino-terminus of the target gene, allowing easy affinity purification and the putative N-terminal mitochondrial targeting sequence has also been removed. Recombinant baculoviruses were generated by cotransfection of transfer plasmids with baculovirus DNA by standard baculovirus techniques. After amplification of the recombinant baculovirus in cultured SF9 insect cells, the virus titer was determined by plaque assay. To overexpress the human pol γA protein, cells were maintained in suspension culture in JRH Excell 420 culture medium supplemented with 100 IU penicillin plus 100 μg/ml streptomycin and grown to ~1.5E6 cells/ml prior to infection with recombinant baculovirus at a multiplicity of infection of approximately 5. Cells were harvested after 96 h postinfection, centrifuged at 2,500 rpm for 10 min, and washed once with TD buffer (134 mM NaCl, 50 mM KCl, 7 mM Na_2HPO_4, and 25 mM Tris pH 7.4). After the second centrifugation, cell pellet was resuspended with 1/20 culture volume of buffer I (same as in Materials and Methods chapter 2) with 300 mM KCl and 2 mM imidazole and homogenized with 0.5% Triton X-100. The homogenate was centrifuged for 1 hour at 35,000 rpm in a Beckman Ti 45 rotor at 4 °C and the supernatant was frozen in liquid nitrogen.

Due to the large volume of crude extract for the first column — the Ni-NTA affinity column, pol γA has been diluted at this stage and further purification was needed to obtain concentrated homogenous protein for biochemical and structural study. Therefore, the final optimized purification protocol is described as the following: For each preparation, crude extracts from ~3 L (~15g) recombinant baculovirus infected SF9 cells were mixed with 3 ml Ni-NTA resin (Qiagen), which is pre-equilibrated with buffer II (same as in Materials and Methods chapter 2) plus 300 mM KCl and 2 mM imidazole. After gently shaking for 1 hour, the 6xHis-tagged protein-resin mixture was spun down and loaded onto a column. After washing with 20 column volumes (cv) buffer II with 0.3 M KCl and 2 mM imidazole, 10 cv buffer II with 0.3 M KCl and 5 mM imidazole and 5 cv buffer-II with 0.3 M KCl and 10 mM imidazole, the protein was eluted with 5 cv buffer II with 0.3 M KCl and 100 mM imidazole. Based on SDS PAGE analysis and Biorad Assay for measuring the total protein concentration of each fraction, fractions of the eluate containing pol γA were pooled and loaded on a hydroxyapatite HCTI-2 column (Amersham Biosciences, total protein limitation is ~28 mg) which has been pre-equilibrated with HAP buffer A (10 mM KPi pH 6.8, 10 mM KCl, 2 mM DTT, 5% glycerol, 0.2 mM PMSF, 1 μg/ml pepstatin A, 5 μg/ml leupeptin and N-64). The column was run with a 15 cv, 0-50% linear gradient in HAP buffer B (HAP Buffer A plus 1 M KPi pH 6.8), and pol γA was eluted at around 30% buffer B. Fractions containing peak absorbance at 280 nm were pooled and stored at -80°C after they have been frozen in liquid nitrogen. Three such stocks were pooled, concentrated to less than 4ml using a

Millipore centricon concentrator (MW exclusion 100) and continued to be purified by size exclusion chromatography (Hiload 16/60 Superdex 200, Amersham Biosciences) and Mono S chromatography (Mono S HR 5/5, Amersham Biosciences) as described for exo⁻pol γA in chapter 2. All chromatographic steps were performed at 4 °C. The enzyme was concentrated to 3 mg/ml using a 100,000*M*r Centricon filtration device. The yield of the wt protein was about 0.1 mg/liter culture.

B. DNA Pol γ Reverse Transcriptase Assays—Polymerase activity of wild type pol γA and exo⁻pol γA was compared in reactions with poly(rA)-oligo(dT) as described previously (INSDORF and BOGENHAGEN 1989). The concentration of wt pol γA was approximately 0.14 mg/ml and the concentration of exo⁻pol γA was 2.5-fold higher than that of wt pol γA as shown in Fig. 3.2B (quantified by densitometry). One unit corresponds to the incorporation of 1 pmol of deoxynucleoside monophosphate to acid-insoluble products at 37°C in a 30-min reaction.

C. Binding of pol γA and holoenzyme to different oligonucleotides by EMSA—Several different oligonucleotides were used for binding analysis. They are shown as following: a. a 12:16-mer primer-template that is a 12-mer (5'-CTAGGACTGGCG-3') annealed to a 16-mer (5'-TACTCGCCAGTCCTAG-3'); b. a 16:24-mer primer-template that is a 16-mer (5'-TACTCGCCAGTCCTAG-3') annealed to a 24-mer (5'- CACGCCAACTAGG ACTGGCGAGTA-3'); c. a 44-hook (5'- GGCGTTGGGTCCGAATTCACTGCCTTTCG

CAGTGAATTCGGACC-3'); d. a 26:45-mer primer-template (CARRODEGUAS and BOGENHAGEN 2000). To compare the binding stability of pol γA or holoenzyme onto these primer-templates, reactions were assembled in 10 μl containing 1.0 μM primer-template, 0.8 μM pol γA or holoenzyme, 20 mM HEPES pH 8.0, 5 mM DTT, 1 mM EDTA, 150 μg/ml BSA, and 50 mM KCl. Binding reactions continued at room temperature for 30 min and then the reaction mixtures were subjected to native gel electrophoresis (6% acrylamide, 0.1% bis-acrylamide, 20 mM HEPES pH 8.0, 0.1 mM EDTA) to check the presence of DNA-bound protein complexes. Gels were stained with EtBr to detect DNA (Fig. 3.3) or with Coomassie Blue to detect protein (data not shown). For reactions to determine the optimal binding concentrations of pol γA or holoenzyme onto the 12:16-mer primer-template, serial concentrations of pol γA or holoenzyme were applied: 0.7, 1.0, 1.8, 2.5 μM for pol γA and 0.6, 1.2, 1.8, 2.5 μM for the holoenzyme.

D. Preparation of Protein-DNA Complexes for Co-crystallization—Proteins used for co-crystallization were prepared as described in Materials and Methods of Chapter 2. Exo$^-$pol γA and reconstituted pol γ holoenzyme were concentrated to 15 mg/ml and 15.4 mg/ml respectively. The 12:16-mer primer-template DNA used for co-crystallization was purchased from Qiagen. Protein and DNA were mixed at a molar ration of 1:1 and complex formation was promoted by microdialysis against the solution containing 20 mM HEPES 8.0, 50 mM KCl, 5 mM MgCl2, 5% Glycerol, 1 mM EDTA, 5 mM BME, 0.2 mM PMSF, 1 μg/ml pepstatin A, 5 μg/ml leupeptin and trace amount of Tris-Base.

The process of dialysis continued for two hours with three buffer changes at 4°C. Before crystallization setup, 10 mM dATP was added to the protein-DNA complex.

E. Crystallization of Human pol γB—Initial crystals of human pol γB were obtained from the crystallization trials of the reconstituted pol γ holoenzyme (protein was prepared as described in Chapter 2) using the TOPAZ® screening chips. The crystallization condition was from OptiMix Reagent Kit 2 (TOPAZ®): 20% PEG MME 5000, 1.0 M KSCN and 0.1 M Bis-Tris propane, pH 6.0. Crystals were reproducible by the hanging drop vapor diffusion method and optimal crystal growth was achieved by mixing 1 μl of 10 mg/ml pol γB protein solution with 1 μl of reservoir solution containing 5% PEG MME 5000, 0.6 M KSCN and 0.1 M Bis-Tris propane, pH 6.0. The crystals were equilibrated in cryoprotectant solutions containing 25% glycerol, 5% PEG MME 5000, 0.6 M KSCN and 0.1 M Bis-Tris propane, pH 6.0 and flash frozen in liquid nitrogen.

F. Data Collection and Structure Determination of Human pol γB—Crystals of human pol γB were analyzed at beam line X26C at the National Synchrotron Light Source, Brookhaven National Laboratories. Data were indexed, integrated and scaled using the HKL software package (MINOR *et al.* 2006; MINOR and OTWINOWSKI 1997). Crystals belong to space group F222 with unit cell dimensions a = 176.7 Å, b = 266.7 Å, and c = 267.1 Å, and contain two homodimers per asymmetric unit. The structure was solved by molecular replacement using the program AMORE (COLLABORATIVE COMPUTATIONAL

PROJECT 1994) and the pol γB homodimer from murine mitochondrial polymerase γ as a search model (PDB entry 1G5H (CARRODEGUAS *et al.* 2001)). Two unambiguous solutions with R-factors of 0.505 and 0.457, and correlation coefficients of 0.362 and 0.535 were obtained, respectively. Several cycles of rigid body refinement were performed with REFMAC (MURSHUDOV *et al.* 1997). Using the program O (JONES *et al.* 1991), murine residues were replaced by the appropriate human residues. Several rounds of restrained refinement in REFMAC alternating with manual building in O were used to improve the model. The structure was analyzed with MOLPROBITY (DAVIS and RICHARDSON 2004). The refinement statistics are summarized in Table 3.3.

G. Limited Proteolysis Study—1 mg/ml pol γA or holoenzyme was incubated with equal volumes of serially-diluted chymotrypsin, 10 or 3.3 μg/ml, at 22° C for 5 min. The reaction was stopped by adding 2 μl of 20 mM PMSF to 20 μl reaction mixtures. Boiled samples were loaded onto a 10% SDS-PAGE, subjected to electrophoresis and the gel was stained with Coomassie Blue. In some cases, following SDS-PAGE, proteolysis products were also transferred onto polyvinylidene difluoride (PVDF) membranes. N-terminal fragments were detected using a 1:5000 dilution of mouse monoclonal His-probe antibody conjugated to horseradish peroxidase (Santa Cruz) and chemiluminescent imaging. Alternatively, fragments containing the pol domain were detected using a 1:5000 dilution of rabbit polyclonal antibody directed against a conserved sequence in the Pol γ active site, KVFNYGRIYGAGC (YE *et al.* 1996)

(Residues 947 to 959 in human pol γA). Bound antibody was detected with goat anti-rabbit IgG secondary antibody and visualized using BCIP/NBT phosphatase substrate (K & P). A parallel blot of a partial chymotryptic digest of pol γA was stained with Coomassie blue and the C-terminal proteolytic fragments were sequenced from the N-terminus by Edman degradation using an automated protein sequencer (Procise 494, Applied Biosystems, CA).

H. Cloning, Overexpression, and Purification of pol γA Fragments—Pol γA fragments in Fig. 3.8 were cloned into vectors for over-expression of the peptides in *E.coli* using standard PCR cloning techniques (Stratagene). Several vectors were used: pET 28a for an N-terminal fused His_6 tag, pET 21b for a C-terminal fusioned His_6 tag, pET 16b for an N-terminal fused His_{12} tag, pTXB1 for a C-terminal fused intein tag, and pGEX-2TK for an N-terminal fused GST tag. The vectors used for cloning of each fragment are summarized in Table 3.4. To overexpress the polypeptides, the vector containing the fragment of interest was transformed to *E.coli* BL21 codon plus RIL cells (in some cases, several cell lines were compared and RIL usually provided the optimal expression). A pre-culture was grown by inoculation of the freshly transformed cells at 37°C overnight. Then I transferred the overnight pre-culture to a bigger culture which was induced with 0.3 mM IPTG at 15°C for 16 hrs when the cell density reached 0.5-0.6 ($O.D_{600}$). The cells were harvested by centrifugation at 6,000 rpm for 15 min using a JA 80:10000 rotor and the resuspended pellet was lysed at 1,000 Pa using a French-press in specific lysis buffer

(in most cases, same as the lysis buffer used for full-lengh exo$^-$pol γA in Chapter 2). For constructs of N-terminal histagged HGA438 and HGA871, lysis buffers containing different salt concentrations (50-300 mM KCl) at different pH (7.0-8.5) were compared to improve the solubility and column affinity of the polypeptides. The purification procedures also varied to optimize the binding of these two polypeptides onto the affinity and/or ion-exchange columns. In general, for his-tag fusion fragments, the purification was performed as described for full-length pol γA in the Materials and Methods section of Chapter 2. For the preparation of intein tagged fragments, the lysate was loaded onto a chitin column preequilibrated with lysis buffer. After ten cv wash with the same buffer, two cv of a buffer containing 100 mM DTT was quickly flushed through the column to induce cleavage which was continued at 4°C overnight. The protein was eluted by several cv lysis buffer. Some of the proteins such as N-terminal histagged HGA438 and HGA550a purified from 6 L culture were concentrated to 1 mg/ml using a 10,000*M*r Centricon filtration device and then frozen in liquid nitrogen.

III. Results:

A. Low Level Expression of WT Pol γA and Crystallization Trials—The initial goal of my research was to purify a sufficient quantity of wt pol γA for X-ray crystallographic studies. Early attempts in our laboratory and others failed to provide a significant yield of soluble pol γA in bacteria. Some laboratories have successfully overexpressed pol γA using baculovirus vectors in insect cells (GRAVES *et al.* 1998; LONGLEY *et al.* 1998b; WANG and KAGUNI 1999) that can provide a eukaryotic environment for recombinant proteins to fold properly. According to the work of Copeland and colleagues, the native and recombinant catalytic subunits are physically and functionally equivalent (LONGLEY *et al.* 1998b). As described under "Materials and Methods", wt pol γA was purified by a procedure consisting of an affinity chromatography on a Ni-NTA (Qiagen) resin and a hydroxyapatite HCTI-2 column (Amersham Biosciences) followed by ion exchange and size exclusion chromatography. In a typical preparation using 45 g of SF9 cells expressing wt pol γA, a final yield of ~1.0 mg of pol γA was obtained. The purity of wt pol γA is shown on the SDS PAGE in Fig. 3.2B. The purified protein was in intact, mature form indicated by MALDI mass spectrometry.

Dynamic Light Scattering (DLS) experiments were performed to characterize the purified protein. DLS (also known as Quasi Elastic Light Scattering [QELS] and Photon Correlation Spectroscopy [PCS]) monitors the fluctuations in scattered light in a solution caused by the Brownian motion induced movement of molecules. DLS can be used to assess the purity of biomolecular samples as well as providing an estimate of their mass.

DLS is used to measure hydrodynamic radii, polydispersities and aggregation effects of protein samples. The method is not invasive and only small sample volumes (20 μl, about 1 mg/ml) are required. A polydispersity below 25% usually indicates that the protein solution is homogenous and suitable for crystallization trials. For wt pol γA, DLS experiments indicated that it forms a dimer in solution with an estimated mass of 238 kDa, compared to 140 kDa of the monomer deduced from the primary sequence, and the final protein solution is fairly homogenous with a polydispersity below 15% at 22°C. Therefore, with the limited amount of wt pol γA available, some hanging drop crystallization trials were attempted using the reagents kits from Hampton Research, Crystal Screen I, II and Clear Strategy Screen I and II. While no crystals were obtained from the original screening, several crystallization conditions appeared to lead to preliminary positive results. The protein concentration, solute concentrations and pH were systematically varied in attempts to obtain crystals. However, no crystal was obtained for wt pol γA.

B. The Polymerase Activity of Exo⁻ Pol γA is Comparable to that of the WT Enzyme—According to the work from the Copeland laboratory, the expression level of a proof-reading deficient pol γA (exo⁻pol γA) was much higher than that of wt pol γA. We therefore obtained a virus expressing this form of the polymerase from their laboratory. In order to obtain sufficient quantities of enzyme for crystallization, exo⁻pol γA was overexpressed in baculovirus infected Sf9 cells and purified to near-homogeneity by a

three-step procedure as described in Materials and Methods of Chapter 2. The yield was about 0.7 mg/L and 7-fold higher than that of the wt enzyme.

Exo$^-$pol γA contains two point mutations in the exonuclease motif I: D198A and E200A. We expected that the exo$^-$pol γA would retain polymerase activity comparable to wt pol γA. A pol γ reverse transcriptase activity assay was performed to compare the polymerase activity between the wild type protein and this pol γA variant (Fig. 3.2). In Fig. 3.2A, the incorporation of TMP by exo$^-$pol γA was approximately 3.5-fold higher than that of wt pol γA. However, considering that the amount of exo$^-$pol γA applied in parallel assays was 2.5-fold higher than that of wt pol γA as shown in Fig. 3.2B (quantified by densitometry), the polymerase activity of exo$^-$pol γA was comparable to that of wild type enzyme.

C. Study of the optimal solvent conditions for crystallization by DLS—In order to determine the optimal solutions for crystallization, a series of solutions containing different salt concentration and different buffer pH were prepared as shown in Table 3.1. Proteins used for this study were prepared as described in "Materials and Methods" of Chapter 2. Prior to analysis by DLS, proteins were diluted with the different solutions and centrifuged for 20 min to remove aggregates. Based on the DLS analysis, the best solution in which exo- pol γA displayed the lowest polydispersity contained 300 mM KCl and 20 mM HEPES pH 8.0 (Data not shown). For the reconstituted holoenzyme, several optimal conditions were obtained as shown in Table 3.1. The solution containing 300 mM

KCl and 20 mM HEPES pH 8.0, which is consistent with the protein storage buffer, was used for crystallization trials.

D. Binding of pol γA and holoenzyme to different primer-templates—The choice of the DNA fragment plays a significant role in the success of a protein-DNA complex crystallization experiment (JORDAN *et al.* 1985). To determine the primer-template suitable for co-crystallization with pol γA and holoenzyme, several oligonucleotides were designed and the binding of pol γA and holoenzyme to them was compared by EMSA. In Fig. 3.3A, when the molar ratio of protein to DNA oligos was 1:1.2, most primer-templates were bound by pol γA and holoenzyme very well. The 12:16-mer apparently bound relatively poorly to pol γA. Nevertheless since a shorter primer-template would provide less flexibility during the process of crystallization, the 12:16-mer was chosen nevertheless for crystallization attempts to obtain the protein-DNA complex. Further EMSA experiments were performed to study the optimal ratio between the protein and the 12:16-mer. As shown in Fig. 3.3B, a 1:1 ratio of protein to 12:16-mer was the minimal ratio required for efficient binding of pol γA and holoenzyme to the DNA.

E. Crystallization Trials of exo⁻pol γA and Reconstituted Holoenzyme in the Absence and in the Presence of Primer-template DNA—Based on the studies above, a number of crystallization trials were conducted using four different preparations: exo⁻pol γA or

reconstituted holoenzyme both in the absence and in the presence of primer-template DNA as summarized in Table 3.2. These trials used variable crystallization formulations from different commercial companies and different crystallization methods.

Originally, only crystallization of exo⁻pol γA was attempted using the reagents from Hampton Research, Crystal Screen Lite (CSL) I, II and Clear Strategy Screen (CSS) I, II by the hanging drop vapor diffusion method. Some preliminary positive results obtained are shown in Fig. 3.4A-D. The picture in Panel A shows some apparent micro-crystals produced in the crystallization trial with 1 μl of 16 mg/ml exo⁻pol γA and 1 μl of reservoir solution containing 0.1 M MES pH 6.5, 6% (W/V) PEG 20,000MME (one formulation of CSL II). Following up this condition, the protein concentration, PEG concentration and pH were systematically varied to improve crystal growth. Since there was no improvement, additive screens (Hampton Research) were applied and added to the original condition. Panels B, C and D show the improved micro-crystals in the additive screens with additives: 4% (v/v) 2,2,2-trifluoroethanol, 0.7% (v/v) n-butanol, 3% (v/v) dimethyl sulfoxide respectively. I was not abable to further impove these crystals by additional attempts such as microseeding and detergent screening.

Assuming that the accessory subunit stabilizes and protects pol γA from oxidation and proteolysis to some extent (GRAZIEWICZ *et al.* 2006), attempts to crystallize the reconstituted holoenzyme were performed in parallel with the crystallization of pol γA alone. In addition to CSL I & II and CSS I & II, Natrix screen (Hampton Research) and Wizard I & II (deCODE Genetics) were tested for exo⁻pol γA and the holoenzyme by the

hanging drop vapor diffusion method. No crystals of pol γA or the holoenzyme were obtained from these crystallization trials. Since the high-throughput crystallization at Hauptman Woodward Medical Research Institute (HWI) uses a crystallization robot to set up the trials with the microbatch under oil method and requires less protein (600 μl, ~10 mg/ml) than the volume usually needed if the setups are made manually with 1536 different reservoir solutions, exo⁻pol γA and the holoenzyme were sent to HWI for high-throughput screening. As shown in Panel F of Fig. 3.4, a crystal of exo⁻pol γA appeared in the drop after two weeks of the high-throughput screening in a solution containing 0.1 M LiCl, 0.1 M Caps pH 10.0, 20% (w/v) PEG 4000. The picture in Panel E shows the clear reservoir solution before the addition of the protein solution. However, the effort to reproduce this crystal by either the microbatch under oil method or the hanging drop vapor diffusion method failed. Unfortunately the original crystal dissolved after the plate was shipped back from HWI. Alternatively, the commercial crystallization formula JBScreen 101 to 108 (Jena Bioscienses) comprising some different formulations from the ones I tested before was applied to exo⁻pol γA and the reconstituted holoenzyme by a crystallization robot in our laboratory using the sitting drop vapor diffusion method. However, no crystals of pol γA or the holoenzyme were obtained.

As indicated by the crystal structures of other DNA polymerases (DOUBLIE *et al.* 1998), the fingers and thumb domains introduce flexibility to the overall structure of DNA polymerase. This flexibility can be reduced upon binding of proper primer-template DNA. Therefore, attempts to co-crystallize exo⁻pol γA or the holoenzyme with

primer-template DNA were also performed. The Natrix screen (Hampton Research) and Wizard I (deCODE Genetics) reagents were tested using the hanging drop vapor diffusion method. No crystal was obtained from these screens. At this point, a new crystallization robot, which requirs far less sample and reagents for screening became available (TOPAZ®). Only 3 to 5 μl of protein solution is required for the analysis of 96 different crystallization trials. For all four combinations of protein and primer-template DNA, 4.96 TOPAZ® screening chips were used for crystallization with OptiMix reagents 1, 2 and 4 (TOPAZ®).

Crystals were obtained from crystallization trials of the holoenzyme through the free interface diffusion technique applied in the TOPAZ system both in the absence and in the presence of primer-template DNA with the reagent containing 20% PEG MME 5000, 1.0 M KSCN, 0.1 M Bis-Tris Propane pH 6.0 (Fig. 3.5Aa). Using the same protein samples, these crystals were reproduced in 8-18% PEG MME 5000, 0.6-1.0 M KSCN, 0.1 M Bis-Tris Propane pH 5.6-6.0 by hanging drop vapor diffusion. In some cases, both needle and cubic crystals were obtained as shown in Fig. 3.5Ab-d. They were frozen separately and examined on beamline X26 at the National Synchrotron Light Source, Brookhaven National Laboratories. It turned out that the cubic crystals were pol γB and the needle crystals were too thin to provide significant diffraction. Using the human pol γB protein (10 mg/ml) alone, the cubic crystals were reproduced and improved in reagents containing 10% PEG MME 5000, 0.6 M KSCN, 0.1 M Bis-Tris Propane pH 5.6 by hanging drop vapor diffusion (Fig. 3.5Ae). Subsequently, optimal crystals were achieved

by mixing 1 μl of 10 mg/ml human pol γB protein solution with 1 μl of 5% PEG MME 5000, 0.6 M KSCN, 0.1 M Bis-Tris Propane pH 6.0 (Fig. 3.5Af). Each type of crystal in Fig. 3.5A was collected from the crystallization drops and subjected to SDS PAGE. As shown in Fig. 3.5B, all crystals are the pol γB protein. This result suggests that the holoenzyme has dissociated under these crystallization conditions. Since pol γB used in e and f of panel A was a 6xhistag fusion protein, it migrated slightly less rapidly on the SDS PAGE of panel B compared to the non-tagged pol γB in the co-purified holoenzyme.

F. Crystal Structure of Human Pol γB—As mentioned above, the original crystal of human pol γB was obtained from TOPAZ crystallization screening as a side product of crystallization attempts of the pol γ holoenzyme. The crystals were reproducible by the hanging drop vapor diffusion method and pol γB used for optimal crystal growth was the C-terminally His-tagged recombinant form containing residues 26-485 of the protein and omitting the N-terminal mitochondrial signal sequence. The structure of human pol γB was solved at 3.1 Å resolution by molecular replacement with the mouse pol γB structure (PDB entry 1G5H) (CARRODEGUAS *et al.* 2001) as search model. Crystals belonged to space group F222 and contain two homodimers per asymmetric unit, with monomers A/B and C/D forming dimers. The N-terminal residues 26-62, internal residues 153-172, residues 220-228, residues 357-368, and the C-terminal Histag were disordered in all four monomers. The crystallographic model was refined to an R factor of 20.8% (R_{free} 26.0%) with non-crystallographic symmetry restraints (Table 3.3). The two independent dimers

of pol γB in the asymmetric unit superimpose with a root-mean-square deviation (rmsd) of 0.334 Å in all atom positions and the rmsd of corresponding atoms after superposition of the monomers is 0.3 to 0.6 Å, indicating that the molecules in the crystal structure have nearly identical structures.

The overall structure of human pol γB is shown in Fig. 3.6A&B, which resembles the structure of mouse pol γB. The rmsd of corresponding C_α atoms after superposition of the monomers (Fig. 3.6D) is 0.667 Å (335 C_α atoms used out of 367) and the rmsd of corresponding C_α atoms after superposition of the dimers (Fig. 3.6E) is 1.45 Å (701 C_α atoms used out of 738). The close similarity between human and mouse pol γB was expected because the identity of primary sequence between them is more than 80% (Fig. 1.5). As for mouse pol γB, the human pol γB structure contains core domain and C-terminal domain besides domain 2 which is essentially missing in the human pol γB structure. The core domain of one monomer in Fig. 3.6 is colored in blue and contains six anti-parallel β-strands and one parallel β-strand which are surrounded by six α-helices and several loops (residues Asp26-Leu130 and Arg182-Gln355). One face of the twisted β sheet forms a pocket that is solvent accessible. The C-terminal domain (residue Leu356-Val485) is colored in yellow in Fig. 3.6 and is comprised of five β strands and three α helices. Domain 2 (residue His131-Leu181, colored in green in Fig. 3.6) is considered to be the dimerization domain according to the deletion experiments, but most part of this domain is disordered in the human pol γB structure. In mouse pol γB structure, this domain consists of a four-helix bundle and a six-stranded short antiparellel β-sheet

(Fig. 1.4A) within the dimer, which provides the major dimerization interface (CARRODEGUAS *et al.* 2001).

As analyzed in Carrodeguas et al. 2001, the structure of pol γB is highly homologous to glycyl-tRNA synthetase from *Thermus thermophilus* (ttGRS; PDB code 1ATI) despite the relatively low sequence identity between ttGRS and pol γB of 20.2%. In Fig. 3.6C, human pol γB is superimposed with ttGRS and the rmsd of corresponding C_α atoms (283) is 3.4 Å (283 C_α atoms used 367). The core domain of pol γB corresponds to the catalytic domain of ttGRS, but the active site of aa tRNA synthetases are not conserved in pol γB and it has been suggested that pol γB cannot function as a tRNA synthetase (CARRODEGUAS *et al.* 2001). The C-terminal domain of pol γB corresponds to the anticodon binding domain of ttGRS. The similarity between the two structures might reflect the DNA binding property of pol γB, which relates to the role of pol γB in RNA primer recognition and binding in mtDNA replication as introduced in the main introduction (FAN *et al.* 1999; MURAKAMI *et al.* 2003). According to the sequence alignment of different pol γB's in Fig. 1.5, the C-terminal domain is highly conserved among different species. This conservation suggests that the C-terminal part may be very important for the basic function of the accessory subunit and may work more directly together with the relatively conserved catalytic subunit to enhance processivity (CARRODEGUAS and BOGENHAGEN 2000; FAN and KAGUNI 2001).

G. Probing the Contacts between Pol γ Subunits by Limited Proteolysis—To explore the

binding relationship between the pol γA and B_2 subunits, limited proteolysis was performed to identify protease cleavage sites that might be protected in the holoenzyme structure. Fig. 3.7 shows that chymotrypsin was able to cleave pol γA at three highly accessible sites that might divide the enzyme into three domains. The fact that only the A subunit contained a His_6 tag, in this case at the N-terminus, enabled the identification of three major N-terminal fragments produced by chymotrypsin labeled b, d and f in Fig. 3.7B. Three major fragments lacking a His_6 tag were found to react with an antibody directed against a conserved sequence within the pol γ polymerase domain, KVFNYGRIYGAGC (YE *et al.* 1996), representing residues 947 to 959 in human pol γ (Fig. 3.7D). These C-terminal fragments are labeled a, c and e in Fig. 3.7. Edman degradation was performed by our collaborator, Dr. Ryuji Kobayashi, to obtain N-terminal sequences of these C-terminal fragments. Fragment a was found to have the sequence IAAKQGKHKQPPT at the N-terminus; fragments c and e started with QKLKGTTELL and TARGGPX(D)TQ, respectively. Therefore, this analysis revealed limited chymotrypsin cleavage of pol γA after residues W312, L549 and L719. It is apparent in Fig. 3.7 that the L549 cleavage site is selectively protected from digestion when the A subunit is bound to the B subunit. This result is consistent with results from other labs indicating that the pol γA protein bearing a mutation at residue 467 is deficient in its ability to bind pol γB_2 (GRAZIEWICZ *et al.* 2006). Taken together, these results imply that pol γB_2 interacts principally with the spacer region of pol γA separating the exo and pol domains, possibly spanning residues that extend from residue A467 to L549.

H. Attempts to Prepare Pol γA Constructs for Crystallization and Interaction Studies with pol γB—Using the limited proteolysis results as a guide, a number of pol γA constructs have been designed for crystallization and interaction studies with pol γB (Fig. 3.8 & Table 3.4). Fig. 3.8 shows an interpretation of the fragments with respect to major sequence features of pol γA. These fragments can be divided into three groups. The first group includes HGA746a, HGA746b, HGA720a, and HGA871 which contain the polymerase domain. The second group includes HGA438, HGA550a, HGA313a and HGA313b which contain all or part of the spacer region. HGA540 and HGA550b, containing both the polymerase domain and most part of the spacer region, can be defined as the third group. All fragments do not contain the N-terminal exonuclease domain. The physical properties of these fragments, such as molecular weight and pKa, are summarized in Table 3.4, as well as the fusion tags, the solubility and the affinity to the corresponding columns. The molecular weight of these fragments ranges from 19.18 to 78.57 kDa and their pKa ranges from 5.3 to 8.7. Most of the pol γA fragments overexpressed in *E.coli* are moderately soluble and have poor affinities to the corresponding affinity columns. Some fragments such as, HGA438 and HGA871, also bound poorly to both an anion and a cation ion-exchang column. Attempts to improve the expression level and solubility of HGA438 by co-expression with CBP tagged pol γB were not successful. The preparations of HGA438 and HGA550a by a three-step procedure as described for full-length pol γA provided several milligram of protein from a 6 L cell culture. However, both of the fragments eluted in the void volume from the size

exclusion chromatography, indicating that the proteins formed aggregates (Data not shown). The protein may have therefore been misfolded and was not suitable for either crystallization or interaction studies with pol γB.

IV. Discussion:

In this study, efforts have been undertaken to crystallize pol γA and the reconstituted holoenzyme both in the absence and in the presence of primer-template DNA. Due to the limited yield of wt pol γA, the proof-reading defective pol γA (exo$^-$pol γA) was used for most crystallization setups. Although this mutant pol γA lost its exonuclease activity, its polymerase activity is as good as that of the wild type protein analyzed by reverse transcriptase assay (Fig. 3.2) indicating that the overall conformation of exo$^-$pol γA is maintained. The proteins used for crystallization have been purified to homogeneity as shown in Fig. 2.1 and DLS analysis indicated that they are suitable for crystallization trials. Originally, the attempt to crystallize pol γA and holoenzyme in the absence of primer-template DNA was performed and some promising conditions for pol γA were obtained as shown in Fig. 3.4. The crystal in Fig. 3.4F was obtained from the high-throughput screening at HWI. The HWI facility provided an opportunity to test 1536 chemical cocktails for crystallization by a robotic procedure using only 600 µl of 9 mg/ml protein solution. Unfortunately the one apparent crystal obtained with this method dissolved before it was shipped back and I was not able to determine if it was really a pol γA crystal. It was more likely to be a protein crystal rather than a salt crystal for two reasons. First, the salt concentration in the crystallization trial was relatively low with 0.05 M Li_2SO_4 and 0.15 M KCl. Second, no such crystal appeared in the same crystallization solution containing the reconstituted holoenzyme. However, I was not able to reproduce this crystal by either the microbatch under oil or the hanging drop vapor

diffusion methods with the same batch of purified pol γA. Other promising crystallization conditions were also obtained and some micro-crystals were produced under those crystallization conditions (Fig. 3.4A-D). Efforts to improve crystallization by many trials, including setup at different temperature, detergent screening and microseeding, didn't improve the crystals. Crystallization of pol γA alone has not been successful. One of the reasons might be that pol γA is not stable by itself and sensitive to oxidative species or proteolytic digest. Upon binding of the accessory subunit, pol γA can be stabilized and protected from oxidation. Therefore, the crystallization of the complex formed between pol γA and pol γB was also attempted. However, this approach did not lead to an improvement. One significant problem is that the complex dissociated into its subunits at least with certain crystallization conditions as indicated by the crystallization trials in Fig. 3.5. Crystals, which grew with 20% PEG MME 5000, 1.0 M KSCN, 0.1 M Bis-Tris Propane pH 6.0 as the reservoir solution from Optimix-2 (TOPAZ®), turned out to be human pol γB crystals, but did not contain pol γA or the holoenzyme by SDS PAGE. The dissociation of the complex into the subunits can be explained by the component of 1.0 M KSCN which might destroy the interactions between the two subunits. Thus, to keep the complex intact during crystallization conditions is a significant concern. Another problem is that the salt concentration in all protein solutions was relatively high, 300 mM KCl. The minimal salt concentration to keep the protein soluble at high protein concentrations and to maintain the complex in the protein solution should be determined and applied for crystallization.

Judging by the known structures of family A DNA polymerases (Fig. 1.3) (DOUBLIE *et al.* 1998), the structure of a DNA polymerase is expected to require flexibility of the fingers and thumb domains. The catalytic subunit of pol γ is much bigger compared to other family A DNA polymerases whose structures have been solved. The length difference is mostly contributed by the linker region separating the exonuclease domain and the polymerase domain (Fig. 1.2) (GRAZIEWICZ *et al.* 2006). Therefore, it is conceivable that the structure of the catalytic subunit pol γA might be even more flexible and therefore prevents crystallization. We considered that the overall conformation of a polymerase could be stabilized by reducing the flexibility between the finger and the thumb domains of a DNA polymerase upon binding of primer-template DNA. Accordingly, several oligonucleotides with different length were designed for co-crystallization with pol γ and their binding to pol γA and holoenzyme was compared by EMSA experiments. Since all these primer-templates bound to pol γA and the holoenzyme applying a certain ratio of protein-DNA concentrations and shorter primer-templates are preferred to reduce flexibility, the shortest oligonucleotide, a 12:16-mer, was used for co-crystallization with pol γ. As shown in Table 3.2, many crystallization trials were made with pol γ proteins and the 12:16-mer primer-template. However, they were not successful.

Only one oligonucleotide has been used for attempted co-crystallization with pol γ and this 12:16-mer is relatively short. This primer-template was selected for these trials since it bind to pol γ, and since short oligonucleotides have been used for

co-crystallization with other polymerases (LI *et al.* 1998). However, recent results of foot-printing and primer-extension experiments in our laboratory designed to study the length of primer required for extension of the template by pol γ indicate that the minimal length of a primer required for efficient extension by pol γ is around 25 nucleotides. Therefore, if attempts to co-crystallize the polymerase with primer-template DNA are repeated, the oligonucleotide should be longer than a 12:16-mer. Since many protein-DNA complexes crystallized under a rather narrow range of solution conditions, the effort is better focused on trying a variety of DNA fragments under a relatively limited set of crystallization conditions, rather than on exploring exhaustive potential crystallization conditions. Thus, there might be a greater chance to obtain crystals of pol γ holoenzyme if several primer-templates with different length were applied.

The crystal of human pol γB was analyzed and the structure was solved at 3.1 Å resolution, a relatively low resolution in comparison to the resolution of 1.95 Å at which the crystal structure of mouse pol γB was determined. The structure of human pol γB closely resembles the structure of its mouse homolog as expected based on high sequence conservation. The rmsd of corresponding C_α atoms after superposition of either monomers or dimers of the two structures is low, 0.667 Å for the monomer superposition (335 C_α atoms used out of 367) and 1.45 Å for the dimer superposition (701 C_α atoms used out of 742). The disordered regions in the mouse pol γB structure are not improved in the human structure. In addition, the four α-helix dimerization bundle and most of the β-strands at the base of the dimerization domain are also disordered in the structure of

human pol γB. Like the mouse pol γB structure, the structure of human pol γB is homologous to aa-tRNA synthetases and the rmsd of corresponding C_α atoms after superposition with the monomer of glycyl tRNA synthetase is 3.4 Å (283 C_α atoms used out of 367). This similarity might reflect the DNA binding property of pol γB and it has been suggested that pol γB might bind to nucleic acids with similar structures as tRNA (CARRODEGUAS and BOGENHAGEN 2000). However, a mutational analysis shows that this binding property of pol γB is not required for stimulation of pol γA activity (CARRODEGUAS *et al.* 2001). It remains a possibility that the DNA binding property of pol γB might play a role in replication initiation as suggested in Carrodeguas and Bogenhagen, 2000, but this has not been demonstrated experimentally.

The structure of pol γB does not elucidate the mechanism by which the accessory subunit engages the catalytic subunit onto the primer-template and increases the processivity of pol γ. Nevertheless, based on the available structural data, biochemical and mutagenesis studies, some mechanisms found in other DNA polymerase accessory factors can be excluded and a mechanism compatible with the existing data can be outlined. The crystal structure provides no evidence that pol γB can form a toroid structure found in sliding clamps, like PCNA and the β subunit of *E.coli* DNA polymerase III (JERUZALMI *et al.* 2001; KONG *et al.* 1992; KRISHNA *et al.* 1994). It indicates that pol γB can not act as a sliding clamp. Of the remaining accessory factors which have been structurally characterized, UL42 binds non-specifically to dsDNA with high affinity and has little structural similarity to pol γB (ZUCCOLA *et al.* 2000). In the T7

DNA replication complex, thioredoxin doesn't interact directly with the DNA in the crystal structure (DOUBLIE *et al.* 1998). As noted above, pol γB can bind to DNA with moderate affinity, but this DNA binding property is not required for pol γA stimulation. This means that pol γB does not bind to DNA tightly during replication and thus pol γB may be similar to thioredoxin at this point. Recently Fan et al. (2006) (FAN *et al.* 2006) presented a hypothetical model for the pol γA-γB interaction in the presence of DNA in light of the T7 DNA polymerase and thioredoxin co-crystal structure. Since the weak structural resemblance of pol γB to thioredoxin is only limited to the C-terminal domain of pol γB (FAN *et al.* 1999) and the thumb region in T7 DNA polymerase which interact with thioredoxin is not conserved in pol γA, such modeling is not very feasible. In their model, it was suggested that the two subunits of pol γ share an extensive binding interface that permits the holoenzyme to substantially encircle the nascent DNA. However, according to the 3D model of the human pol γ holoenzyme provided by our recent EM studies (Fig. 3.9), one pol γB subunit dominates the contacts with the catalytic subunit while the second B subunit is largely exposed to solvent. This result is consistent with our previous mutagenesis and biochemical studies (YAKUBOVSKAYA *et al.* 2006) which demonstrated that one pol γB molecule contributes most of the interaction energy with pol γA. Our results fail to support the clamp type pol γ-DNA complex formation proposed by Fan et al. (2006) (FAN *et al.* 2006). Currently there is limited knowledge on the interaction sites of the two subunits. The 3D model of human pol γ in Fig. 3.9 demonstrates that the N-terminal core domain of pol γB mediates most contacts with pol

γA. Nevertheless, the remarkable difference on pol γA stimulation and processivity increase by the wild type pol γB compared to the monomeric pol γB mutant I_4 suggested that the second pol γB molecule has an important role in mtDNA replication. The EM model also explained the properties of some pol γB mutations that affect its ability to stimulate pol γA. To explore the binding relationship between the pol γA and B_2 subunits, limited proteolysis was performed to identify protease cleavage sites that might be protected in the holoenzyme structure. Fig. 3.7 clearly shows that the L549 cleavage site is selectively protected from digestion when the A subunit is bound to the B subunit. This result is consistent with results from other labs indicating that a pol γA protein bearing a mutation at residue 467 is deficient in its ability to bind pol γB_2 (GRAZIEWICZ *et al.* 2006). Taken together, these results imply that pol γB_2 interacts principally with the spacer region of pol γA separating the exo and pol domains, possibly spanning residues that extend from residue A467 to L549. However, to fully understand the interaction of the two subunits and their functions in the replication, it is still necessary to obtain the structure of the holoenzyme.

While it is most desirable to crystallize the intact pol γA or holoenzyme, it has to be considered that flexible regions of the protein will interfere with the formation of a well-ordered crystal lattice. In principle, the probability of obtaining crystals will be increased if the flexible and non-functional parts are removed. A common procedure for the indentification of a minimal folded protein fragment for crystallization is limited proteolysis. Using the limited proteolysis results as a guide, a number of pol γA

constructs have been designed for crystallization and interaction studies with pol γB (Fig. 3.8 & Table 3.4). As shown in Fig. 3.7, six major fragments were obtained by limited chymotrypsin digestion. Since we currently focus on the activity of the polymerase and its interaction with pol γB, the fragments containing the polymerase active sites and/or the spacer region which is proposed to be the principal pol γB interaction region in pol γA, were subjected to cloning into vectors for overexpression in *E.coli*. In some cases, the predicted secondary structure was also considered for designing the truncated fragments of pol γA as shown in Panel A of Fig. 3.8, except for construct HGA871 which was specifically designed to obtain the smallest polymerase functional domain containing only three polymerase motifs (GRAZIEWICZ *et al.* 2006). The fragments in Panel B of Fig. 3.8 were designed solely according to the results of limited proteolysis. Among these fragments, construct HGA438 is important to our studies since it contains the whole spacer region which is expected to be sufficient for the interaction with the accessory subunit. Efforts have been carried out to optimize the overexpression and purification of this fragment. However, this fragment formed aggregates during purification indicating that it was either misfolded or exposed hydrophobic amino acids into the solvent due to the truncation. Another fragment, HGA550a was observed to form similar aggregates as HGA438 during preparation. It might be a common problem for other pol γA constructs since most of them displayed moderate solubility and poor binding to columns, indicating that the truncated fragments might not be able to fold properly in solution. Further limited proteolysis experiments on pol γA and the holoenzyme in the presence of DNA should be

performed to compare the results of limited proteolysis on pol γA and the holoenzyme in the absence of DNA. Some useful knowledge might be obtained to explain the poor behavior of the pol γA fragments designed here.

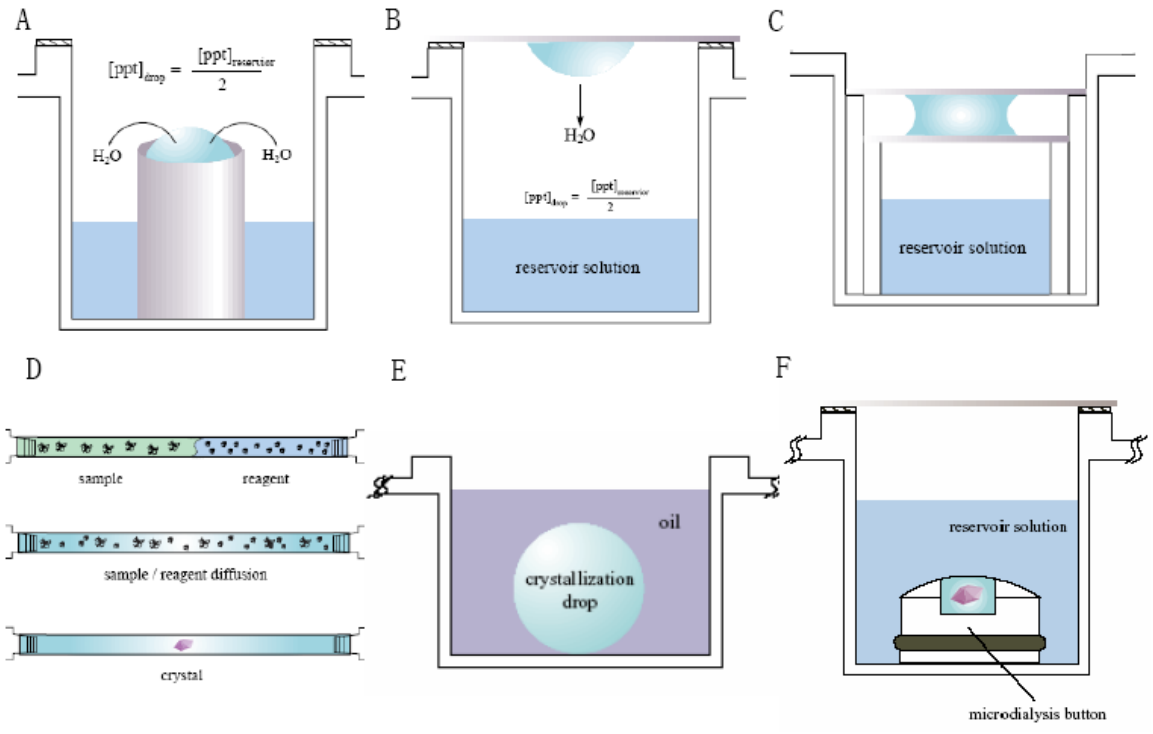

Figure 3.1: Crystal growth techniques. ***(A)*** Sitting drop vapor diffusion crystallization. ***(B)*** Hanging drop vapor diffusion crystallization. ***(C)*** Sandwich drop crystallization. ***(D)*** Free interface diffusion crystallization. ***(E)*** Microbatch under oil crystallization. ***(F)*** Microdialysis crystallization. (Figures from Crystal Growth 101 Literature of Hampton Research)

A

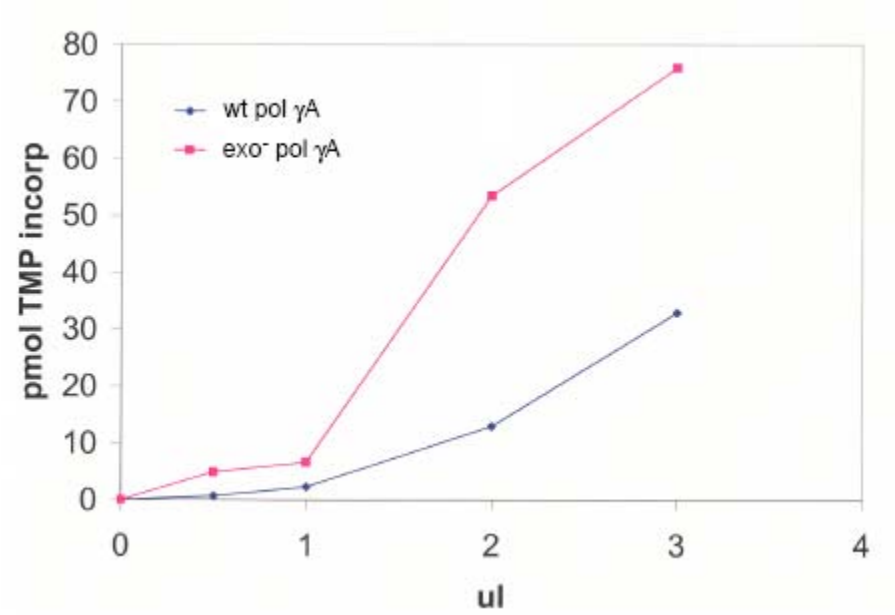

B

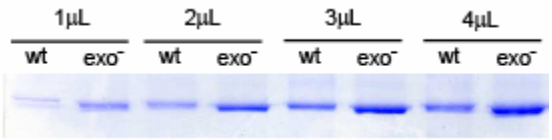

Figure 3.2: Comparison of the polymerase activity of exo⁻ pol γA to wt pol γA by reverse transcriptase assays. ***(A)*** Pol γ activity assays. The blue line is for wt pol γ and the red line is for exo⁻pol γA. ***(B)*** The amount of wt pol γA and exo⁻ pol γA used for the assays were compared on Coomassie Blue stained SDS PAGE.

Table 3.1. Study of the optimal solvent conditions for crystallization by Dynamic Light Scattering at 22°C.

Solvent Condition (20 mM HEPES)	Cumu MW(kDa)	I MW(kDa)	M MW(kDa)	Cumu P (%)	IP (%)	MP (%)
50 mM KCl, pH 7.0	341.7	364.4	260.6	51.2	21.2	21.3
100 mM KCl, pH 7.0	306.9	329.8	237.9	52.2	22.0	20.5
200 mM KCl, pH 7.0	334.9	383.4	218.3	51.7	29.5	27.1
300 mM KCl, pH 7.0	236.9	287.5	257.3	45.2	10.3	13.3
50 mM KCl, pH 7.5	420.9	422.3	273.9	57.2	25.6	23.7
100 mM KCl, pH 7.5	290.4	279.7	246.8	49.0	11.3	13.9
200 mM KCl, pH 7.5	339.6	390.0	217.3	52.3	31.3	26.8
300 mM KCl, pH 7.5	259.6	293.1	250.4	51.1	14.1	15.1
50 mM KCl, pH 8.0	461.1	411.8	302.8	57.5	19.2	21.1
100 mM KCl, pH 8.0	272.2	268.2	233.1	47.5	12.4	14.5
200 mM KCl, pH 8.0	359.8	518.5	205.6	64.3	39.6	33.6
300 mM KCl, pH 8.0	266.8	274.7	240.6	48.9	11.8	14.2
500 mM KCl, pH 8.0	218.7	252.5	217.1	52.5	13.6	14.6

The protein studied in this table was the co-purified holoenzyme. Optimal solvent conditions and DLS analysis results are colored in blue. I: Intensity, M: Mass, P: Polydispersity.

This figure was contributed by Elena Yakubovskaya and Zhixin Chen.

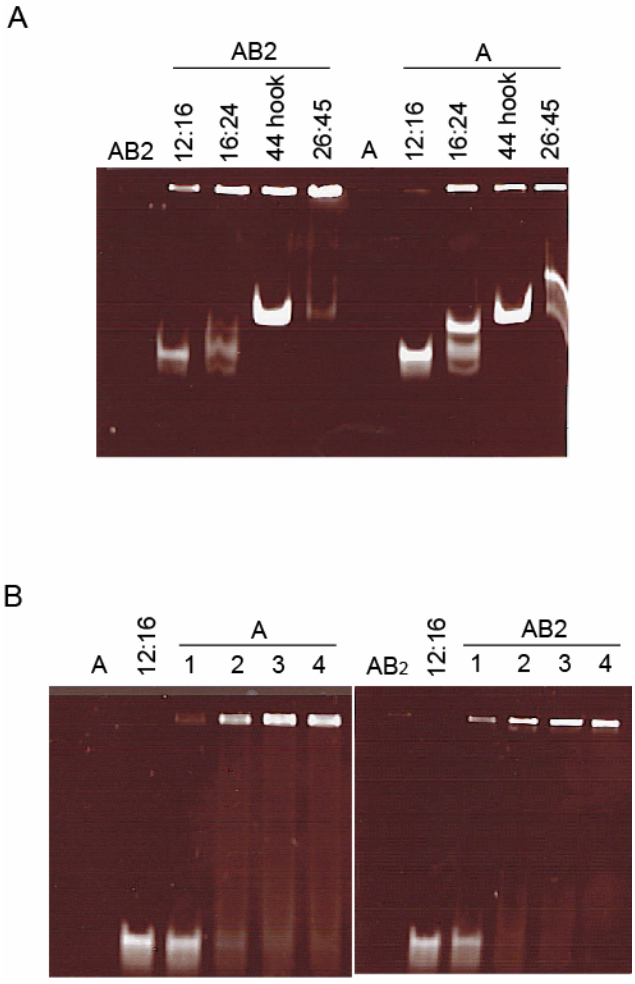

Figure 3.3: Binding of pol γA and holoenzyme to different primer-templates assayed by EMSA. ***(A)*** Assays comparing the binding stability of pol γA and holoenzyme on four different primer-templates. The concentration ratio between protein and primer-template DNA was 1:1.2. ***(B)*** Assays to determine the optimal binding concentration of pol γA and holoenzyme on the 12:16-mer primer-template. The concentration of 12:16-mer was 1 μM. The concentration of pol γA was 0.7, 1.0, 1.8, 2.5 μM in lane 1 to 4. The concentration of holoenzyme was 0.6, 1.2, 1.8 and 2.5 μM in lane 5 to 8.
This figure was contributed by Elena Yakubovskaya.

Table 3.2. Summary of crystallization trials of exo⁻ pol γA, reconstituted holoenzyme in the absence and in the presence of primer-template DNA.

	exo⁻pol γA	exo⁻pol γA +DNA	Reconstituted Holoenzyme	Reconstituted Holoenzyme+DNA	Crystallization Method
CSL I & II	+		+		**Hanging drop vapor diffusion**
CSS I & II	+		+		
Natrix	+	+	+	+	
Wizard I	+	+	+	+	
Wizard II	+		+		
HTS at HWI	+		+		**Microbatch under oil**
Optimix-1	+	+	+	+	**Free interface diffusion**
Optimix-2	+	+	+	+	
Optimix-4	+	+	+	+	
JBScreen 101 to 108	+		+		**Sitting drop vapor diffusion**

A plus sign indicates conditions that were tried. A blue (+) means promising conditions were obtained and a red (+) means crystals were obtained from this group of conditions. Proteins used for these crystallization trials were prepared as described in "Materials and Methods" of chapter 2 after appropriate concentration. The primer-template used for crystallization was the 12:16-mer shown in Fig 3.2.

This figure was contributed by Elena Yakubovskaya and Zhixin Chen.

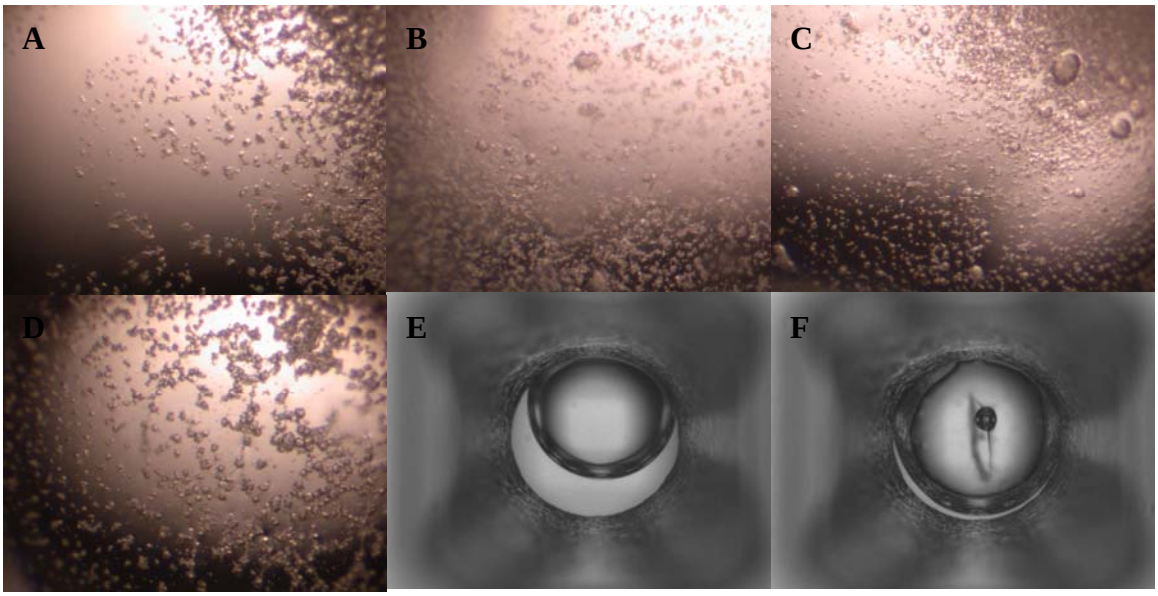

Figure 3.4: Some promising crystallization screening results for exo$^-$ pol γA. ***(A)*** Crystallization setup in 0.1 M MES pH 6.5, 6% (W/V) PEG 20,000MME (original protein concentration was 16 mg/ml) by the hanging drop vapor diffusion method. ***(B)***, ***(C)*** and ***(D)*** Crystallization follow-ups of ***A*** with additional additives: 4% (v/v) 2,2,2-trifluoroethanol, 0.7% (v/v) n-butanol, 3% (v/v) Dimethyl sulfoxide respectively. ***(E)*** and ***(F)*** Crystallization setup in 0.1 M LiCl, 0.1 M Caps pH 10.0, 20% (w/v) PEG 4000 (original protein concentration was 9 mg/ml) by the microbatch under oil method, ***E*** shows the drop right after the setup was made, and ***F*** shows a crystal that appeared in the drop after two weeks. We were, however, not able to reproduce this crystal by either the microbatch under oil method or the hanging drop vapor diffusion method.

A

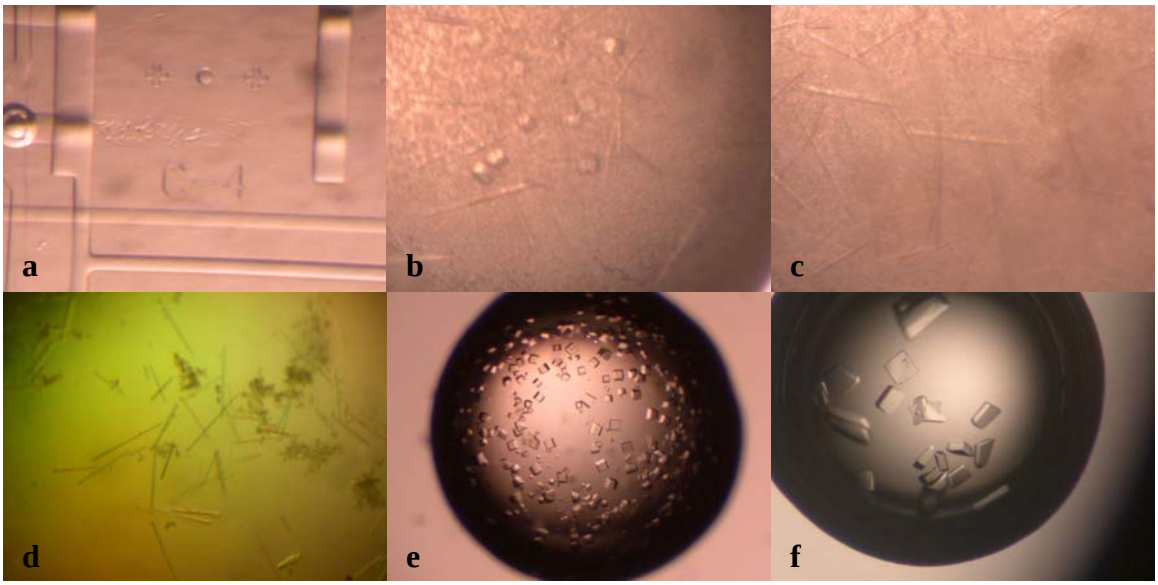

B

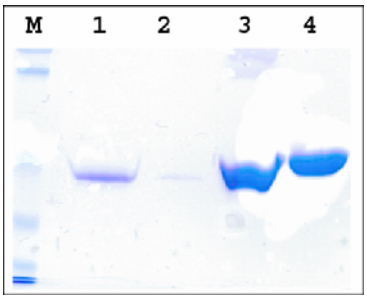

Figure 3.5: Crystals of human pol γB. ***(A.a)*** Original needle crystals obtained using the Fluidigm chip with the free interface diffusion method (the concentration of co-purified holoenzyme was 15.44 mg/ml; the crystallization condition was 20% PEG MME 5000, 1.0 M KSCN, 0.1 M Bis-Tris Propane pH 6.0 from OptiMix-2). ***b***, ***c*** and ***d*** show the reproduced crystals in 12% PEG MME 5000, 0.8 M KSCN, 0.1 M Bis-Tris Propane pH 6.0 by the hanging drop vapor diffusion method using the same holoenzyme protein as in ***a***. In ***d***, most of the precipitate in the setup has been removed. ***e*** and ***f*** show the optimal crystals achieved by mixing 1 µl of 10 mg/ml human pol γB protein solution with 1 µl of 10% PEG MME 5000, 0.6 M KSCN, 0.1 M Bis-Tris Propane pH 5.6 or with 1 µl of 5% PEG MME 5000, 0.6 M KSCN, 0.1 M Bis-Tris Propane pH 6.0 by the hanging drop vapor diffusion method. ***(B)*** Coomassie blue stained SDS PAGE showing the proteins of the crystals in panel ***A***. Lane 1: protein sample from the crystals collected from ***d***, lane 2: the cubic crystals collected from ***b***, lane 3: the crystals collected from **c**, and lane 4: the crystals collected from **e**. Since pol γB used in ***e*** and ***f*** of panel ***A*** was the 6xhistag fusion protein, it shifted up a little bit on the SDS PAGE compared to the non-tagged pol γB in the co-purified holoenzyme. Review "Purification of Proteins" in Chaper 2.

Table 3.3. Data collection and refinement of human pol γB	
Data collection statistics	
Space group	F2,2,2
Cell dimensions	a = 176.7 Å, b = 266.7 Å, and c = 267.1 Å
Maximum resolution (Å)	3.1
Completeness	99.7 (99.5)
Mean redundancy	4.4 (4.4)
R_{sym}	0.098 (0.557)
<I/sigI>	18.8 (2.9)
Refinement	
Resolution limits (Å)	20.0-3.1
Number of reflections	53327
R_{cryst} (R_{free})	0.208 (0.260)
Deviation from ideal values in	
Bond distances (Å)	0.017
Bond angles (°)	1.452
Chiral volumes (Å)	0.100
Planar groups (Å)	0.009
Torsion angles (°)	6.2/33.5/17.1
Ramachandran statistics	91.33%/7.14%/1.53%

$R_{sym}=\sum_{hkl}\sum_i| I_i-<I>| \sum_{hkl}\sum_i I_i$ where I_i is the i^{th} measurement and , <I> is the weighted mean of all measurements of I. <I/sigI> indicates the average of the intensity divided by its standard deviation. Numbers in parentheses refer to the respective highest resolution data shell in each data set. $R_{cryst}=\sum|\,|F_o|-|F_c|\,|/\sum|F_o|$ where F_o and F_c are the observed and calculated structure factor amplitudes. R_{free} is the same as R_{cryst} for 2% of the data randomly omitted from refinement. Ramachandran statistics indicate the fraction of residues in the most favored, allowed, and disallowed regions of the Ramachandran diagram as defined by MOLPROBITY (DAVIS and RICHARDSON 2004).

This figure was contributed by James J. Truglio and Zhixin Chen.

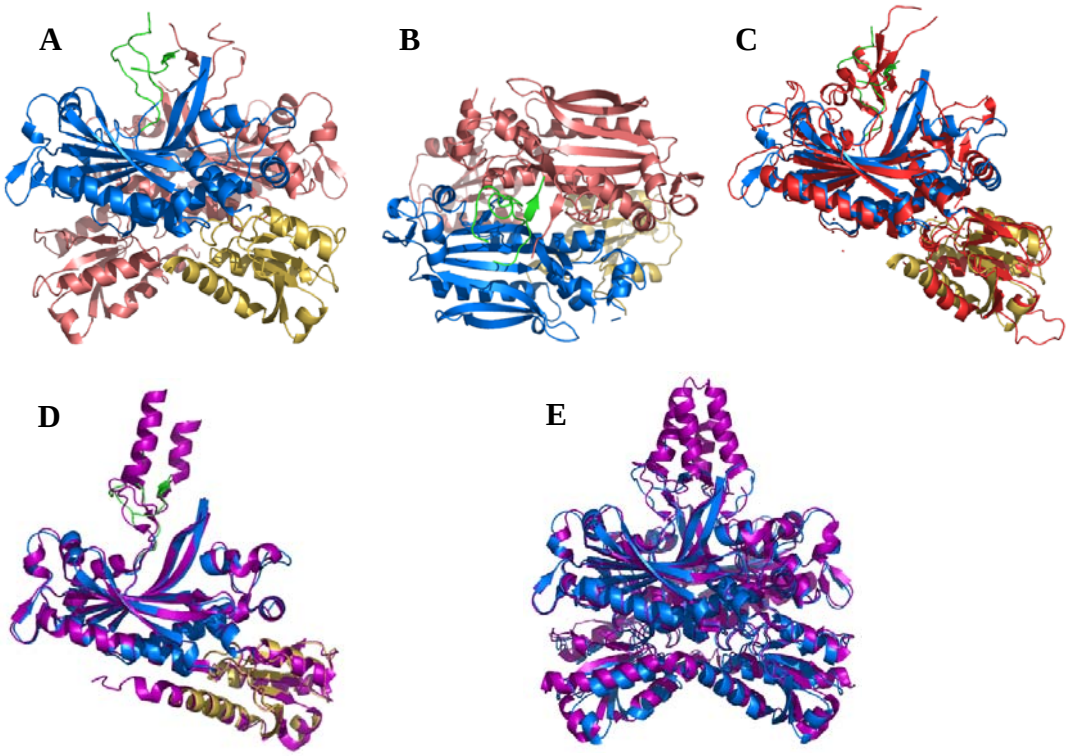

Figure 3.6: Crystal structure of human pol γB. ***(A)*** Overall structure of the human pol γB dimer, with one subunit colored by domains (the core domain is colored in marine, domain 2 is colored in green and the C-terminal domain is colored in yelloworange) and the other in salmon. ***(B)*** The structure in ***A*** is rotated 90° along the X-axis. ***(C)*** Superposition of human pol γB and a ttGRS monomer. Pol γB is colored by domains as in ***A***, and ttGRS (PDB code 1ATI) is shown in red. ***(D)*** Superposition of human and mouse pol γB monomers. The human monomer is colored by domains as in ***A***, and the mouse monomer is in purple. Note: the two helix bundle in the mouse structure is clearly visible whereas it is disordered in the human protein. ***(E)*** Superposition of human and mouse pol γB dimers. The human dimer is shown in marine and the mouse dimer is in purple.

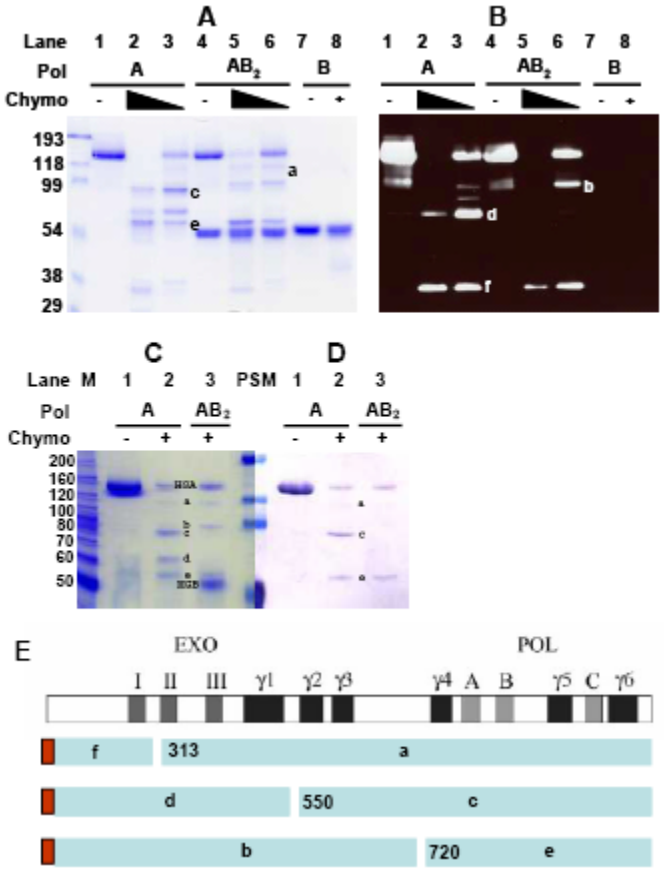

Figure 3.7: Protection of a chymotrypsin cleavage site in pol γA upon interaction with pol γB. Partial proteolysis of pol γ components was used to identify protease-resistant domains. Chymotrypsin was used to treat either N-terminally his-tagged pol γA alone *(lanes 1-3 in **A** & **B**, lanes 1-2 in **C** & **D**)*, or the same tagged pol γA complexed with untagged pol γB *(lanes 4-6 in **A** & **B**, lanes 3 in **C** & **D**)*, or pol γB alone (lanes 7, 8). Reactions were stopped by addition of PMSF and polypeptides were subjected to SDS-PAGE. ***(A)*** & ***(C)*** Coomassie stained gel analysis. ***(B)*** An immunoblot to detect N-terminal proteolytic fragments using an anti-histag antibody. ***(D)*** An immunoblot to detect C-terminal proteolytic fragments using an antibody to a sequence near the polymerase active site. Six major fragments of pol γA were identified as products of three proteolytic cleavages. Fragments ***b***, ***d*** and ***f*** identified in ***B*** retained the N-terminal his-tag. Fragments ***a***, ***c*** and ***e*** identified in ***A*** and ***C*** did not contain a his-tag, but were recognized to be C-terminal fragments in ***D***. No discrete degradation products of pol γB were observed under these conditions. ***(E)*** An interpretation of the pol γA fragments with respect to major sequence features. Subsequent N-terminal sequence analysis of fragments ***a***, ***c*** and ***e*** identified cleavage sites as shown in the figure and discussed in the text.

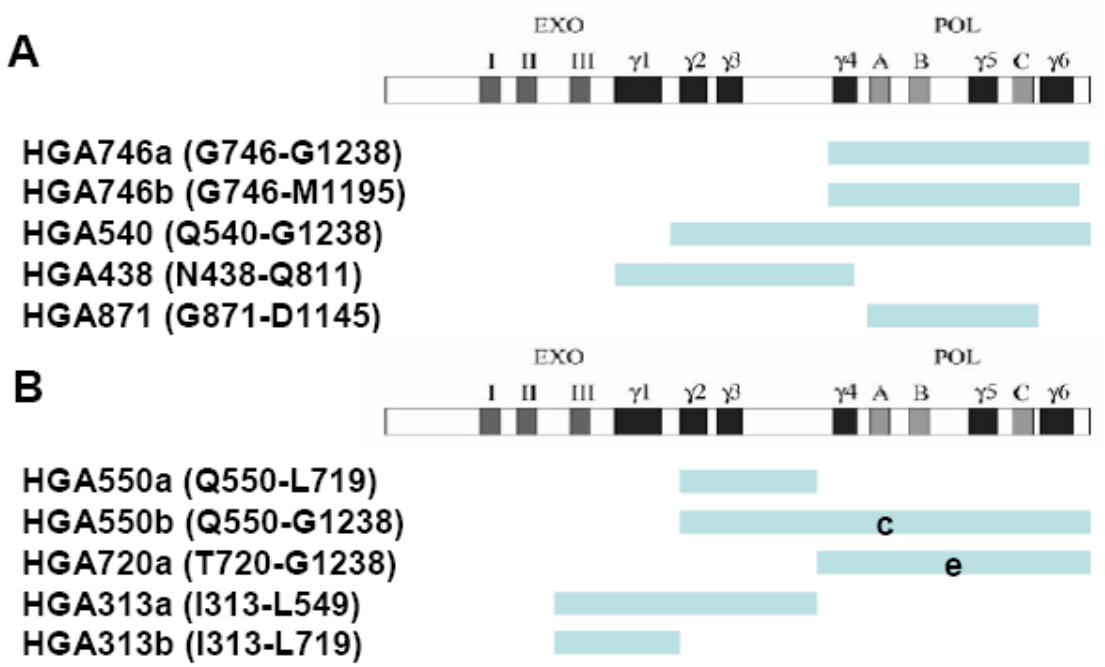

Figure 3.8: Interpretation of designed pol γA fragments with respect to major sequence features. The fragments in ***A*** were designed based on the predicted secondary structure of pol γA in addition to the results of limited proteolysis. The fragments in ***B*** were designed solely according to the results of limited proteolysis. ***c*** and ***e*** are corresponding to the fragments obtained by limited proteolysis digestion in Fig. 3.7.

Construct	Peptides	MW (kDa)	pKa	Tag	Solubility	Affinity to column	Notes
HGA746a	G746-G1238	55.51	8.61	N-6His	Moderate	Poor	Different Ni column tried and no improvement on affinity to the column.
				C-6His	Moderate	Poor	
				C-intein	Moderate	Poor	
HGA746b	G746-M1195	50.75	8.68	N-6His	Moderate	Poor	--
HGA540	Q540-G1238	78.57	8.14	N-6His	Moderate	Poor	--
HGA438	N438-Q811	42.09	5.71	N-6His	Moderate	Poor	1.Different lysis buffer tried and no improvement on both solubility and affinity to Ni column. 2.Different ion exchange column. 3.Coexpression with CBP-HGB.
				N-10His	Moderate	Poor	
				C-6His	Moderate	Poor	
				None	Moderate	--	
HGA871	G871-D1145	31.25	6.22	N-6His	Moderate	Poor	1.Different lysis buffer tried and no improvement on both solubility and affinity to Ni column. 2.Amonium sulfate precipitation. 3.Different ion exchange column.
				N-10His	Moderate	Poor	
				C-6His	Moderate	Poor	
				C-intein	Poor	Poor	
HGA550a	Q550-L719	19.18	6.58	N-6His	Moderate	Moderate	--
				N-GST	--	--	
HGA550b	Q550-G1238	77.45	8.16	N-6His	--	--	--
HGA720a	T720-G1238	58.38	8.45	N-6His	--	--	--
HGA331a	I331-L549	27.16	5.30	N-6His	Moderate	--	--
				H-GST	--	--	--
HGA331b	I331-L719	46.32	5.73	N-6His	Moderate	--	--
				N-GST	--	--	--

Table 3.4: Summary of pol γA constructs. Ni affinity columns are Ni-NTA (Qiagen), Ni-IDA (Amersham Biosciences), and Talon metal affinity resin (Clontech). Ion exchang columns have been tested are DEAE sepharose, Sp sepharose, ANX sepharose, Mono S, and Mono Q (all from Amersham Biosciences). Constructs colored in red indicate that extensive attempts to improve the purification of these constructs have been performed.

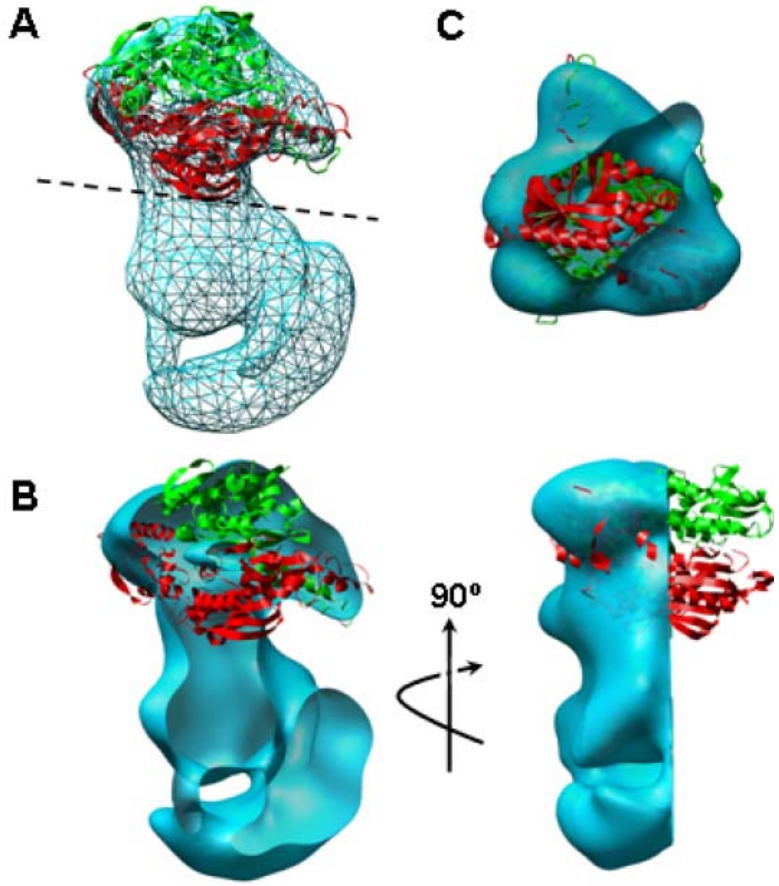

Figure 3.9: Docking the X-ray structure of human DNA pol γB onto the 3D model of the pol γ holoenzyme. The structure of the pol γ holoenzyme was obtained at 17 Å resolution using negative-stain electron microscopy method. Different pol γB subunits are colored red and green**.** ***(A)*** View of the entire model. ***(B)*** Clipped model in two orthogonal orientations. ***(C)*** The model is cut near the surface delimiting catalytic and accessory parts of the molecule. The level and direction of the cut is shown as a dashed line in Panel ***A***. It can be clearly seen that the contact area between the B dimer *(top)* and the pol γ catalytic subunit *(bottom)* is formed mostly by one *(red)* subunit of the dimer.
Yakubovskaya and Bogenhagen, et al, submitted

CHAPTER 4: Concluding Discussion

Mitochondrial DNA polymerase γ (pol γ) is responsible for replication and repair of mtDNA and is mutated in individuals with genetic disorders such as chronic external ophthalmoplegia, Parkinsonism, Alpers syndrome etc (LUOMA *et al.* 2004; NAVIAUX and NGUYEN 2004; VAN GOETHEM *et al.* 2001). Pol γ is also an adventitious target for toxic side effects of several antiviral compounds, and mutation of its proofreading exonuclease leads to accelerated aging in mouse models (KUJOTH *et al.* 2005; TRIFUNOVIC *et al.* 2004). Human pol γ is isolated from mitochondria as a complex containing two subunits, a catalytic subunit, pol γA, of 139 kDa and an accessory subunit, pol γB, of 53 kDa. The catalytic subunit is a family A DNA polymerase with separate polymerase and 3'→5' exonuclease domains. The processivity and substrate binding properties of pol γA are enhanced by complex formation with the accessory subunit. Initial characterization of pol γ suggested that the enzyme forms a heterodimer containing one copy of each subunit. However, when the crystal structure of mouse pol γB was solved, it became apparent that this accessory factor is itself a homodimer with remarkable structural similarity to prokaryotic tRNA synthetases (PDB code 1G5H (CARRODEGUAS *et al.* 2001)).

The work in this dissertation describes the first extensive investigation of the assembly of the pol γ holoenzyme. The results of analytical ultracentrifugation equilibrium experiments clearly show that pol γB forms a dimer in solution. Thus it is very unlikely that the dimerization of pol γB is a crystal packing artifact. Further studies by analytical gel filtration and isothermal titration calorimetry established that the pol γB dimer binds tightly to the pol γA monomer to form a heterotrimer with the structure AB_2.

This is the first detailed study of the association of these subunits in the absence of DNA. Moreover, the K_D of 27 nM for the subunit interaction determined by SPR, agrees well with the binding affinity measured in the presence of DNA in the enzyme kinetic studies of Johnson *et al* (JOHNSON et al. 2000). Meanwhile, to take advantage of the differences between the dimeric wt pol γB and the monomeric pol γBΔI4, the contribution of the accessory subunit to the interaction of the polymerase with DNA primer-templates was explored. Results of both electrophoretic mobility shift assays and SPR experiments showed that the heterodimeric enzyme formed by association of pol γBΔI4 to pol γA binds tightly to primer-template and dissociates slowly in the presence of competitor primer-template, demonstrating that one pol γB molecule contributes most of the interaction energy with pol γA. This is further supported by the 3D model of the human pol γ holoenzyme according to our recent EM studies. In this model, one pol γB subunit dominates the interaction surface with the catalytic subunit while the second B subunit is largely exposed to solvent. However, the tight binding of pol γBΔI4 to pol γA and the consequent stabilization of the enzyme on primer-templates does not lead to stimulation of polymerase activity, revealing that the second molecule in the pol γB dimer plays an important functional role. Therefore, the functional human holoenzyme forms a heterotrimer with two copies of the processivity factor and one copy of the catalytic subunit.

To view the interaction of the two pol γ subunits at the atomic level and to elucidate the mechanism whereby the accessory subunit keeps the catalytic subunit engaged on the

primer-template and stimulates the activity of the enzyme, crystallization of pol γ has been attempted in this dissertation, for both the catalytic subunit alone and for the reconstituted holoenzyme in the absence and in the presence of primer-template DNA. Although a sufficient quantity of homogeneous protein was obtained after a simplified preparation scheme was established, no crystal of pol γA or the holoenzyme was obtained. The crystallization of the recombinant holoenzyme in the presence of DNA was expected to be more promising, because pol γB can protect pol γA from oxidation and the primer-template is believed to stabilize the conformation of pol γA by reducing the flexibility of the fingers and thumb domains upon DNA binding. Another possible advantage was that, upon the formation of the protein-DNA complex, the solubility of pol γ would be improved and thus the protein solution used for crystallization could contain a relatively low concentration of salt, which would facilitate the process of crystallization. However, the DNA oligo used for co-crystallization with pol γ might not be the proper one. More attempts should be conducted to screen proper DNA lengths and a number of DNA sequences should be applied rather than extensive crystallization conditions.

The human pol γB structure was solved at 3.1 Å resolution by molecular replacement. As expected from the high sequence conservation, the human pol γB structure closely resembles the structure of its mouse homolog. However, both structures are not homologous to other processivity factors such as PCNA and the β subunit of *E.coli* pol III that form toroidal structures to stabilize polymerase binding to DNA by encircling the DNA duplex (KRISHNA *et al.* 1994). The structure of the pol γB dimer

doesn't provide any clue to explain the mechanism whereby this protein keeps the catalytic subunit engaged on the primer-template. The interaction between pol γB_2 and pol γA is most likely structurally distinct compared to that of most other pairs of processivity factors with their cognate polymerases.

For a better understanding of the subunit interaction, regions within pol γB and pol γA required for complex formation were studied by limited proteolysis experiments. A pol γB interacting domain was mapped to the spacer region of pol γA which is located between the catalytic domain and the exonuclease domain of pol γA. Our result is consistent with the biochemical and mutagenesis studies on *Drosophila* pol γ (FAN and KAGUNI 2001; LUO and KAGUNI 2005; LUOMA *et al.* 2005) which suggested that the two subunits interact with each other in more than one region and part of the pol γB interaction domain of pol γA might be located in some of the conserved sequences of the linker region, but this model might have predicted a more extensive protection against proteolysis. The EM model obtained for the pol γ holoenzyme features a rather restrictive interaction between pol γA and mainly one pol γB protomer.

Using the limited proteolysis results as a guide, a number of pol γA constructs, containing the polymerase domain and/or the spacer region, have been designed to remove the flexible regions for crystallization and interaction studies with pol γB. These pol γA fragments were cloned into vectors for overexpression in *E.coli* rather than insect cells. This might be one of the reasons that the folding and conformation of these fragments did not produce soluble monomeric protein. The protein tended to form

aggregates during purification. Furthermore, attempts to compare the limited proteolysis of pol γA and the holoenzyme in the presence of DNA might provide more information to identify the pol γA fragments suitable for X-ray crystallographic studies.

In summary, the work in this dissertation has used a variety of biophysical and functional approaches to study the interaction of the human pol γ catalytic subunit with both the wild-type accessory factor, pol γB, and a deletion derivative that is unable to dimerize and consequently is impaired in its ability to stimulate processive DNA synthesis. Our studies clearly showed that the functional human holoenzyme contains two subunits of the accessory factor and one catalytic subunit, thereby forming a heterotrimer.

The structure of pol γ seems to be variable, ranging from a single catalytic subunit in yeast to a heterodimer in *Drosophila* and a heterotrimer in mammals. It will be interesting to compare the structures of a variety of pol γ proteins. According to the primary sequence alignment of *Drosophila* pol γB and human pol γB, the only significant internal deletion in the alignment of the two proteins suggests that the *Drosophila* protein contains a discrete deletion of domain 2 of the mammalian proteins containing the two-helix structure, a deletion similar to that used to generate human pol γBΔI4. Our observation that pol γBΔI4 is able to stabilize pol γ on primer-templates suggests that this deleted protein could retain substantial function. Additional mutations may have occurred to enable monomeric *Drosophila* pol γB to stimulate its catalytic partner. *S. cerevisiae* pol γ, containing only one catalytic subunit, has been reported to be highly processive (ERIKSSON *et al.* 1995). However, the DNA polymerase assay used to examine the

processivity of *S. cerevisiae* pol γ in Eriksson et al. 1995 is not very convincing. Unlabeled primer-template should be used as a competitor in the assay to avoid the possibility that pol γ that dissociates from the labeled primer-template may rebind a labeled molecule. Then the processivity of the enzyme might be evaluated properly. It will be interesting to know if the 200-aa C-terminal extension of *S. cerevisiae* pol γ, instead of pol γB, contributes to the processivity of *S. cerevisiae* pol γ.

Our limited proteolysis analysis mapped a pol γB interaction part of pol γA which is the spacer region separating the catalytic domain and the exonuclease domain of pol γA. Additional mutational and structural studies on human pol γ are necessary to understand the interactions between the two subunits and the processivity mechanism.

References:

ANDERSON, S., A. T. BANKIER, B. G. BARRELL, M. H. DE BRUIJN, A. R. COULSON *et al.*, 1981 Sequence and organization of the human mitochondrial genome. Nature **290:** 457-465.

APPLETON, B. A., A. LOREGIAN, D. J. FILMAN, D. M. COEN and J. M. HOGLE, 2004 The cytomegalovirus DNA polymerase subunit UL44 forms a C clamp-shaped dimer. Mol Cell **15:** 233-244.

ATTARDI, G., 1985 Animal mitochondrial DNA: an extreme example of genetic economy. Int Rev Cytol **93:** 93-145.

ATTARDI, G., and G. SCHATZ, 1988 Biogenesis of mitochondria. Annu Rev Cell Biol **4:** 289-333.

BEDFORD, E., S. TABOR and C. C. RICHARDSON, 1997 The thioredoxin binding domain of bacteriophage T7 DNA polymerase confers processivity on Escherichia coli DNA polymerase I. Proc Natl Acad Sci U S A **94:** 479-484.

BEESE, L. S., V. DERBYSHIRE and T. A. STEITZ, 1993 Structure of DNA polymerase I Klenow fragment bound to duplex DNA. Science **260:** 352-355.

BIENSTOCK, R. J., and W. C. COPELAND, 2004 Molecular insights into NRTI inhibition and mitochondrial toxicity revealed from a structural model of the human mitochondrial DNA polymerase. Mitochondrion **4:** 203-213.

BOGENHAGEN, D. F., 1999 Repair of mtDNA in vertebrates. Am J Hum Genet **64:** 1276-1281.

BOGENHAGEN, D. F., and D. A. CLAYTON, 2003a Concluding remarks: The mitochondrial DNA replication bubble has not burst. Trends Biochem Sci **28:** 404-405.

BOGENHAGEN, D. F., and D. A. CLAYTON, 2003b The mitochondrial DNA replication bubble has not burst. Trends Biochem Sci **28:** 357-360.

BOLDEN, A., G. P. NOY and A. WEISSBACH, 1977 DNA polymerase of mitochondria is a gamma-polymerase. J Biol Chem **252:** 3351-3356.

BOWMAKER, M., M. Y. YANG, T. YASUKAWA, A. REYES, H. T. JACOBS *et al.*, 2003

Mammalian mitochondrial DNA replicates bidirectionally from an initiation zone. J Biol Chem **278:** 50961-50969.

BRAITHWAITE, D. K., and J. ITO, 1993 Compilation, alignment, and phylogenetic relationships of DNA polymerases. Nucleic Acids Res **21:** 787-802.

BREYER, W. A., and B. W. MATTHEWS, 2001 A structural basis for processivity. Protein Sci **10:** 1699-1711.

BROWN, T. A., C. CECCONI, A. N. TKACHUK, C. BUSTAMANTE and D. A. CLAYTON, 2005 Replication of mitochondrial DNA occurs by strand displacement with alternative light-strand origins, not via a strand-coupled mechanism. Genes Dev **19:** 2466-2476.

BURGERS, P. M., E. V. KOONIN, E. BRUFORD, L. BLANCO, K. C. BURTIS *et al.*, 2001 Eukaryotic DNA polymerases: proposal for a revised nomenclature. J Biol Chem **276:** 43487-43490.

CANN, I. K., and Y. ISHINO, 1999 Archaeal DNA replication: identifying the pieces to solve a puzzle. Genetics **152:** 1249-1267.

CARRODEGUAS, J. A., and D. F. BOGENHAGEN, 2000 Protein sequences conserved in prokaryotic aminoacyl-tRNA synthetases are important for the activity of the processivity factor of human mitochondrial DNA polymerase. Nucleic Acids Res **28:** 1237-1244.

CARRODEGUAS, J. A., R. KOBAYASHI, S. E. LIM, W. C. COPELAND and D. F. BOGENHAGEN, 1999 The accessory subunit of Xenopus laevis mitochondrial DNA polymerase gamma increases processivity of the catalytic subunit of human DNA polymerase gamma and is related to class II aminoacyl-tRNA synthetases. Mol Cell Biol **19:** 4039-4046.

CARRODEGUAS, J. A., K. G. PINZ and D. F. BOGENHAGEN, 2002 DNA binding properties of human pol gammaB. J Biol Chem **277:** 50008-50014.

CARRODEGUAS, J. A., K. THEIS, D. F. BOGENHAGEN and C. KISKER, 2001 Crystal structure and deletion analysis show that the accessory subunit of mammalian DNA polymerase gamma, Pol gamma B, functions as a homodimer. Mol Cell **7:** 43-54.

CHAN, S. S., M. J. LONGLEY and W. C. COPELAND, 2005 The common A467T mutation in the human mitochondrial DNA polymerase (POLG) compromises catalytic

efficiency and interaction with the accessory subunit. J Biol Chem **280:** 31341-31346.

CLAYTON, D. A., 1982 Replication of animal mitochondrial DNA. Cell **28:** 693-705.

CLAYTON, D. A., 1991 Nuclear gadgets in mitochondrial DNA replication and transcription. Trends Biochem Sci **16:** 107-111.

COLLABORATIVE COMPUTATIONAL PROJECT, N., 1994 The CCP4 suite: programs for protein crystallography. Acta Crystallogr D Biol Crystallogr **50:** 760-763.

CROTEAU, D. L., and V. A. BOHR, 1997 Repair of oxidative damage to nuclear and mitochondrial DNA in mammalian cells. J Biol Chem **272:** 25409-25412.

CROTEAU, D. L., R. H. STIERUM and V. A. BOHR, 1999 Mitochondrial DNA repair pathways. Mutat Res **434:** 137-148.

DAVIS, A. F., P. A. ROPP, D. A. CLAYTON and W. C. COPELAND, 1996 Mitochondrial DNA polymerase gamma is expressed and translated in the absence of mitochondrial DNA maintenance and replication. Nucleic Acids Res **24:** 2753-2759.

DAVIS, L. W., and D. C. RICHARDSON, 2004 MOLPROBITY: structure validation and all-atom contact analysis for nucleic acids and their complexes. Nucleic Acids Research **32:** W615-W619.

DOUBLIE, S., S. TABOR, A. M. LONG, C. C. RICHARDSON and T. ELLENBERGER, 1998 Crystal structure of a bacteriophage T7 DNA replication complex at 2.2 A resolution. Nature **391:** 251-258.

EOM, S. H., J. WANG and T. A. STEITZ, 1996 Structure of Taq polymerase with DNA at the polymerase active site. Nature **382:** 278-281.

ERIKSSON, S., B. XU and D. A. CLAYTON, 1995 Efficient incorporation of anti-HIV deoxynucleotides by recombinant yeast mitochondrial DNA polymerase. J Biol Chem **270:** 18929-18934.

FAN, L., and L. S. KAGUNI, 2001 Multiple regions of subunit interaction in Drosophila mitochondrial DNA polymerase: three functional domains in the accessory subunit. Biochemistry **40:** 4780-4791.

FAN, L., S. KIM, C. L. FARR, K. T. SCHAEFER, K. M. RANDOLPH *et al.*, 2006 A novel

processive mechanism for DNA synthesis revealed by structure, modeling and mutagenesis of the accessory subunit of human mitochondrial DNA polymerase. J Mol Biol **358:** 1229-1243.

FAN, L., P. C. SANSCHAGRIN, L. S. KAGUNI and L. A. KUHN, 1999 The accessory subunit of mtDNA polymerase shares structural homology with aminoacyl-tRNA synthetases: implications for a dual role as a primer recognition factor and processivity clamp. Proc Natl Acad Sci U S A **96:** 9527-9532.

FERNANDEZ-SILVA, P., J. A. ENRIQUEZ and J. MONTOYA, 2003 Replication and transcription of mammalian mitochondrial DNA. Exp Physiol **88:** 41-56.

FOURY, F., 1989 Cloning and sequencing of the nuclear gene MIP1 encoding the catalytic subunit of the yeast mitochondrial DNA polymerase. J Biol Chem **264:** 20552-20560.

FRIDLENDER, B., M. FRY, A. BOLDEN and A. WEISSBACH, 1972 A new synthetic RNA-dependent DNA polymerase from human tissue culture cells (HeLa-fibroblast-synthetic oligonucleotides-template-purified enzymes). Proc Natl Acad Sci U S A **69:** 452-455.

FRIED, M., and D. M. CROTHERS, 1981 Equilibria and kinetics of lac repressor-operator interactions by polyacrylamide gel electrophoresis. Nucleic Acids Res **9:** 6505-6525.

GILL, S. C., and P. H. VON HIPPEL, 1989 Calculation of protein extinction coefficients from amino acid sequence data. Anal Biochem **182:** 319-326.

GRAVES, S. W., A. A. JOHNSON and K. A. JOHNSON, 1998 Expression, purification, and initial kinetic characterization of the large subunit of the human mitochondrial DNA polymerase. Biochemistry **37:** 6050-6058.

GRAY, H., and T. W. WONG, 1992 Purification and identification of subunit structure of the human mitochondrial DNA polymerase. J Biol Chem **267:** 5835-5841.

GRAZIEWICZ, M. A., M. J. LONGLEY, R. J. BIENSTOCK, M. ZEVIANI and W. C. COPELAND, 2004 Structure-function defects of human mitochondrial DNA polymerase in autosomal dominant progressive external ophthalmoplegia. Nat Struct Mol Biol **11:** 770-776.

GRAZIEWICZ, M. A., M. J. LONGLEY and W. C. COPELAND, 2006 DNA polymerase gamma

in mitochondrial DNA replication and repair. Chem Rev **106:** 383-405.

HOLT, I. J., and H. T. JACOBS, 2003 Response: The mitochondrial DNA replication bubble has not burst. Trends Biochem Sci **28:** 355-356.

HOLT, I. J., H. E. LORIMER and H. T. JACOBS, 2000 Coupled leading- and lagging-strand synthesis of mammalian mitochondrial DNA. Cell **100:** 515-524.

INSDORF, N. F., and D. F. BOGENHAGEN, 1989 DNA polymerase gamma from Xenopus laevis. I. The identification of a high molecular weight catalytic subunit by a novel DNA polymerase photolabeling procedure. J Biol Chem **264:** 21491-21497.

ITO, J., and D. K. BRAITHWAITE, 1991 Compilation and alignment of DNA polymerase sequences. Nucleic Acids Res **19:** 4045-4057.

JERUZALMI, D., M. O'DONNELL and J. KURIYAN, 2001 Crystal structure of the processivity clamp loader gamma (gamma) complex of E. coli DNA polymerase III. Cell **106:** 429-441.

JOHNSON, A. A., Y. TSAI, S. W. GRAVES and K. A. JOHNSON, 2000 Human mitochondrial DNA polymerase holoenzyme: reconstitution and characterization. Biochemistry **39:** 1702-1708.

JONES, T. A., J. Y. ZOU, S. W. COWAN and M. KJELDGAARD, 1991 Improved methods for building protein models in electron density maps and the location of errors in these models. Acta Crystallogr A **47 (Pt 2):** 110-119.

JORDAN, S. R., T. V. WHITCOMBE, J. M. BERG and C. O. PABO, 1985 Systematic variation in DNA length yields highly ordered repressor-operator cocrystals. Science **230:** 1383-1385.

KAGUNI, L. S., 2004 DNA polymerase gamma, the mitochondrial replicase. Annu Rev Biochem **73:** 293-320.

KELMAN, Z., and M. O'DONNELL, 1995 Structural and functional similarities of prokaryotic and eukaryotic DNA polymerase sliding clamps. Nucleic Acids Res **23:** 3613-3620.

KIEFER, J. R., C. MAO, J. C. BRAMAN and L. S. BEESE, 1998 Visualizing DNA replication in a catalytically active Bacillus DNA polymerase crystal. Nature **391:** 304-307.

KIEFER, J. R., C. MAO, C. J. HANSEN, S. L. BASEHORE, H. H. HOGREFE *et al.*, 1997 Crystal structure of a thermostable Bacillus DNA polymerase I large fragment at 2.1 A resolution. Structure **5:** 95-108.

KIM, Y., S. H. EOM, J. WANG, D. S. LEE, S. W. SUH *et al.*, 1995 Crystal structure of Thermus aquaticus DNA polymerase. Nature **376:** 612-616.

KONG, X. P., R. ONRUST, M. O'DONNELL and J. KURIYAN, 1992 Three-dimensional structure of the beta subunit of E. coli DNA polymerase III holoenzyme: a sliding DNA clamp. Cell **69:** 425-437.

KOROLEV, S., M. NAYAL, W. M. BARNES, E. DI CERA and G. WAKSMAN, 1995 Crystal structure of the large fragment of Thermus aquaticus DNA polymerase I at 2.5-A resolution: structural basis for thermostability. Proc Natl Acad Sci U S A **92:** 9264-9268.

KRISHNA, T. S., X. P. KONG, S. GARY, P. M. BURGERS and J. KURIYAN, 1994 Crystal structure of the eukaryotic DNA polymerase processivity factor PCNA. Cell **79:** 1233-1243.

KUJOTH, G. C., A. HIONA, T. D. PUGH, S. SOMEYA, K. PANZER *et al.*, 2005 Mitochondrial DNA mutations, oxidative stress, and apoptosis in mammalian aging. Science **309:** 481-484.

LANG, B. F., M. W. GRAY and G. BURGER, 1999 Mitochondrial genome evolution and the origin of eukaryotes. Annu Rev Genet **33:** 351-397.

LEBOWITZ, J., M. S. LEWIS and P. SCHUCK, 2002 Modern analytical ultracentrifugation in protein science: a tutorial review. Protein Sci **11:** 2067-2079.

LEFAI, E., M. A. FERNANDEZ-MORENO, A. ALAHARI, L. S. KAGUNI and R. GARESSE, 2000 Differential regulation of the catalytic and accessory subunit genes of Drosophila mitochondrial DNA polymerase. J Biol Chem **275:** 33123-33133.

LEWIS, W., E. S. LEVINE, B. GRINIUVIENE, K. O. TANKERSLEY, J. M. COLACINO *et al.*, 1996 Fialuridine and its metabolites inhibit DNA polymerase gamma at sites of multiple adjacent analog incorporation, decrease mtDNA abundance, and cause mitochondrial structural defects in cultured hepatoblasts. Proc Natl Acad Sci U S A **93:** 3592-3597.

LI, Y., S. KOROLEV and G. WAKSMAN, 1998 Crystal structures of open and closed forms

of binary and ternary complexes of the large fragment of Thermus aquaticus DNA polymerase I: structural basis for nucleotide incorporation. Embo J **17:** 7514-7525.

LIM, S. E., M. J. LONGLEY and W. C. COPELAND, 1999 The mitochondrial p55 accessory subunit of human DNA polymerase gamma enhances DNA binding, promotes processive DNA synthesis, and confers N-ethylmaleimide resistance. J Biol Chem **274:** 38197-38203.

LONGLEY, M. J., D. NGUYEN, T. A. KUNKEL and W. C. COPELAND, 2001 The fidelity of human DNA polymerase gamma with and without exonucleolytic proofreading and the p55 accessory subunit. J Biol Chem **276:** 38555-38562.

LONGLEY, M. J., R. PRASAD, D. K. SRIVASTAVA, S. H. WILSON and W. C. COPELAND, 1998a Identification of 5'-deoxyribose phosphate lyase activity in human DNA polymerase gamma and its role in mitochondrial base excision repair in vitro. Proc Natl Acad Sci U S A **95:** 12244-12248.

LONGLEY, M. J., P. A. ROPP, S. E. LIM and W. C. COPELAND, 1998b Characterization of the native and recombinant catalytic subunit of human DNA polymerase g: Identification of residues critical for exonuclease activity and dideoxynucleotide sensitivity. Biochemistry **37:** 10529-10539.

LONGLEY, M. J., P. A. ROPP, S. E. LIM and W. C. COPELAND, 1998c Characterization of the native and recombinant catalytic subunit of human DNA polymerase gamma: identification of residues critical for exonuclease activity and dideoxynucleotide sensitivity. Biochemistry **37:** 10529-10539.

LOREGIAN, A., B. A. APPLETON, J. M. HOGLE and D. M. COEN, 2004 Residues of human cytomegalovirus DNA polymerase catalytic subunit UL54 that are necessary and sufficient for interaction with the accessory protein UL44. J Virol **78:** 158-167.

LUCAS, P., J. P. LASSERRE, J. PLISSONNEAU and M. CASTROVIEJO, 2004 Absence of accessory subunit in the DNA polymerase gamma purified from yeast mitochondria. Mitochondrion **4:** 13-20.

LUO, N., and L. S. KAGUNI, 2005 Mutations in the spacer region of Drosophila mitochondrial DNA polymerase affect DNA binding, processivity, and the balance between Pol and Exo function. J Biol Chem **280:** 2491-2497.

LUOMA, P., A. MELBERG, J. O. RINNE, J. A. KAUKONEN, N. N. NUPPONEN *et al.*, 2004

Parkinsonism, premature menopause, and mitochondrial DNA polymerase gamma mutations: clinical and molecular genetic study. Lancet **364:** 875-882.

LUOMA, P. T., N. LUO, W. N. LOSCHER, C. L. FARR, R. HORVATH *et al.*, 2005 Functional defects due to spacer-region mutations of human mitochondrial DNA polymerase in a family with an ataxia-myopathy syndrome. Hum Mol Genet **14:** 1907-1920.

MICHIKAWA, Y., F. MAZZUCCHELLI, N. BRESOLIN, G. SCARLATO and G. ATTARDI, 1999 Aging-dependent large accumulation of point mutations in the human mtDNA control region for replication. Science **286:** 774-779.

MINOR, W., M. CYMBOROWSKI, Z. OTWINOWSKI and M. CHRUSZCZ, 2006 HKL-3000: the integration of data reduction and structure solution--from diffraction images to an initial model in minutes. Acta Crystallogr D Biol Crystallogr **62:** 859-866.

MINOR, W., and Z. OTWINOWSKI, 1997 Processing of X-ray diffraction data collected in oscillation mode. Methods Enzymology **276:** 307-326.

MURAKAMI, E., J. Y. FENG, H. LEE, J. HANES, K. A. JOHNSON *et al.*, 2003 Characterization of novel reverse transcriptase and other RNA-associated catalytic activities by human DNA polymerase gamma: importance in mitochondrial DNA replication. J Biol Chem **278:** 36403-36409.

MURSHUDOV, G. N., A. A. VAGIN and E. J. DODSON, 1997 Refinement of macromolecular structures by the maximum-likelihood method. Acta Crystallogr D Biol Crystallogr **53:** 240-255.

NAVIAUX, R. K., and K. V. NGUYEN, 2004 POLG mutations associated with Alpers' syndrome and mitochondrial DNA depletion. Ann Neurol **55:** 706-712.

OHMORI, H., E. C. FRIEDBERG, R. P. FUCHS, M. F. GOODMAN, F. HANAOKA *et al.*, 2001 The Y-family of DNA polymerases. Mol Cell **8:** 7-8.

OLLIS, D. L., P. BRICK, R. HAMLIN, N. G. XUONG and T. A. STEITZ, 1985 Structure of large fragment of Escherichia coli DNA polymerase I complexed with dTMP. Nature **313:** 762-766.

OLSON, M. W., Y. WANG, R. H. ELDER and L. S. KAGUNI, 1995 Subunit structure of mitochondrial DNA polymerase from Drosophila embryos. Physical and immunological studies. J Biol Chem **270:** 28932-28937.

PINZ, K. G., and D. F. BOGENHAGEN, 1998 Efficient repair of abasic sites in DNA by mitochondrial enzymes. Mol Cell Biol **18:** 1257-1265.

PINZ, K. G., and D. F. BOGENHAGEN, 2000 Characterization of a catalytically slow AP lyase activity in DNA polymerase gamma and other family A DNA polymerases. J Biol Chem **275:** 12509-12514.

RECORD, M. T., JR., P. L. DEHASETH and T. M. LOHMAN, 1977 Interpretation of monovalent and divalent cation effects on the lac repressor-operator interaction. Biochemistry **16:** 4791-4796.

SAWYER, D. E., and B. VAN HOUTEN, 1999 Repair of DNA damage in mitochondria. Mutat Res **434:** 161-176.

SCHMITT, M. E., and D. A. CLAYTON, 1993 Conserved features of yeast and mammalian mitochondrial DNA replication. Curr Opin Genet Dev **3:** 769-774.

SCHULTZ, R. A., S. J. SWOAP, L. D. MCDANIEL, B. ZHANG, E. C. KOON *et al.*, 1998 Differential expression of mitochondrial DNA replication factors in mammalian tissues. J Biol Chem **273:** 3447-3451.

SHADEL, G. S., and D. A. CLAYTON, 1997 Mitochondrial DNA maintenance in vertebrates. Annu Rev Biochem **66:** 409-435.

STEITZ, T. A., 1999 DNA polymerases: structural diversity and common mechanisms. J Biol Chem **274:** 17395-17398.

TRIFUNOVIC, A., A. WREDENBERG, M. FALKENBERG, J. N. SPELBRINK, A. T. ROVIO *et al.*, 2004 Premature ageing in mice expressing defective mitochondrial DNA polymerase. Nature **429:** 417-423.

VAN GOETHEM, G., B. DERMAUT, A. LOFGREN, J. J. MARTIN and C. VAN BROECKHOVEN, 2001 Mutation of POLG is associated with progressive external ophthalmoplegia characterized by mtDNA deletions. Nat Genet **28:** 211-212.

WANG, J., J. P. SILVA, C. M. GUSTAFSSON, P. RUSTIN and N. G. LARSSON, 2001a Increased in vivo apoptosis in cells lacking mitochondrial DNA gene expression. Proc Natl Acad Sci U S A **98:** 4038-4043.

WANG, Y., and L. KAGUNI, 1999 Baculovirus expression reconstitutes *Drosophila* mitochondrial DNA polymerase. J. Biol. Chem. **274:** 28972-28977.

WANG, Y., Y. MICHIKAWA, C. MALLIDIS, Y. BAI, L. WOODHOUSE *et al.*, 2001b Muscle-specific mutations accumulate with aging in critical human mtDNA control sites for replication. Proc Natl Acad Sci U S A **98:** 4022-4027.

WERNETTE, C. M., and L. S. KAGUNI, 1986 A mitochondrial DNA polymerase from embryos of Drosophila melanogaster. Purification, subunit structure, and partial characterization. J Biol Chem **261:** 14764-14770.

WOLF, Y. I., and E. V. KOONIN, 2001 Origin of an animal mitochondrial DNA polymerase subunit via lineage-specific acquisition of a glycyl-tRNA synthetase from bacteria of the Thermus-Deinococcus group. Trends Genet **17:** 431-433.

YAKUBOVSKAYA, E., Z. CHEN, J. A. CARRODEGUAS, C. KISKER and D. F. BOGENHAGEN, 2006 Functional human mitochondrial DNA polymerase gamma forms a heterotrimer. J Biol Chem **281:** 374-382.

YANG, M. Y., M. BOWMAKER, A. REYES, L. VERGANI, P. ANGELI *et al.*, 2002 Biased incorporation of ribonucleotides on the mitochondrial L-strand accounts for apparent strand-asymmetric DNA replication. Cell **111:** 495-505.

YE, F., J. A. CARRODEGUAS and D. F. BOGENHAGEN, 1996 The gamma subfamily of DNA polymerases: cloning of a developmentally regulated cDNA encoding Xenopus laevis mitochondrial DNA polymerase gamma. Nucleic Acids Res **24:** 1481-1488.

ZUCCOLA, H. J., D. J. FILMAN, D. M. COEN and J. M. HOGLE, 2000 The crystal structure of an unusual processivity factor, herpes simplex virus UL42, bound to the C terminus of its cognate polymerase. Mol Cell **5:** 267-278.